

REPORT No. 252

GEOLOGICAL SURVEY OF JAPAN

GEOLOGIC REMOTE SENSING OF  
THE KUSATSU—MANZA GEOTHERMAL AREA,  
CENTRAL JAPAN

By

Hirokazu HASE

GEOLOGICAL SURVEY OF JAPAN

Hisamoto, Takatsu-ku, Kawasaki-shi, Japan

1974







550.36:551.21:550.836:778.35 (521.24)

**REPORT No. 252**

GEOLOGICAL SURVEY OF JAPAN

Isamu KOBAYASHI, Director

**Geologic Remote Sensing of  
the Kusatsu – Manza Geothermal Area,  
Central Japan**

By  
Hirokazu HASE



## CONTENTS

	Page
Abstract .....	1
Introduction .....	2
Acknowledgments .....	3
I. Geologic Setting .....	4
I.1 Basement rocks of the Kusatsu-Shirane Volcano .....	6
I.2 Sedimentary rocks .....	6
I.3 Quaternary volcanic rocks .....	7
II. Thermal Activity of the Kusatsu-Manza Area .....	8
II.1 Volcanic activity of the Kusatsu-Shirane Volcano in historic times .....	9
II.2 Fumaroles and steam dominated hotgrounds .....	13
II.2.1 Sesshō-gawara .....	13
II.2.2 Karafuki .....	14
III. Remote Sensing Data for Geologic Procedures and Results .....	18
III.1 Thermal infrared remote sensing .....	20
III.1.1 Basic concept on the use of thermal infrared imagery for geothermal purpose .....	21
III.1.2 Experimental result on the detection of geothermal anomaly .....	26
III.2 Photogeologic structural analysis .....	26
III.2.1 Reliability of structural analysis data by aerial photographs .....	28
III.2.2 Film sandwich method .....	29
III.3 Aerial thermal infrared imagery of the area .....	33
III.3.1 Interpretation of imagery .....	34
III.3.2 Data analysis by the automatic data reduction system .....	39
IV. Interpretation of Structural Control .....	39
IV.1 Field measurement of the fracture system .....	39
IV.2 Lineagenic structural characteristics of the Kusatsu-Manza area .....	41
Conclusion .....	43
References .....	44
Appendix .....	49
要 旨	
Plates 1 ~ 6	

## List of Illustrations

### Figures

1. Index map of the Kusatsu–Manza area, central Japan .....	4
2. Geologic map of the Kusatsu–Manza area .....	Facing Page 8
3. Past major topographic changes recorded at the summit area of Shiranesan .....	12
4. Location map of the Sesshō-gawara geothermal spot .....	13
5. Heat discharge contour map at the southern slope of Sesshō-gawara .....	Facing Page 14
6. Noon time shallow underground (10 cm) temperature contour map of the southern slope of Sesshō-gawara .....	15
7. Temperature vs. depth data of the “center” geothermal spot at Karafuki .....	18
8. Correlation figures of temperature measurement point and thermal infrared imagery of the “center” geothermal spot at Karafuki .....	19
9. Temperature measurements sites YS–1, 2, and YS–3 at the heat discharge contour map of the Sulphur Cauldron, Yellowstone, U.S.A. ....	22
10. Temperature vs. depth curve (tautochrones) at YS–1 .....	23
11. Tautochrones at YS–2 .....	24
12. Tautochrones at YS–3 .....	25
13. Index map of aerial photographs used .....	30
14. An example of linear feature analysis by the film sandwich method using 1: 20,000 aerial photograph .....	31
15. An example of linear feature analysis by the film sandwich method using 1: 40,000 aerial photograph .....	32
16. Index map showing the area covered by aerial thermal infrared imaging flight .....	34
17. Explanatory figure of aerial thermal infrared imagery at the Shiranesan–Kusatsu Hotsprings area .....	36
18. Explanatory figure of aerial thermal infrared imagery at the Manza area .....	38
19. Structural geologic map of the eastern part of the Chikuma river, central Japan .....	Facing Page 38
20. Field measurement of fractures .....	40
21. Schmidt net diagram of fracture system of the Manza area and near the Shirane Sulphur mine .....	42

### Tables

1. Geologic development of the Kusatsu–Manza area .....	5
2. Temperature measurement data at the “center” geothermal spot at Karafuki .....	17
3. Experimental data for the lowest intensity of heat discharge amount .....	27
4. Specification of aerial thermal infrared flights .....	34
5. Measurement data of fracture system .....	40

### Plates

1–1. View of the Karafuki geothermal spot looking toward south (northern face)
1–2. Nighttime thermal infrared imagery mosaic of the Karafuki geothermal spot
2. Aerial thermal infrared imagery of a part of the Sesshō Lava near at Sesshō-gawara
3. Aerial thermal infrared imagery of the Kusatsu–Shirane Volcano—Kusatsu Hotsprings area
4. Aerial thermal infrared imagery of the Manza area
5. Automatically processed thermal infrared imagery of Sesshō-gawara
6–1. Automatically processed aerial thermal infrared imagery of the Yugama crater lake
6–2. View of the Yugama crater lake looking toward south



## Geologic Remote Sensing of the Kusatsu-Manza Geothermal Area, Central Japan

Hirokazu HASE\*

### Abstract

Geothermal systems are primarily controlled by geology and geologic structure. Macroscopically, it is quite decisive to state that the systems are understood geologically since much heat energy is delivered to the earth's surface from the deep underground mainly by the convective heat transfer system along major faults and fractures formed under the regional stress field of the area concerned. But local and shallow depth underground geothermal problems can not be solved by such sense.

To understand the geologic control of the geothermal system particularly in terms of local sense, photogeologic and thermal infrared studies were made selecting the Kusatsu-Manza area, Gunma Prefecture, central Japan, as a model field.

Techniques on pictorial expressions of electromagnetic radiation beyond the visible wavelength region have progressed rapidly in the decade and provide many earth data.

The author has been engaged in the study of the application of thermal infrared imagery for the understanding of geothermal problems for several years. In this study some experiments were made for the purpose.

The Kusatsu-Manza area is situated at the junction of the southwestern end of the Northeast Japan Arc and the northern end of the Izu Bonin Arc. Arc tectonism known as the Green-tuff Movement that commenced in the middle Tertiary characterizes the geology and volcanism of the area. The area is in the geanticlinal uplift zone of the early stage of the Green-tuff Movement and marine sedimentary rocks are lacking. The "basement" rock in the area therefore consists of altered volcanic rocks and pyroclastic rocks derived from terrestrial volcanism, and is intruded by igneous rocks. Successive volcanic activity during the Quaternary period formed the present volcano-geologic characteristics of the area. The Quaternary volcanic rocks are all andesitic and can be divided into many stratigraphic units. The Kusatsu-Shirane Volcano which occupies the central part of the area is a composite volcano consisting of two summit peaks, Shiranesan (north peak) and Moto-Shirane (south peak). The volcano showed explosion activities in historic times but is now thought to approach a dormant stage. Many geothermally anomalous spots are observed in the area among which the summit craters area of Shiranesan, Sesshō-gawara, Kusatsu Hotsprings, and the Manza area are dominant.

Structural geologic analysis of the area was made mainly by the use of aerial photographs on which the major linear features were plotted by stereoscopic observation and the minor linear features by the film sandwich method. Aerial photographs used are on the scale of approximately 1: 20,000 and also 1: 40,000. The result of analysis was correlated with field measurement data of the fracture system mainly in the Manza area. Thermal infrared imaging flights were made on Dec. 18th, 1971 and on Aug. 19th, 1972 at predawn to just after sunrise by the InSb detector mounted scanners. Particularly, the thermal infrared imagery obtained on Aug. 19th, 1972 successfully covered the major geothermal spots in the area. Another thermal infrared imaging test was made using a land thermal infrared scanner at Karafuki in the Manza geothermal area. The scanner used was provided with a HgCdTe detector.

All the data were utilized to interpret the structural control of the surface geothermal anomalies

---

\* Water Resources and Engineering Geology Department

and several conclusions were obtained. These are: 1) The existence of regional arrangements of linear features with the trend of NW-SE was recognized in the eastern part of the Chikuma River, northern Fossa Magna region. 2) The concentration zone of the minor linear features plotted by the film sandwich method showed good parallelism with the major linear features plotted by the stereoscopic observation of aerial photographs in terms of their general trend and also they showed good agreement with field measurement data in the Manza area. 3) Geothermal anomaly at the northern slope outside of the summit craters area of Shiranesan is formed along a ring-shaped fracture system around the outer side of the summit craters area. 4) Geothermal anomaly shown as convective dominated-hotground at Manza has N-S trend and is inferred to be related to the Manza Fault. 5) Heat discharge contour map was made of the southern slope of Sesshō-gawara utilizing snowfalls as calorimeters and the geothermal distribution pattern suggested the existence of a fracture system related to the Kusatsu Fault. 6) The lowest intensity of heat discharge amount by thermal infrared imagery distinguished as "geothermal anomaly" from the adjacent thermal pattern is hoped to be the order of or one order higher of the crustal heat flow value. One of the experimental result correlated with the heat discharge contour map and aerial thermal infrared imagery at Sesshō-gawara by use of the automatically processed data analysis-system showed that the limitation boundary of the lowest geothermal heat discharge amount distinguished from the surrounding thermal pattern had an amount much smaller than  $800 \mu\text{cal}/\text{cm}^2 \text{ sec}$ . 7) The distribution of geothermally anomalous spots at Sesshō-gawara and also the location of sulphur mines suggested that these thermally related features were formed at the intersections of the radial fracture system and ring type fracture system of the volcanic body.

### Introduction

Remarkable repeated linear patterns of geologic or topographic features have attracted deep interest for regional structural geologists for more than 60 years. Concerning the origin of structural linear patterns, MEINESZ (1947) developed a concept on the occurrence of worldwide shear pattern caused by the flattening of the earth ellipsoid following the shift of the rotation axis. Attention to the linear features is now focused as an evidence of the theory of today's global tectonism and the economic importance. The term "lineageny" was first proposed by HILLS in his text book of structural geology (HILLS, 1963, p. 315) as a tectonic movement independent of other movements such as orogeny, epirogeny, and taphrogeny. He states "It is proposed to call these lineagenic movements (lineageny), because of their effects in forming major geological lineaments. The movements are mainly horizontal block displacements, but secondary folds and faults may arise along the major strike-slip faults." KUTINA (1969) expressed a striking new concept of structural control of hydrothermal ore deposits distributed in the western United States where the major ore deposits are situated at intersections of two sets of deep-seated fracture zones, based upon regularities in distribution of the actual faults and ore veins in the continental area and on the eastward continental prolongation of the large fracture zones of the northeastern Pacific known as the Mendocino and the Pioneer fracture zone. WERTZ (1970) discussed on the economic significance of the "Texas lineament."

Detailed mapping data of fault and joint system provide us with the fundamental structural geologic knowledge and it is going to be made possible remotely by use of *remote sensing data* such as radar imagery, satellite imagery, thermal infrared imagery, multispectral photograph/imagery, and so on, together with conventional aerial photograph.

With regard to geothermal heat transfer system, heat energy in the deep underground is transferred to the surface most efficiently through vertical fracture paths. Development of a possible fracture system may be theoretically analyzed if we know the stress field of the area

concerned, or vice versa by knowing stress ellipsoid of the conjugate fault sets observed. However, our knowledge on the stress field changes, as load increases with increasing depth, is not so complete to take into consideration the occurrence of the local fracture system (KAKIMI, 1971).

Another problem often encountered in the field survey of a geothermal area is the lack of information of the area. The geothermal area is often situated in inaccessible mountainous areas and the outcrops are often thermally altered thus preventing detailed field survey.

Many stratigraphers and structural geologists have challenged the geothermal fields and tried to clarify the interrelation with the geothermal system and geologic structure. The conclusion is believed to be quite cogent in view from the regional geologic or structural geologic standpoint. But the conclusion is too remote to apply for local geothermal problems which are, in many cases, closely related to our daily life.

Photogeologic structural analysis has been thought to be very effective to understand the structural geologic control of the geothermal area and the acquisition technique by this method has progressed very rapidly beyond the visible wavelength region. That is, ultraviolet, thermal infrared, and microwave wavelength region is being used as the pictorial data source of the earth not only the aircraft altitude but also the spacecraft altitude. Also spectral understanding of the earth's material is being made in wider wavelength range of electromagnetic rays including the visible wavelength region. These data acquisition techniques are ambiguously called "remote sensing." One side of geologic remote sensing can be said to be the practical outgrowth of photogeology (LYON, 1970a).

The author has been engaged in the study of use of thermal infrared imagery as an aid for solving geologic problems, particularly for the purpose of structural analysis of the geothermal area.

One of the geothermal areas Kusatsu-Manza area, Gunma Prefecture, central Japan was selected for the purpose, and the photogeologic and thermal infrared remote sensing methods were applied.

In this paper the result of the study is given and a consideration of the geothermal system in view of lineagenic structural control is made. The surface heat flow study for quantitative use of thermal infrared imagery is included.

In use of new terms, the definitions are made on each occasion. As a general usage of structurally significant fissures suggesting faults and joints, the term "fractures" are used in this paper. Fissures may or may not be related to fractures.

### Acknowledgments

Deep gratitude is expressed to Dr. Kyuya MATSUNO, chief of the Water Resources and Engineering Geology Department, Geological Survey of Japan, who introduced the author to the study on the application of thermal infrared imagery for geologic purpose, for his valuable suggestions, selection of the Kusatsu-Manza area for study and encouragement throughout the course of study. Appreciation is due to Mr. Kashihiro NISHIMURA, photogrammetrist of Geologic Remote Sensing Laboratory in Geological Survey of Japan for his kind assistance both in the field and laboratory, and also for his valuable suggestions on the photogrammetric work. Thanks are expressed to Mr. Tatsumi KURASAWA and members of the Enterprise Bureau of Gunma Prefectural Government for their assistance in the field.

Concerning the data acquisition and analysis, special thanks are due to: Dr. Sumizo FUJII and members of the Fujitsu Co. for permission to use the land thermal infrared scanner at Karafuki in the Manza geothermal area. They collaborated in obtaining daytime and nighttime thermal infrared imagery at the spot. Mr. Masataka FUCHIMOTO and members of the Asia

Aerial Survey Co. provided aerial thermal infrared imagery near Sesshō-gawara. Mr. Sei WATANABE and his colleague of the Nakanihon Kōku Aerial Survey Co. made thermal infrared flight over the area and provided the data which were very useful in this study. Mr. Chitao MIYAKOZAWA of the Kimoto Co. permitted the author to use the automatic data processing system developed by the company.

He also wishes to thank Dr. Taichi OSHIMA, Institute of Industrial Science and Technology, University of Tokyo and the Japan Society of Photogrammetry for their assistance in the series of thermal infrared geological studies at the Manza area.

Gratitude is expressed to: Dr. Isamu KOBAYASHI, Director of Geological Survey of Japan, for his encouragement in various ways; Professor RONALD J. P. LYON of Stanford University and Dr. DONALD E. WHITE of the U. S. Geological Survey for their suggestions and guidance on thermal infrared imagery for geothermal purpose.

The author also expresses his thanks to Professors Kotora HATAI, Nobu KITAMURA, and Kiyoshi ASANO of the Tohoku University, Dr. Kiyoshi SUMI, chief of the Environment Geology Section, Geological Survey of Japan, who read the manuscript for their valuable guidance and suggestions and also to Associate Professors, Tamio KOTAKA, Yokichi TAKAYANAGI, and Hisao NAKAGAWA of the Tohoku University for their valuable suggestions.

### I. Geologic Setting

The Kusatsu-Manza area is a mountainous upland in central Japan (Fig. 1). The area is about 160 km northwest of Tokyo and lies at the southwestern end of the physiographic region called the Mikuni Mountains, and forms the central part of the Jōshin-etsu Highlands National Park.

Macroscopically, the area is situated at the junction of southwestern end of the Northeast Japan Arc and the northern end of the Izu-Bonin Arc. The tectonism started in the middle Tertiary and continuously active to today is characterized by the general geology, geologic structure, or volcanism of the area. Recent volcanic activity, geothermal activity, and a high

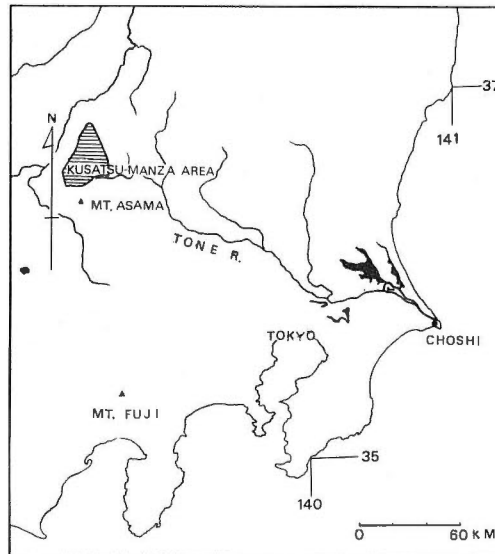


Fig. 1. Index map of the Kusatsu-Manza area, central Japan.

rate of crustal heat flow are the general thermo-geologic characteristics of the inner belt of the Northeast Japan Arc and the Izu-Bonin Arc.

Rocks in the area are in large part composed of the products of the Kusatsu-Shirane Volcano and its basement rocks. The Kusatsu-Shirane Volcano is a composite volcano consisting of two summit peaks with central craters. The peaks are called Shiranesan (north peak) and Moto-Shirane (south peak). The volcano had explosion activity in historic times but the vapor explosion type of the activities suggests that the volcano is approaching a dormant stage. There are many geothermally anomalous spots in the area among which the central craters area of Shiranesan, Sesshō-gawara, Kusatsu Hotsprings, and the Manza area are dominant.

The geologic history of the area is retroactive to Miocene time. The crustal depression first occurred in northern central Japan in the early stage of the Miocene and a geosynclinal sedimentary basin is formed followed by marine transgression in the tectonically depressional region. This tectonic movement is a part of the Neogene Tertiary tectonism or more popularly, the Green-tuff Movement. Thick piles of marine sedimentary rocks together with vast amount of submarine volcanic products are deposited in the geosynclinal basin during this stage. The marine transgression reaches the maximum in the middle Miocene time and a geanticlinal movement is initiated first in the basin accompanied with acidic plutonic intrusive rock masses composed of porphyrites and granodiorites. Regional tectonic movements in northern central Japan (the northern Fossa Magna region) is studied and summarized by IJIMA (1962 and 1963) who proposed the name of the Central Uplift Zone for the NNE-SSW trend culmination zone with plutonic intrusion. The area studied is located in part in the axial belt of the Central Uplift Zone. In Late Miocene time the area is subjected to a terrestrial erosional environment and volcanic activity is comparatively calm but fierce volcanic activity again takes place in Pliocene time and it lasts until the Quaternary period forming the present Kusatsu-Shirane Volcano and other adjacent volcanoes.

The development of the geologic history of the area is tabulated in accordance with IJIMA's stage names (Table 1).

The earliest descriptions of the geologic observations and studies of the area were made by

Table 1. Geologic development of the Kusatsu-Manza area.

GEOLOGIC AGE		STANDARD (Central Japan)	KUSATSU — MANZA AREA	
QUATERNARY	RECENT		Kusatsu-Shirane Volcano	Younger Lava
	PLEISTOCENE			Older Lava { Shirane Pumice Flow Shirane Tuff Brec. Takai Lava
TERTIARY	PLIOCENE	KOMORO GROUP	Kadokai F.	Swarm Eruption → Vent Eruption → Steam Explosion Block Movement ↑ Uplift ↑
		OGAWA F.	Acidic Plutonic Rocks	
	AOKI F.			
	MIOCENE	BESSHO F.	Propylite	
		UCHIMURA F.	Rhyolite	

IWASAKI (1897) at the end of the nineteenth century. The most complete study on general geology of the area in the early days is the splendid work of OHASHI (1914). In 1932, volcanic explosion whose activity was the most intense in the past hundred years took place from the cluster of small craters at the summit of Shiranesan and many investigation reports were published in the same year and the following year (for example, TSUYA, 1932; TSUYA, 1933). The recent geologic study was mainly by OTA (1957) in his geologic sheet map "Kusatsu" on the scale of 1: 50,000 and the adjacent sheet map "Suzaka" on the same scale (OTA and KATADA, 1955). More recently, reinvestigation of the Kusatsu-Shirane Volcano was made by OTA and MATSUNO (1970), and detailed stratigraphical sequences and the geologic structure were reported with the aid of photogeologic interpretation. The area studied is mostly included in their geologic map and the geologic description in this paper is largely based upon their work.

### **I.1 Basement rocks of the Kusatsu-Shirane Volcano**

The oldest basement rocks of the Kusatsu-Shirane Volcano are those of the Neogene Tertiary period which are widely distributed westwards and eastwards of the area. But they are not observed in the area covered with Quaternary volcanic rocks. According to OTA and KATADA (1955) and OTA (1957), the oldest rocks in the Kusatsu geologic sheet map are rhyolites which crop out east of the area and are not geologically mapped in this paper. They are composed of the alternation of lavas and pyroclastic rocks. The lava rarely contains lapilli of propylites or fragments of black colored shale, and some parts becoming compact due to secondary silicification. Volcanic rocks are mostly intermediate in chemical composition and regionally metamorphosed into propylites. Igneous rocks including granite-porphry, quartz porphyry, aplite, and hornblende-quartz diorite intrude both the rhyolite and porphyrite rock masses. Their widespread distribution is seen in the Suzuka geologic sheet map, west of the present area and only isolated small rock masses crop out in the east of the area. Quartz porphyrites are known to change into quartz diorite (OTA and KATADA, 1955). The small outcrop of porphyrite observed at the east of the area is composed almost all of thick lava and the bedding plane is obscure. Pyroxenes in the phenocryst of porphyrite are partly altered into chlorite, and in general it gives a grayish green to dark green color to the rocks.

The geologic age of a granodiorite sampled at 12 km south-southwest of the Kusatsu-Shirane Volcano is radiometrically dated, and gives  $2.1 \times 10^7$  year or Middle Miocene age (KAWANO and UEDA, 1966). Volcanic rocks stratigraphically subdivided into many eruption units in the area are all products of the post igneous intrusion. No radiometric data are available for them. Some of the volcanic rock bodies are highly dissected and do not show their initial topographic features, suggesting that they are products of Neogene Tertiary to Pleistocene volcanism. These dissected volcanic units are named in ascending order, the Takai Lava, the Horaguchi Lava, the Older-Shirane Lava, and the Yokote-yama Lava, all of which consist of augite-hypersthene andesite to quartz bearing augite-hypersthene andesite lava and their pyroclastics. The Takai Lava had been considered to be a member of the Green-tuff rocks but today it is accepted to be younger and to overlie the Green-tuff rocks group. The Older-Shirane Lava also had been considered to be younger than the Yokote-yama Lava, and to form the lower part of the Kusatsu-Shirane Volcano (OTA, 1957), but according to the recent field investigation by OTA and MATSUNO (1970), the lava is a formation of the basement rocks group of the volcano and stratigraphically older than the Yokote-yama Lava.

### **I.2 Sedimentary rocks**

Through the later stage of the Green-tuff tectonism, the area was mostly subjected to a terrestrial environment with volcanic activity, therefore the distribution of the Tertiary sedimentary rocks is limited. Outcrops of the sedimentary rocks are found along the Manza River

and the Agatsuma River at the southwestern margin of the area. They are named the Kadokai Formation and consist of an irregular alternation of sandstone, conglomerate, and volcanic ashes reaching a total thickness of at least 100 m. The general trend of strike of the bedding plane is NE-SW and the strata are folded with the same axial trend. No fossil remains have been reported and the age of the formation or sedimentary environment (marine or nonmarine) can not be determined directly. Although the basement contact is not observed, the formation appears to be stratigraphically conformable or with a little time hiatus with the underlying rocks. The formation is thought to be the products of the uppermost Neogene Tertiary to early Pliocene time. Quaternary sedimentary rocks are more or less related to the volcanic activities. Pyroclastic-flow deposits, pumice-flow deposits, and mud-flow deposits derived mainly from the active Asama Volcano (see Fig. 1) situated at 26 km south of the Kusatsu-Shirane Volcano are deposited along the Agatsuma River, other valleys, or buried topographic lows. Volcanic materials seem to have dammed up the Agatsuma River in the past and lake sediments such as gravel, sand, and clay were deposited.

The Kusatsu Hot Springs are situated on the talus deposits at the eastern foot of the volcano.

### I.3 Quaternary volcanic rocks

The Plio-Pleistocene age of the Kusatsu-Manza area is characterized by continuous volcanic activities, which resulted in the distribution and the formation of the present volcanic features. The volcanic activities gradually changed from the swarm rift eruption in the early stage of the Green-tuff volcanism to isolated individual vent eruptions in the later stage (Pliocene to Quaternary). Adjacent centers of the volcanic eruption to the Kusatsu-Shirane Volcano are the Omeshi Volcano at the west and the Azumaya Volcano at the southwest, both of which form independent volcanic bodies today; they consist of andesitic rocks. Some volcanic products from the Omeshi Volcano and the Azumaya Volcano are distributed in the area. Except for them, all of the Quaternary rocks described briefly in the following are those of the Kusatsu-Shirane Volcano.

The first volcanic products of the Kusatsu-Shirane Volcano are mainly thick andesitic tuff breccia intercalating lava flow beds, 3 to 5 m in thickness. The distribution of the rocks was first thought to be limited at the southwestern slope of the volcano but by the recent geologic survey by OTA and MATSUNO (1970), the rock mass cropping out on the east to southeast slope of the volcano and forming isolated topographic high on the gentle surface slope are of the same rock-stratigraphic units. This andesitic tuff breccia is called the Shirane Tuff Breccia and the distribution pattern of the volcano reminds us of the first formation of conical volcanic body on the older basement rocks. The conical shape of the volcano is broken only on the north and northwest side. The topographic high of the southern edge of the Yokote-yama Volcano at the time might be preclusive of the northern distribution of the tuff breccia, but the lack of it on the northwestern side of the volcano, seems to have resulted from structural geologic control as discussed in the later chapters (III and IV).

The total thickness of the Shirane Tuff Breccia attains about 300 m.

The most widespread rocks by the volcanic activity of the Kusatsu-Shirane Volcano, are the thick dacitic pyroclastic materials which are called the Shirane Pumice Flow (OTA, 1957) or the Kusatsu-Shirane Pyroclastic Flow Deposits (ARAMAKI, 1968). The locus of eruption is probably beneath the Moto-Shirane, from where the flow formed a gentle conical slope, the present surface feature. The formation was formed by intermittent eruptions and as many as five flow units are observed. The lower part of a single flow unit is usually welded and often manifests columnar joints that serve for easy counting of the flow units.

The volcanic activity following the pumice flow is subdivided into the older and the younger activity. The older volcanic products are in ascending order: 1) the Yatoko Lava crops out

near the Shirane Sulphur Mine and the Ishizu Sulphur Mine. This consists of quartz bearing pyroxene andesite and its pyroclastics. The lava is easily cracked into plates 3 to 4 cm in thickness. 2) the Matsuo-zawa Lava is distributed in the vicinity of the Agatsuma Sulphur Mine and forms the mother rock of sulphur ore. It consists of massive andesitic tuff breccia at the mine. 3) the Aoba Lava crops out typically at the northwestern portion of Sesshō-gawara forming a steep caldera wall. The lava is glassy andesite and its viscous property is a cause of the topographic steepness not seen in the other flows. 4) the Yahazu-daira Lava is distributed along the sightseeing toll road at the western part of the area, showing a barb-shaped narrow distribution sandwiched by the Shirane Tuff Breccia at the lower part and by the Udogo-sawa Lava at the upper part. The rocks are pyroxene andesite. 5) the Udogo-sawa Lava is of pyroxene andesite but can be distinguished from the Yahazu-daira Lava by its coarse-grained groundmass. 6) the Komenashi Lava forms a gentle surface slope at the southern part of the volcano. The lava is pyroxene andesite and is easily cracked into plates 3 to 4 cm thick. 7) the Moto-Shirane-West Lava is a product of the volcanic eruption that took place from a parasitic lateral crater at the southwestern slope of the Kusatsu-Shirane Volcano. 8) the Yumiike Lava crops out at the saddle between the two peaks, Shiranesan and Moto-Shirane. It is compact pyroxene andesite and the fresh rock shows a dark bluish green color. 9) the Futago-yama Lava Dome and the Ainomine Cinder Cone are the products of the eruption of the parasitic volcanoes of the Kusatsu-Shirane Volcano.

The volcanic products from the Yatoko Lava to the Ainomine Cinder Cone are distinguished as the older lava flow group of the volcano and they are strongly related to the formation of the primary caldera of the Kusatsu-Shirane Volcano. The western half of the primary caldera preserves topographic features today and its diameter attains more than 15 km in the elongated N-S direction. After the formation of the above-mentioned volcanic product, some other volcanic eruptions took place in the area and also several secondary calderas were formed. The secondary calderas are comparatively small on scale and the units of the lava flows that erupted are called the younger volcanic products. The younger lavas keep their original topographic shape well and are easily distinguished on aerial photographs. The main eruption center was at the summit area of Moto-Shirane. The Yamada-toge Lava is the first of the products in this younger stage. The lava overlies the Takai Lava at the northern portion of Shiranesan and forms a lava dome. The Moto-Shirane Lava is distributed at the southeastern portion of the volcano and a lava front is observed at the Ishizu Sulphur Mine. The Heibei-ike Lava was produced by the eruption of Shiranesan and it is distributed at the northern part of the area overlying the Aoba Lava. The Sesshō Lava is from the eruption of Moto-Shirane and the center of the eruption-vent is near the summit. The flow of the lava took two courses flowing down along the eastern and southern slopes of the volcano. The lava is glassy black-colored pyroxene andesite. The last product of the eruption of Moto-Shirane is called the Moto-Shirane Cinder Cone. On the other hand, the latest volcanic activities in historic times are only at the summit craters area of Shiranesan.

The distribution of the rocks is shown in the geologic map (Fig. 2).

## II. Thermal Activity of the Kusatsu-Manza Area

There are many active volcanoes and numerous hot springs in northern central Japan including the present area. Obviously, crustal thermal activity in the region resulted mostly from heat energy of the Tertiary granitic intrusion mass since the area occupies a part of the structural culmination zone. Regional structural geologic control under the Green-tuff tectonism in the region is most significant. The deep-seated major fracture system may control the arrangement of the Quaternary volcanoes.



Recent thermal activities in the area studied are the vapor explosion type of volcanic activity without the flow of lava at the summit craters area of Shiranesan, steam issuing fumarole, hot springs and hotpools at the crater-bowls, and convective and conductive hotground.

The Kusatsu-Shirane Volcano is now in a quiescent stage after the explosion in 1939 and only manifests thermal activity represented by steam issuing fumarole at the northern portion of the summit and around the crater wall of the Mizugama. The summit craters area is covered with the recent volcanic ejecta and lacks vegetation. Its desolated scenery attracts sightseers every year.

Among the summit craters, the Yugama is the largest and contains the deepest water (deeper than 30 m) and the Yugama, the Mizugama, and the Yumiike crater-bowls contain shallow lake water (not deeper than 2 m) at their bottom. The water temperature of the Yugama is a little higher than the "normal" because of the subaqueous heat source.

In the area, there are two well known hot spring resorts called Kusatsu Hot Springs and Manza Hot Springs. The Kusatsu Hot Springs whose discovery is retroactive to more than 1,000 years boasts of the abundance of hotwater. It discharges 32.24 m<sup>3</sup>/min of sulphurated acid alumivtrial hot spring water (average temperature of 57°C), or a total calorimetric amount of 1,575 × 10<sup>6</sup> cal/min. By this abundant hot spring water, it is ranked one of the leading hot springs in Japan. Almost all of the hot springs are found along the Yukawa (English meaning of hotwater creek).

Manza Hot Springs is also comparable with the Kusatsu Hot Springs. It discharges 3.60 m<sup>3</sup>/min of arsenic acid alum hot spring water and sulphurated acid hot spring water (average temperature of 90°C), or equivalent of 291.6 × 10<sup>6</sup> cal/min (calorimetric calculation value is based upon Yuhara's unpublished data). The area is located at the deepest of the Manza River. The Manza area characteristically shows many fumaroles, and convective and conductive hot-grounds other than hot springs. The area is situated at an elevation of about 1,750 m, or 600 m higher than the Kusatsu Hot Springs and it is the third hot springs in elevation in Japan.

Among other geothermally anomalous spots in the area, the Sesshō-gawara is the most dominant. No hot spring water nor surface water is seen at the spot and Sesshō-gawara forms a typical vapor issuing convective and conductive hotground geothermal spot. The thermal activities of these spots are described in this chapter.

### II.1 Volcanic activity of the Kusatsu-Shirane Volcano in historic times

The volcano has been active ten times during the last ninety years. The form falls into a category of the late stage of volcanic activity and its activity is vapor explosion or explosion without the eruption of lavas. The oldest report on the activity which describes that the explosion resulted in ash fall that extended to the northwestern district of the volcano, is in 1805 (OTA, 1957). The volcano kept quiescent for seventy-seven years until the explosion took place on August 6, 1882.

The volcanic activities after 1882 to today are reported by many persons on the occasion of every explosion. The summarized description is given by TSUYA (1933) and OTA (1957). The activities during 1882 to 1932 are mainly in TSUYA's detailed report. The selected passage of his report given in the following is focused on the change of the volcanic topographic features. Description of the explosion of 1937-39 is based upon MINAKAMI's report (MINAKAMI, 1939).

(i) The activity of 1882: The rumbling sound began in the previous summer beneath the summit craters area. The explosion took place on Aug. 6th, in the floor of the Yugama crater-bowl and eight other places near it, resulting in the formation of numerous hollows, from which vapors, hotwater, mud, and stones were thrown out. These hollows were of varying sizes and depths, the largest being about 150 m in diameter and about 90 m in depth. Following the explosion of Aug. 6th, numerous openings, the largest of which about 5.5 m in diameter were

observed at noon of Aug. 9th, near the crater rim on the southeast side, and from these openings hotwater poured out for a week until Aug. 16th. Before this explosion, the ground in and around the Yugama crater-bowl had been covered with a pool of cold water at the center of the crater-bowl, but by the explosion the trees and bushes were completely ruined, and the position of the pool changed to another part near the base of the northern crater-wall, its old site becoming partly dry ground and partly a new pool of hot water.

E. NAUMANN visited this mountain on Sept. 5th and 7th of the same year, and reported that fairly strong emissions of dense vapor clouds were taking place from several fissures on the northern wall of the Yugama crater-bowl, as well as from the horseshoe-shaped explosion crater and hot fountain at the bottom of the crater-bowl.

(ii) The explosion of 1897: On July 8th, 1897, dominant explosive activity took place at the northeastern rim of the Yugama crater. As a preliminary sign of this explosion, vapors mixed with sulphur actively issued from the Yugama since a month previously and slight earthquakes were frequently felt on the mountain. Since the afternoon of July 7th, roarings were of frequent occurrence, until about 4 A.M. the next day, and an explosion took place ejecting volcanic ashes and sand from an opening of about 100 m in circumference and 20 m in depth, between the rocky ridges, and about 200 m northeast of the former explosion crater in the Yugama crater-bowl. An hour later, a second explosion occurred on the southwest side of the explosion crater and lasted for about three hours. As a result of this explosion, another explosion crater was formed, about 80 m in diameter and opening into the former pool. On July 31st of the same year, an explosion took place at about 5 A.M. with slight earthquakes. Several explosion holes were formed in front of the lock-gate of the drainage tunnel at the southern slope of the pool. About 40 m eastward of these holes there appeared a fissure through which hot mud and blocks were projected northwestward over the crater rim during the explosion.

The next year (1898), according to JIMBO, it was found that, as a result of the last explosions, the level of the former pool had fallen about 5 m. When he visited the mountain on Aug. 17th, vapor clouds were issuing from the northeast corner of the pool.

(iii) The explosion of 1900: On Oct. 1st, 1900, feeble rumblings and explosions were felt at about 3 A.M.

(iv) The explosion of 1902: On July 15th, 1902, an explosion occurred at about 4 P.M. in a small conical mound on the northeastern shore of Yumiike, an explosion crater lake on the saddle between Moto-Shirane, and Shiranesan. Emissions of vapors and ejections of rock fragments continued to the next evening. Four days later, on July 19th, only a faint vapor-cloud was issuing.

On Oct. 18th, hotwater was seen spouting from several places in the crater at the top of the conical mound near the Yumiike crater. Through all the explosions of this year the Yugama crater-bowl remained quiet. Lake water increased in acidity since the year.

(v) The explosion of 1905: In 1910, according to OHASHI, it was said that the steam was issuing from the hotwater pool at the bottom of the Yugama crater, near the base of the inside northern wall. In 1906, feeble fumaroles and fountains were observed at several places in the hotwater pool inside the Yugama crater. A very active fumarole was noticed in the northwestern part of the pool. At that time the water in the pool was about 50°C. The Yugama crater-bowl contained little water at that time.

(vi) The explosion of 1925: On Jan. 22nd, 1925, an explosion took place at the inside northern wall of the Yugama crater, ejecting ash-laden clouds and rock fragments with rumblings. On Jan. 25th, it was found that a new explosion pit, about 20 m by 7 m, had opened near the upper rim of the inside northern wall of the crater. The Yugama crater-bowl was as before, emitting feeble vapor clouds from its floor.

(vii) On Dec. 31st, 1927, an explosion occurred at about 11 A.M. The explosion shot out

enormous columns of vapor heavily charged with volcanic ashes from a fissure nearly 100 m long at the base of the inside northern wall of the Yugama crater, as well as from numerous other fissures on the southern flank adjoining the southern rim of the Yugama crater, which formerly had been a vertical cliff, caved in. As a result of its explosion, the vent that opened in 1925 ceased activities, the water in the Yugama crater-bowl rose in temperature from 15°C to 24°C, while its level sank about 14 m. On the southern flank near the south rim of the crater, a hot spring of 80°C began to gush out. Since then fairly strong emissions of vapor-clouds continued during the following three months, but these gradually decreased in intensity.

(viii) The explosion of 1932: The explosive activities of 1932 began on Oct. 1st. The first explosion occurred at the inside northeastern wall of the Yugama crater, as well as in the fissures on the outside of the southern rim of the crater. After the explosion of Oct. 1st, the mountain was relatively quiet, and a number of people visited and photographed the sites of vapor issuing from the crevices in the inside northeastern wall of the Yugama crater and also from the fissures on the outside of the southern rim of the crater. The explosion lasted until Oct. 27th.

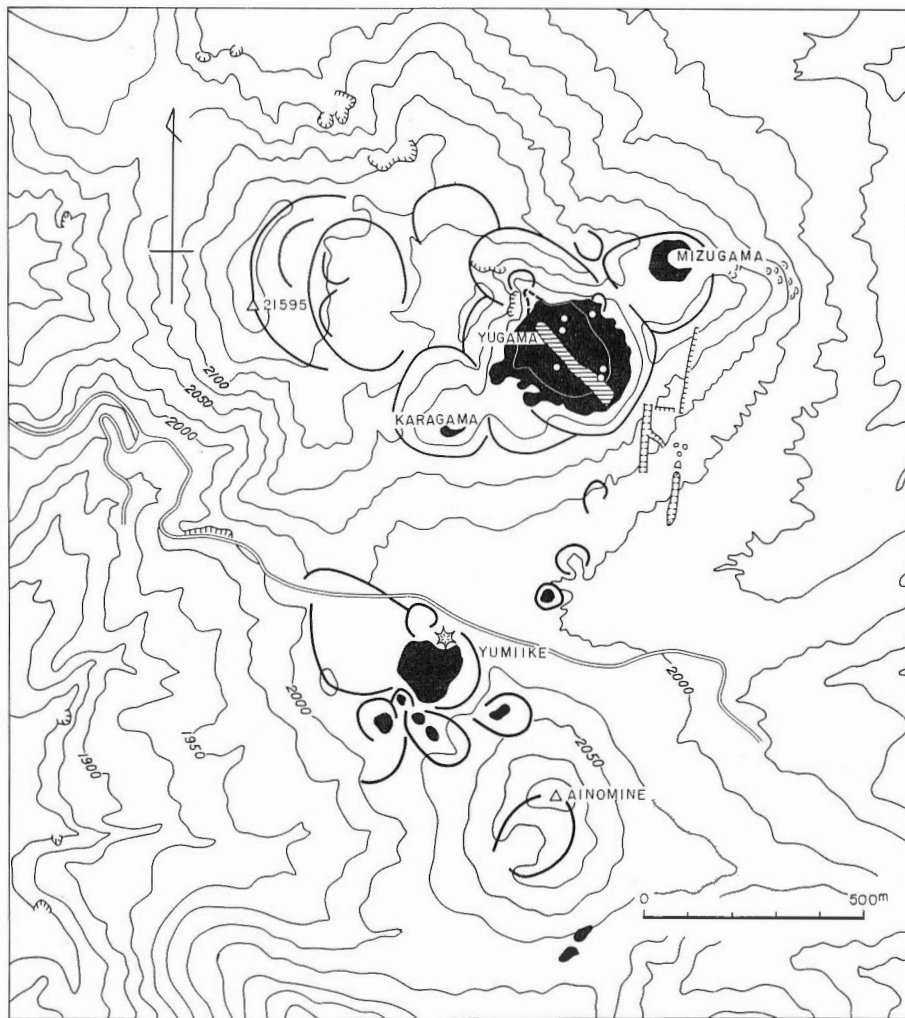
The noticeable topographic change of this time of explosion was fissuring, both inside and outside the Yugama crater-bowl.

(ix) The explosion of 1937-39: The explosion took place suddenly on Nov. 27th, 1937 at the Yugama crater. MINAKAMI, who was under geophysical investigation of the Kusatsu-Shirane Volcano, had a chance to visit the summit craters area soon after the first explosion. Continuous explosive activities were recorded five times during the same year. In the following year, 1938, explosive activities were more frequent, counting eleven times a year, and the activity continued until mid 1939. Most of the explosions took place in and around the rim of the Yugama crater depositing volcanic ejecta and ashes in the crater. According to MINAKAMI (1939), the southern rim of the crater where the fissures were formed during the explosion of 1932, was still actively emitting vapor from the former vents, and after the explosion the vapor clouds became dominant. Water level of the Yugama crater was lower than at the time of the explosive activity in 1932. A fissure zone of NW-SE trend across the bottom of the crater was formed issuing vapor and fumaroles along the fissure zone.

Through the volcanic activities of the Kusatsu-Shirane Volcano during the past ninety years, the topographic feature change at the summit craters area was noticeable. This aroused deep interest of the investigators, and some of them recorded the changes on topographic sketch maps. The earliest topographic sketch map of the summit craters area was made by KAJIMA and GOMI, whose map was introduced in TSUYA's report (1932b). TSUYA himself made a map of the same area after the explosion of Oct. 23rd, 1932, and another one on Aug. 8th, 1933 when he visited the site again. MINAKAMI made the same kind of map after the explosion of 1937 and correlated it with TSUYA's map. These records give interesting information on the changes of the topographic features following the construction or destruction of hollows and pits, the location of vents and fissure zone, and the distribution of water in the craters beside the explosion spots which are subaqueous today.

The previously reported sketch maps were superimposed on the present topographic map (1965) allowing some errors by the author (Fig. 3).

Through the explosion activities in the past ninety years, the linear arrangements of fumarole vents, hollows, and pits are noticeable. Two parallel rows of fissure zones formed by the explosion of 1932 have NNE-SSW trend at the eastern slope of the Yugama crater. The explosion activity of 1937-39 formed a NW-SE direction of the fissure zone across the bottom of the Yugama crater. As later explained, linear fissure zones that developed around the Yugama crater were understood to form a segment of a ring type fracture outside the summit craters, the Yugama, the Mizugama, and the Karagama in this paper.










-  crater rim
-  crater lake and pool of water
-  beach line at the time of 1927
-  fissure zone formed at the explosion of 1937-39
-  fissure zones formed at the explosion of 1932
-  subaqueous hot spring previously recorded
-  conical mound where the explosion of 1902 took place

Fig. 3. Past major topographic changes recorded at the summit area of Shiranesan.

## II.2 Fumaroles and steam dominated hotgrounds

Many spots of geothermal activities represented by hot springs, fumaroles, or hot grounds in the area are fundamentally related to the active volcano, Kusatsu-Shirane.

Two major geothermal spots, Sesshō-gawara and Karafuki of Manza are described below.

### II.2.1 Sesshō-gawara

This name of the spot comes from the emitting of sulphurous acid gas and hydrogen sulphide gas killing birds and animals at the place. The location is about 1,550 m above sea level and situated 3 km southeast of the summit of Shiranesean. The sightseeing park road crosses the spot and is one of the attractive places in the national park.

The surface rock of the spot consists of the Quaternary Sesshō Lava whose distribution is easily distinguished on aerial photographs by the tonal difference from the adjacent rocks and the aa type of surface texture. The surface is usually covered with shrubby trees. Sesshō-gawara occupies a part of the northern margin of the eastside flow where a pressure ridge is formed along the margin of the flow with several meters high topographic feature. The geothermally altered area extends in E-W to ENE-WSW direction forming an irregular oval-shaped planal distribution with the longer axis 500 m and the shorter axis 150 m in length (Fig. 4).

The lava flow shows an irregular rugged surface and various sizes of volcanic ejecta are settled on the surface of the flow. The vertical columnar section of the lava flow unit is therefore very porous. On the other hand, the geothermally altered zone has comparatively smooth surface. The surface is coated with reduced free sulphur, and cracks and openings in the lava are filled with free and sublimated sulphur. Fragmented altered bedrock materials of 30–100 cm thickness cover the flat surface but not thicker than 30 cm on the slope. Vegetation is lacking at the place and a feeble fumarole is observed here and there in the central 300 m long and 60 m wide zone. The most intensive geothermal anomaly is observed on the topographically high pressure ridge limiting the flow unit.

The earliest description on Sesshō-gawara was by IWASAKI (1897), and according to him, there was a round water pool with diameter of about 10 m. Today there is no topographic feature suggesting it and no surface water is observed around the spot. A feeble vapor issuing from a hollow of the outer rim of about 150 m in diameter is observed 300 m south of Sesshō-gawara but this is not mentioned in his description.

The spot has once been surveyed for geothermal power generation from 1954 to 1956 by the

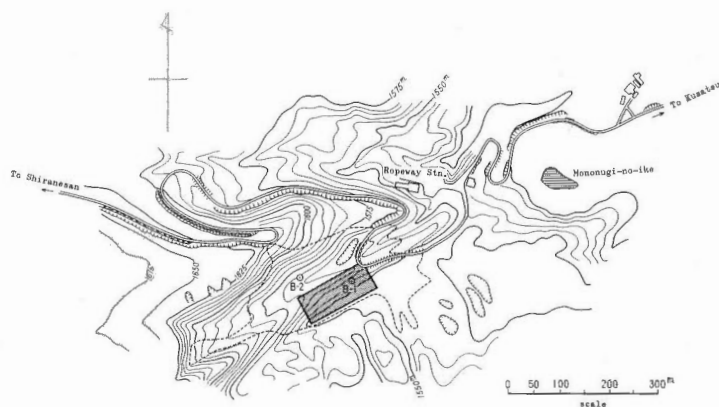


Fig. 4. Location map of the Sesshō-gawara geothermal spot (area surrounded by dotted line is thermally altered area).

Tokyo Electric Co. and the Chubu Electric Co. Two test bore holes were dug for this purpose and several studies were made. The study of geochemical and rock alteration was done utilizing the core samples by ANDO (1957). The bore holes were left unused and utilizing one of the bore holes (another one was buried in March, 1958), conductive heat flow measurement was made (UYEDA and others, 1958). They obtained approximately constant (i.e.  $24.2^{\circ}\text{C}/100\text{ m}$ ) temperature gradient 170 m below the surface to the bottom (250 m), and by the average of ten samples of thermal conductivity value of altered andesite ( $K = 4.48 \times 10^{-3}\text{ cal/cm sec }^{\circ}\text{C}$ ), they determined the conductive heat flow-rate of the spot to be  $10.8\text{ }\mu\text{cal/cm}^2\text{ sec}$ , or about seven times the normal crustal heat flow value.

A stratigraphical columnar section based on the core sample showed that the thickness of the Sesshō Lava was about 20 m at the spot, and below the lava to the bottom (250 m), the rock was composed of the Aoba Lava which includes a strongly altered silicified zone. The surface water is easily percolated through the porous rock downward and the groundwater level is lower than 250 m below the surface so that the spot shows fumarole and steam dominated-hotground geothermal anomaly at the surface.

Mapping of the surface heat discharge pattern was made by the author (HASE, 1971) utilizing individual heavy snowfalls as calorimeters during Nov. 30th to Dec. 2nd, 1970 at the southern slope of the spot ( $8,000\text{ m}^2$ )(see Fig. 4). Many people have noticed that snowfalls at a geothermally anomalous spot melt in relation to heat discharge and WHITE (1969a) first tried a quantitative measurement of the total heat discharge by snowfalls at the geothermal grounds in Yellowstone National Park, the United States. The same kind of measurement in Japan was first done by SEKIOKA and YUHARA (1970) at Hakone, Japan.

The boundary between a bare ground and snow covered surface which is called the snow line is mapped as a time function, so that iso-heat discharge contour lines are drawn and the amount of total heat discharge is calculated calorimetrically using snowfalls on the thermally insulated plate put adjacent to the anomalous spot. For an area of very high heat discharge this method can not be applied because of no snowfalls, and the amount of low heat discharge is excluded from the mapping due to the considerable error expected. But this method is considered one of the most effective and non-instrumental way of obtaining the amount of total heat discharge and the distribution which is difficult and requires much time.

During the period of the snowfall calorimetric survey, 20 cm thick heavy snowfalls mostly within 24 hours were recorded without considerable wind effect which favored the mapping condition. The result of measurements is shown on the heat discharge map, which has two iso-heat discharge contour lines of 800 and  $1,320\text{ }\mu\text{cal/cm}^2\text{ sec}$  and two other qualitative sub-contour lines (Fig. 5).

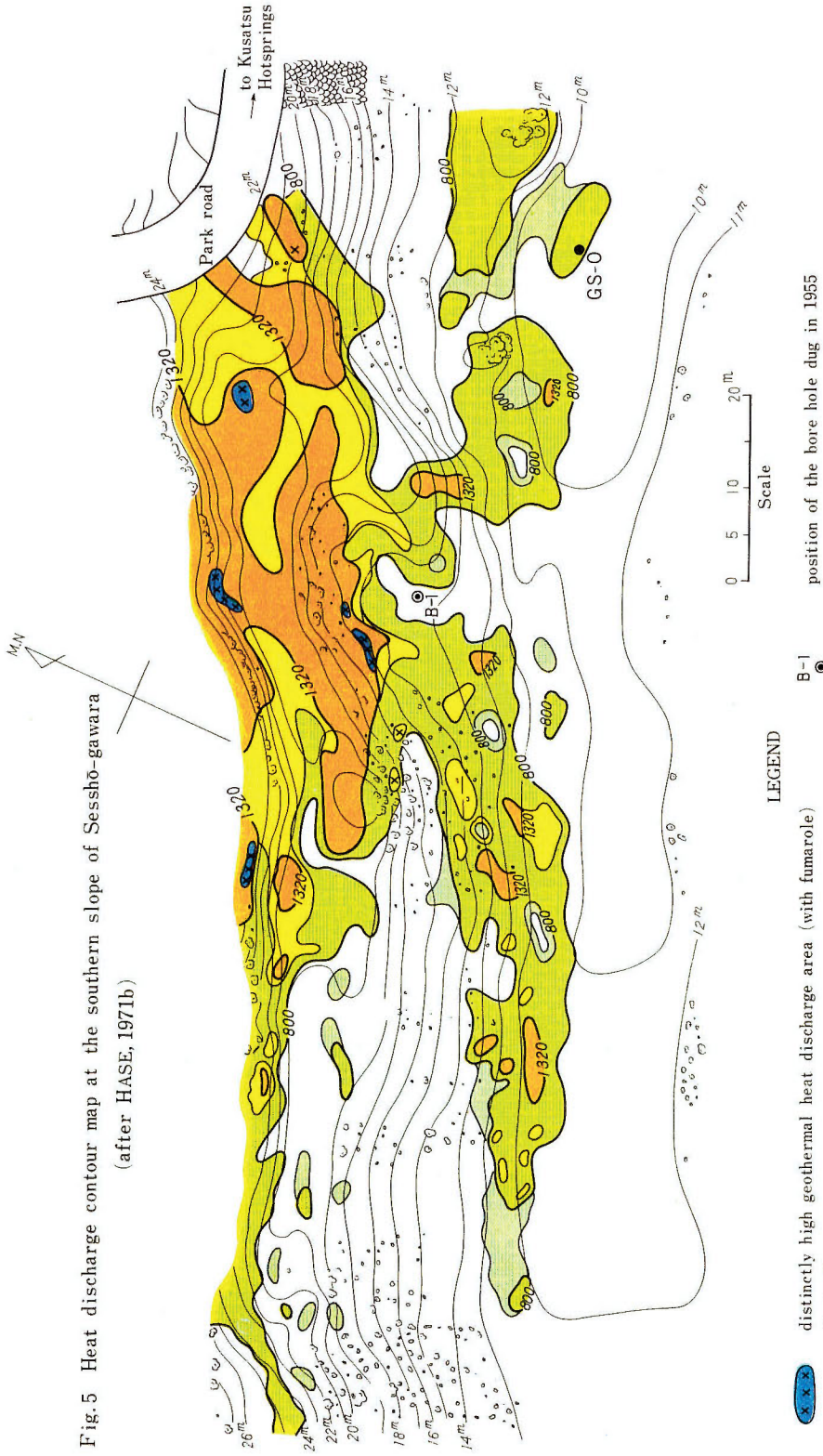
The map indicates that the intensive geothermal heat discharge at Sesshō-gawara is along the narrow linear zone, the result, however, was unexpected because of the porous characteristics of the Sesshō Lava. This fact may suggest that the heat discharge at the spot is along the fracture zones as is discussed in the next chapter.

Preceding the snowfall calorimetric survey, shallow subsurface temperature measurements were done at 12.5 m by 5 m intervals over the same area and the result of measurements at noon of Nov. 27th to 29th was averaged as shown on the shallow underground (10 cm depth) temperature contour map (Fig. 6). This map shows good correlation with the snowfall heat discharge map in view of the thermal distribution pattern but is less effective to know the linear thermal distribution pattern.

### II.2.2 Karafuki

The spot is a part of the Manza geothermal area and is situated geographically at an elevation of 1,700–1,800 m above sea level. The summit craters area of Shiranesan is about 2 km to the east. Another face of the area is a well known winter skiing resort, and several hotels and inns,

Fig. 5 Heat discharge contour map at the southern slope of Sesshō-gawara  
(after HASE, 1971b)



LEGEND

- distinctly high geothermal heat discharge area (with fumarole)
- area of heat discharge greater than 1,320  $\mu\text{cal}/\text{cm}^2 \text{sec}$  (measured on Nov. 30, 1970)
- area of heat discharge  $x < 1,320 \mu\text{cal}/\text{cm}^2 \text{sec}$  (x is obtained from the sub-snow line contour measured on Nov. 30, 1970 ;  $800 \mu\text{cal}/\text{cm}^2 \text{sec} < x < 1,320 \mu\text{cal}/\text{cm}^2 \text{sec}$ )
- area of heat discharge greater than 800  $\mu\text{cal}/\text{cm}^2 \text{sec}$  and smaller than 1,320  $\mu\text{cal}/\text{cm}^2 \text{sec}$  (measured on Dec. 2, 1970)
- area of heat discharge  $y < 800 \mu\text{cal}/\text{cm}^2 \text{sec}$  (y is obtained from the sub-snow line contour measured on Dec. 2, 1970 ;  $y < 800 \mu\text{cal}/\text{cm}^2 \text{sec}$ )

B-1 position of the bore hole dug in 1955

\* the contour line of the topographic map was drawn deciding the position of the base point GS-O to be 10.0m





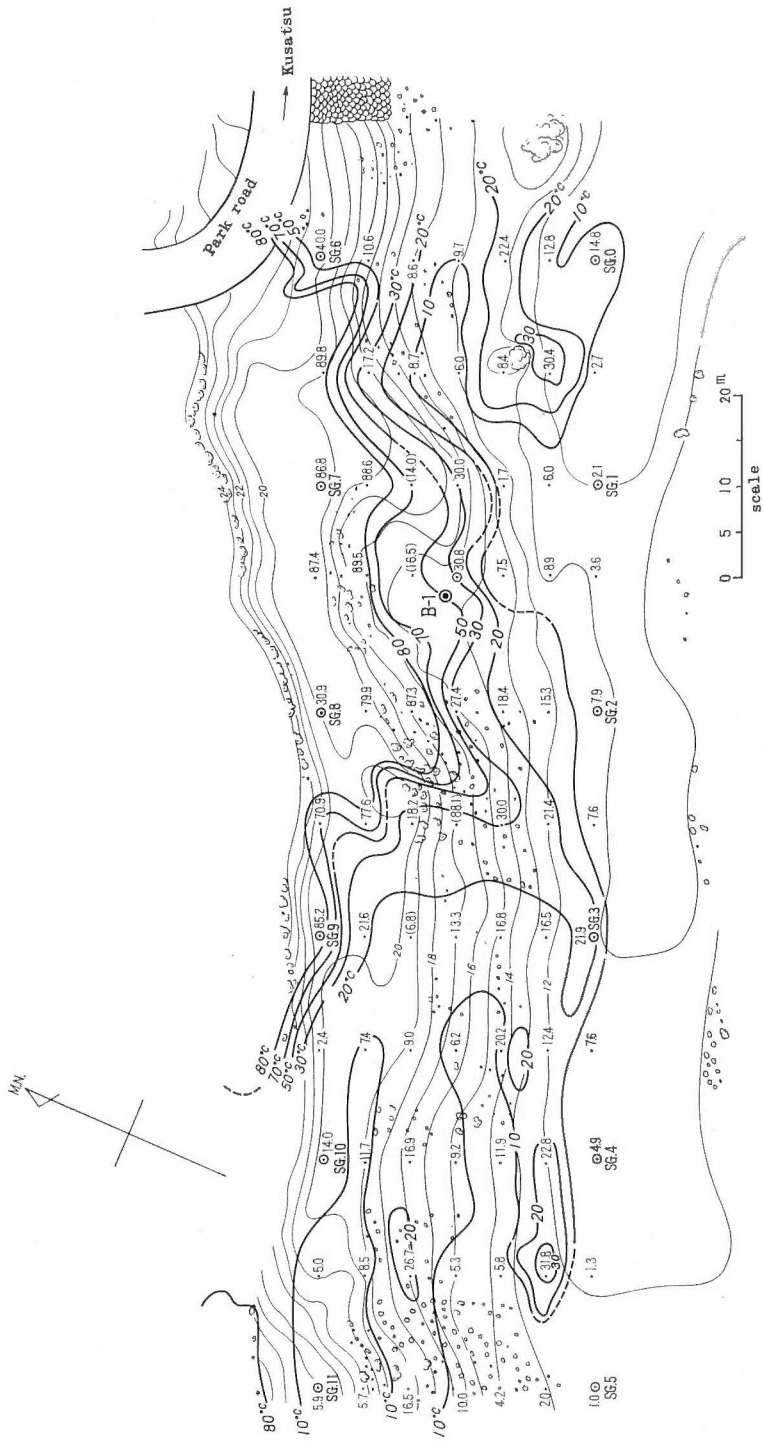


Fig. 6. Noon time shallow underground (10 cm) temperature contour map of the southern slope of Sesshō-gawara (after HASE, 1971b).

the oldest of those is said to have been opened retroactive to 1875. Almost all of the geothermally anomalous spots are seen within 1 km distance along the upper course of the Manza River and its tributaries, the Nigayusawa and the Hoshozawa creek (refer to Fig. 18).

The rocks cropping out in the area are of the Plio-Pleistocene Takai Lava which consists of massive altered pyroxene andesite lava. The rocks encountered hydrothermal alteration change into green color due to the bearing of chlorite and have partly undergone secondary silicification. Another characteristics of the Takai Lava is the development of fracture systems.

Strongly altered geothermal spots lack surface vegetation, and these merge into areas with shrubby bamboo grass to densely vegetated tall conifer and birch forest. Small outcrops of limonite deposits which were formed as the result of groundwater seepage containing volcanic water are seen along the river.

The Manza geothermal area has once been an object site for a geothermal power generation plant and preliminary ground survey was done in 1954 by the Chubu Electric Co. But the plan was interrupted for several reasons including the problem of high acidity of the hot spring water there.

Karafuki is one of the major geothermal spots characterized by fumarole and steam dominated-hotground. But the groundwater level at the spot is near the surface. The spot is distributed along the northern slope of the Hoshozawa creek 300 m upper stream from the junction of the Manza River. This slope shows a typical landslide topography characterized by horse-shoe-shaped steps and wavy surface pattern parallel across the slope. The bottom of the slope, 500 m in width, faces the creek. Intensive geothermal anomaly is seen at the central core part where the basement Takai Lava is cropping out, but the rock mass seems to have slid down to some extent (*Pl. I-I*).

The rock surface of the Takai Lava is coated with reduced free sulphur and most fractures developed in the lava are filled with sublimated sulphur of yellowish white to grayish yellow in color. The most intensive geothermal manifestation is seen in the sublimated sulphur zone and two fumaroles and other feeble vaporish grounds are observed in the zone. Surrounding the central core part, there is a strongly altered bedrock zone changing into clay. The clayey zone gradually changes outwards into weakly altered soil to non-altered loamy soil.

A number of dead tree stumps definitely over the age of several tens of years are observed at the northern slope surrounding the geothermal spot. Many of the tree stumps are slanted and a large scale landslide activity seems to have taken place in the past not older than several tens of years.

The chemical property of the hot spring water was studied by NAKAMURA and HIRUKAWA (1957) at the spot and according to them, it is characterized by strong acidity and high content of  $\text{Cl}^-$  and  $\text{SO}_4^{2-}$ , and the condensed water of both fumaroles and hot spring water have similarity showing that the spot is strongly affected by underground water with boiling temperature.

A trial study to obtain the geothermal pattern by thermal infrared imagery at the spot was done during Aug. 31st to Sept. 2nd, 1972, using the land-use thermal infrared scanning instrument called the Infra-Eye 501 constructed by the Fujitsu Co. in the same year. The instrument is a portable one and favorable for field purpose. The dimension of the instrument is  $37 \times 23 \times 20$  cm for the optical head and  $20 \times 28 \times 47$  cm for the indicator part, and 25 kg (both for the optical head and indicator part) on total weight. The efficiency of the instrument is: Instantaneous field view of the scanning head is 1.3 m rad. Total field view of a single imagery is  $15^\circ$  for horizontal direction and  $10^\circ$  for vertical direction. An up-to-date liquid nitrogen cooled HgCdTe detector is used covering 8 to 13  $\mu\text{m}$  wavelength region (the description of the thermal infrared imagery is given in the next chapter).

The scanner was set on a terrace in front of a hotel on the opposite side of the Karafuki geothermal spot. The optical head was positioned as perpendicular as possible to the geothermal

spot. The average distance between the optical head and the spot was 200 m and thus a circumference of 26 cm in diameter was recorded as a signal energy power of unit (radiance). The horizontal scanning with sequential sweeping of the instantaneous field view is made by rotating the hexahedral mirror, and the vertical coverage of the lines is made by a swinging plane mirror, thus the unit frame of imagery is generated by two mirror combinations. The frame time of a single imagery is one second. By moving the optical head horizontally and vertically, the total geothermal spot area can be imaged. The imagery of a single frame is shown on the Braun tube in the indicator part and it is photographed using a conventional 35 mm B/W film.

One example of nighttime thermal infrared imagery mosaic is shown (*Pl. 1-2*). This was obtained during the night of Aug. 31st, 1972, between 21:30 and 21:36. The weather condition was calm (wind velocity was less than 2.5 m/sec), cloud cover changed from 20 to mostly 100%, and the air temperature was 18.2 to 17.6°C.

Preceding the imaging test, a surface temperature measurement survey was done traversing the Karafuki geothermal spot. Particularly, surface to shallow underground detailed temperature measurements were made at a part of the isolated geothermal spot seen in the central portion of the imagery mosaic (refer to *Pl. 1-2*). Namely, temperature measurement was made

Table 2. Temperature measurement data at the "center" geothermal spot at Karafuki.

point	temperature in °C (depth in cm)			average temp. gradient	conductive heat flow*	rock, soil
a	36.0 (68.0)	—	—	—	—	loose debris
b	93.2 (75.7)	—	—	—	—	boundary soil/rock
c	38.7 (9.0)	69.7 (43.6)	93.0 (80.0)	0.77°C/cm	3,450	clayey bed rock
d	49.7 (18.5)	66.4 (36.8)	93.2 (76.0)	0.80°C/cm	3,580	do.
e	93.8 (69.0)	—	—	—	—	do.
f	32.6 (16.8)	—	—	—	—	altered soil
g	55.6 (2.0)	71.2 (4.8)	—	5.57°C/cm	24,750	compact bedrock
h	93.8 (8.0)	—	—	—	—	compact bedrock
i	29.4 (7.6)	—	—	—	—	debris, water seepage
j	75.7 (72.0)	—	—	—	—	bedrock (clayey)
k	35.0 (5.7)	51.1 (19.0)	63.0 (40.2)	0.89°C/cm	3,990	do.
l	75.0 (23.2)	90.6 (80.0)	—	0.28°C/cm	1,250	do.
m	62.1 (85.4)	—	—	—	—	do.
n	47.2 (30.5)	75.4 (59.9)	—	0.96°C/cm	4,300	do.
o	40.8 (84.6)	—	—	—	—	do.

\*  $\mu$  cal/cm<sup>2</sup> sec; thermal conductivity value  $4.48 \times 10^{-3}$  cal/sec cm °C measured at Sesshō-gawara by Uyeda and others (1958) was utilized in the calculation.

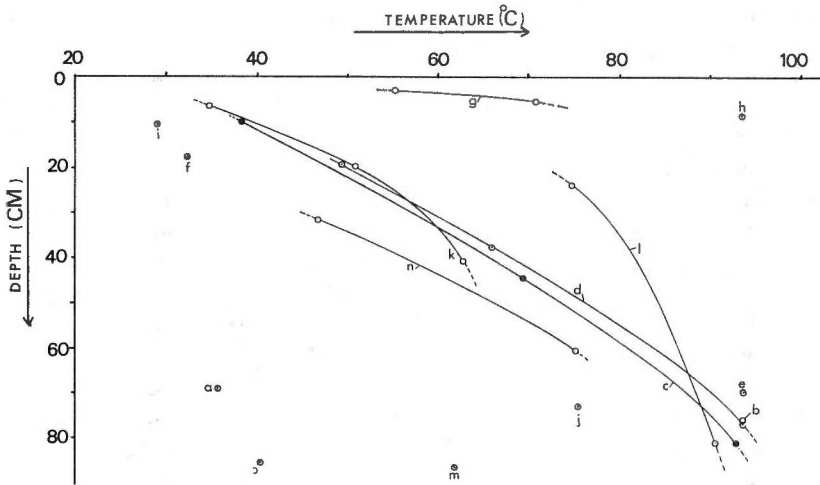


Fig. 7. Temperature vs. depth data of the "center" geothermal spot at Karafuki (refer to Fig. 8, Table 2, and Pl. 1-2).

on three meter grid traverse system making 15 measurement points at the depths of 2 to 85.4 cm from the surface. Conventional mercury thermometers were used for measuring the bottom temperature of the holes dug by a specially made hand auger rod. These temperature data are tabulated (Table 2) and the temperature versus depth curve diagram is shown (Fig. 7).

For the qualitative correlation with thermal infrared imagery and photograph, they are enlarged into approximately equal scale and shown (Fig. 8). Temperature measurement points were marked by red paint and some of them are visible on the enlarged photograph taken for terrain photogrammetry of the spot from the opposite side of the creek. Exact correlation with temperature measurement data and the tonal difference of the imagery is still difficult because the thermal pattern generated by recording radiance from the geothermal surface on the imagery and the tonal change of the photograph recording differential reflectance of the surface materials are different. However we can easily identify the exact distribution of the geothermal anomaly (distribution of surface radiant power) by thermal infrared imagery which is very difficult to obtain by other methods. Most of the "center" geothermal spot manifests distinctly high geothermal anomaly (conductive heat flow measured tended  $1,250-24,750 \mu\text{cal}/\text{cm}^2 \text{ sec}$ ) and thus all the temperature measurement points should appear brighter (higher) compared with background in the nighttime thermal infrared imagery (the explanation is made in later). The geothermal distribution pattern of Karafuki shown on the imagery shows a net type heat discharge pattern recording higher radiant temperature distribution from open cracks including the systematic and nonsystematic fractures developed in the rock mass.

### III. Remote Sensing Data for Geologic Procedures and Results

For an area lacking surface geologic evidence such as the Kusatsu-Manza area, some procedures of analysis are necessary to understand the geologic structure, stratigraphic sequence, and so on. The use of aerial photographs for the purpose may be the most prevalent method. The application of geologic remote sensing data will furnish good and better realistic results.

In this chapter one of the remote sensing methods, aerial thermal infrared sensing is introduced and used to understand the geothermal distribution in view of geologic structure together

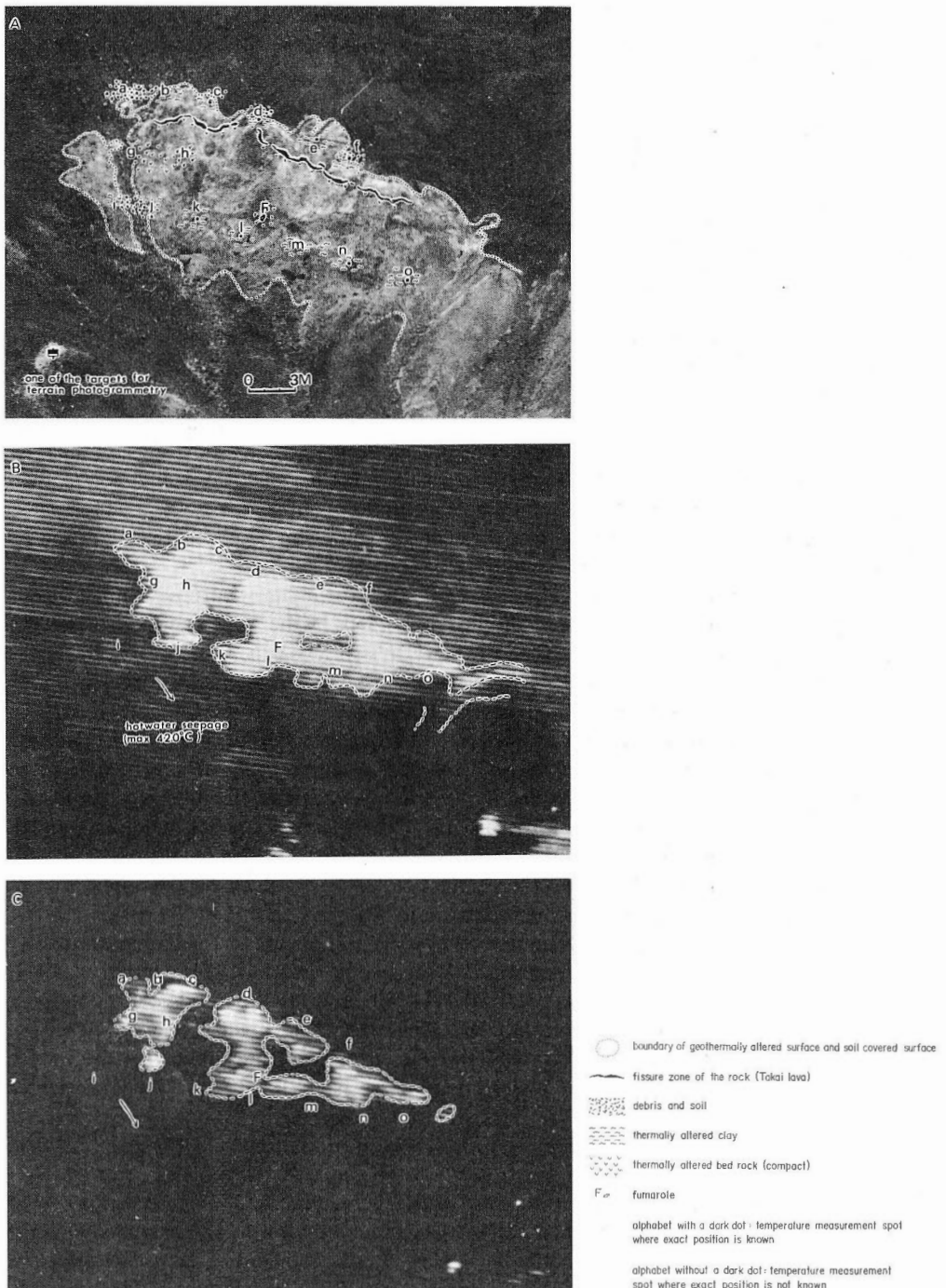


Fig. 8. Correlation figures of temperature measurement point and thermal infrared imagery of the "center" geothermal spot at Karafuki.

- A. Enlarged photograph of the spot
- B. Nighttime thermal infrared imagery of the spot (narrow temperature range imagery)
- C. Nighttime thermal infrared imagery of the spot (wide temperature range imagery).

with aerial photographs. Thermal infrared imagery is still unpractical in Japan and holds many problems and thus the surface heat flow studies for quantitative utilization of the thermal infrared imagery made by the author is introduced.

### III.1 Thermal infrared remote sensing

Study on infrared radiation has a long history retroactive to 1,800 A.D., the first discovery of it by William HARSHEL and numerous studies have been done to date with regard to radiation physics, technology, and application. But the knowledge on the electromagnetic rays in the wavelength region of far infrared portion of spectrum (5.6–1,000  $\mu\text{m}$ ) has been left unknown till the recent. The main reason was the lack of an effective detector sensitive to this wavelength region.

Recent technological progress in semi-conductive materials has made possible the production of high sensitive and fast response quantum detectors effective to far infrared wavelength region covering 8–14  $\mu\text{m}$  "atmospheric window."

All natural objects whose temperature are above absolute zero emit electromagnetic rays and for the surface materials whose temperature are about room temperature, most of the radiant energy are distributed in the 8–14  $\mu\text{m}$ , or in a part of the infrared wavelength region. This region is no more sensitive to photographic emulsions and a quantum detector is used for generating the electric signal in proportion to the radiance (temperature) collected and focused on the detector, in turn, it is amplified and converted into a visible form.

Infrared technology belonged to a secret research field for military purposes until 15 years ago. For earth science's purposes, it was unveiled early 1960s by the American geologists. They were interested in the thermal information of the earth's surface which was treated merely as "background noise" for military purposes, and also the spectral characteristics of rock and rock forming minerals in the thermal infrared wavelength region.

The year 1964 is a remarkable year because several geologic studies based upon infrared rays were reported. The term "Infrared Geology" was first proposed by CANTRELL (1964) and in the same year FISCHER and others certified that the infrared scanner could be adopted for the mapping of geothermal distribution of the volcanic area in Hawaii (FISCHER and others, 1964). Characteristics of minerals and rocks in the thermal infrared wavelength region have been spectroscopically studied by LYON who further concentrated his study on the application of it for the remote compositional mapping of lunar and planetary soils (LYON, 1964).

After these pioneer's works, several papers were published utilizing thermal infrared imagery for the mapping of geothermal distribution (MCLERRAN and MORGAN, 1965; MOXHAM, 1969; FRIEDMAN and others, 1969; PALMASON and others, 1970), and for structural geologic purpose (WALLACE and MOXHAM, 1967). Also surface heat flow studies were made by measuring surface radiance (DECKER and PECK, 1967). In relation to spectroscopic study following the LYON's work, the study was made in view of geologic remote sensing (VINCENT and THOMSON, 1972a and b).

In Japan, the first information of thermal infrared imagery was brought by FISCHER (FISCHER, 1962).

In 1964, the first experimental laboratory use of the thermal infrared imaging sensor named Infravision-I was started by the Nippon Electric Co. Using this sensor, an experimental study of mapping of the geothermal distribution at the test sites of Sesshō-seki, Nasu Volcano, and Owakudani, Hakone Volcano was done by members of the Geological Survey of Japan and the Nippon Electric Co. These tests were successful in obtaining several useful data for both technical development and geologic purpose. It was noticed that the airborne system was more necessary for the full face mapping of the geothermal distribution by a rapid scan, and it was tried at the end of the year using the first airborne thermal infrared scanner constructed by the

same company for geologic and general purposes. Detailed case history of the technical development of Japanese thermal infrared scanner up to 1967 was reported by MATSUNO and others (1969).

Fundamental physics, optics, and technical problems on thermal infrared imagery were introduced by the author (HASE and MATSUNO, 1967; HASE, 1971a).

Today, several private companies own airborne thermal infrared scanners for exploration and environmental purposes in Japan, and thus opportunities are enlarged to utilize them for geologic purpose. The author has been engaged in the study on the application of thermal infrared imagery since 1965. Particularly his study for the time being was concentrated to know the limit of detectable geothermal heat energy in terms of heat flow unit. The result of his experiment may be helpful for the quantitative mapping of other crustal heat energy problems such as the mapping of oxidizing heat energy of sulphide ore deposit and so on.

Temperature measurement surveys have been made so far by using thermometers or thermistors for measuring the subsurface temperature at some depths, say 1 m from the surface, to avoid the diurnal solar temperature fluctuation effect. This method is easy and noninstrumental but time consuming, and temperature measurement points are limited to know detailed thermal distribution (refer to Fig. 8). Complete mapping of geothermally anomalous pattern is desirable particularly for the mapping of the heat discharge from fractures (refer to Figs. 5 and 6 for comparison). Thermal infrared imagery provides us rapid and complete coverage of the thermal pattern at the area concerned. On the other hand, the imagery obtained is that of radiance of the surface which is strongly affected by solar energy. Surface geothermal behavior therefore should be studied first.

### III.1.1 Basic concept on the use of thermal infrared imagery for geothermal purpose

Temperature of the earth's surface is basically solar energy dependent. It may be said that the heat input from solar radiation provides about 99.97 percent of the heat energy required for the physical processes taking place in the earth-atmospheric system (SELLERS, 1965). Solar energy is supplied to the earth's surface with a periodic motion and thus the surface energy level value is variable. Such changes of energy level cause movement of heat energy (temperature fluctuation). There exist three types of temperature fluctuations; the diurnal change, the annual change, and the nonperiodic temperature fluctuation. Two depths can be defined by the two periodic temperature fluctuations. One is the depth affected by the diurnal temperature change and the other is the depth affected by the annual temperature change. Non-periodic temperature fluctuation is local and temporary, and will perturb both waves (and depths) to some extent. Usually we can consider that there is no diurnal temperature change below 70–80 cm from the surface and there is no annual temperature change below 15–20 m from the surface.

The mean diurnal subsurface temperature curve plotted at shallower depth "rides" on the mean annual underground temperature curve. In May, for example, last winter's underground temperature may be observed at 3–7 m depth. Low intensity geothermal heat flow is masked by the annual temperature change or, in other words, signal to noise ratio of the geothermal surface anomaly\* (S/N ratio of the geothermal surface anomaly) is too small to be distinguished.

Factors influencing surface temperature distribution are: 1) Climatologic factors such as wind, evaporation and coagulation, cloud cover, precipitation and frost, temperature change due to rainfall and snowfall with different temperature from ambient temperature, and advective movement of air mass. 2) Microtopographic effect. 3) Physical factors such as heat capacity, thermal conductivity, porosity, water content, density, specific heat, and the difference of emittance. 4) Chemical factor such as photosynthesis. Some of them are minor factors and can

\* S/N ratio of the geothermal surface anomaly may be defined to be the ratio of the surface temperature given by geothermal heat energy (signal) to background normal temperature decided by solar incident energy (noise). This noise level is higher in the daytime and comparatively lower in the nighttime.

be neglected and some others are unusual.

A heat budget equation at a comparatively lower geothermally anomalous ground surface will be written by several principal factors as follows excluding topographic effect.

where

$$I + LE + P = G$$

I: effective outgoing radiation  
 LE: evaporation or coagulation  
 P: heat exchange by forced convection (wind)  
 G: geothermal heat energy

Radiation factor in the equation is the main temperature function in the thermal infrared imagery.

Surface temperature system is interdependently affected by the combinations of many factors cited above, and surface temperature anomaly shown by the comparatively low geothermal energy may be overlooked or on the contrary, temperature pattern resulted from non-geothermal cause may be misinterpreted as geothermal anomaly. Therefore the next considerations will at least be inevitable to conclude anomalously high surface temperature pattern shown on thermal infrared imagery to be geothermal cause. These are: 1) Observation of local cloud cover preventing outgoing radiation particularly at night. 2) The possibility of difference of thermal property of surface materials. 3) The difference of emittance of surface materials which

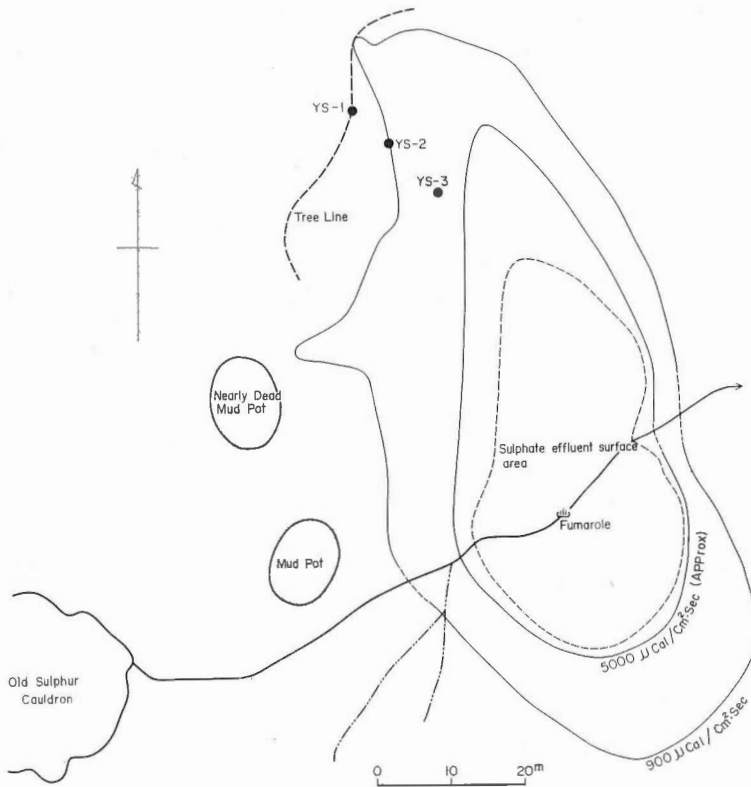


Fig. 9. Temperature measurements sites YS-1, 2, and YS-3 at the heat discharge contour map of the Sulphur Cauldron, Yellowstone, U.S.A. (heat discharge contour by D. WHITE).





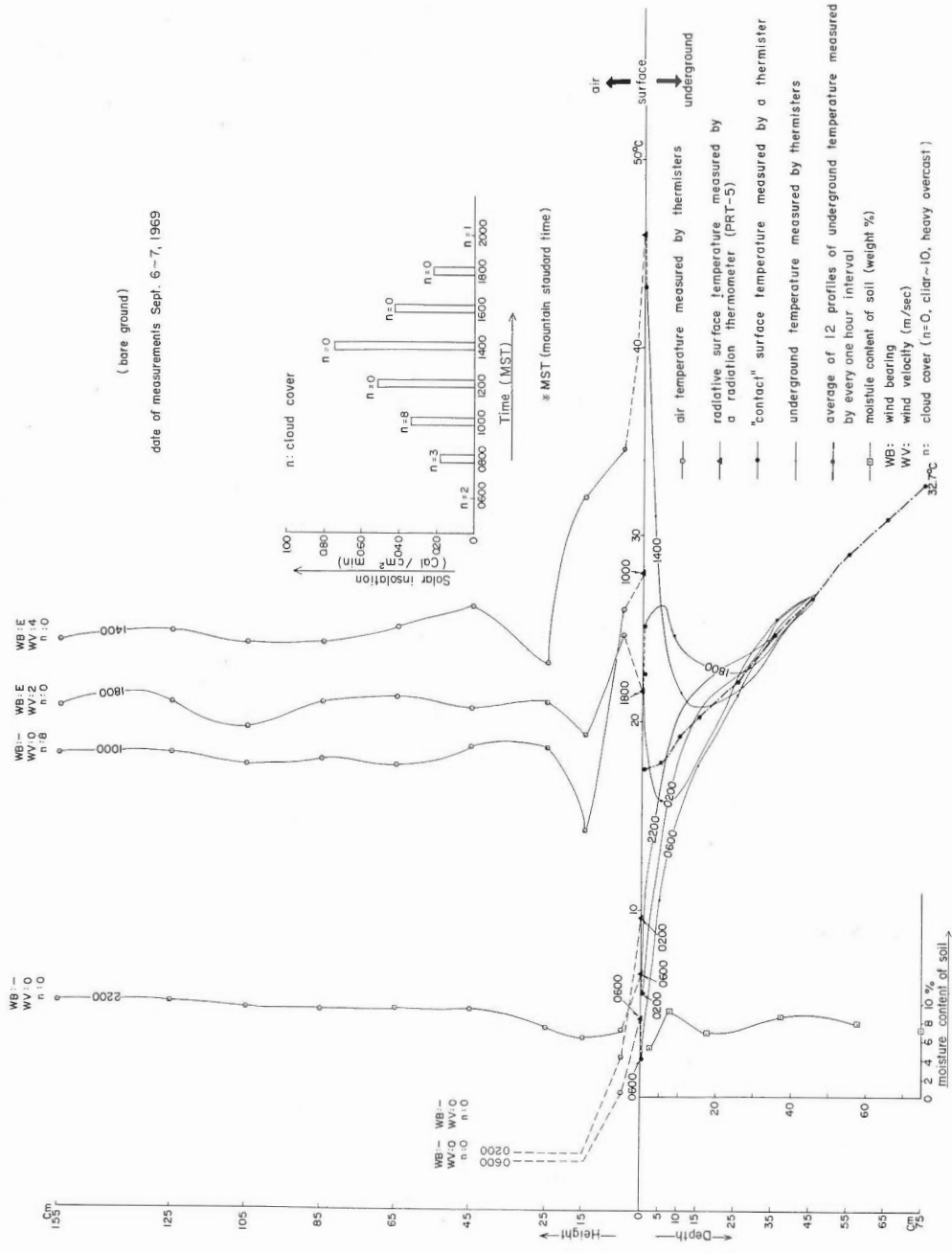


Fig. 11. Tautochrones at YS-2.

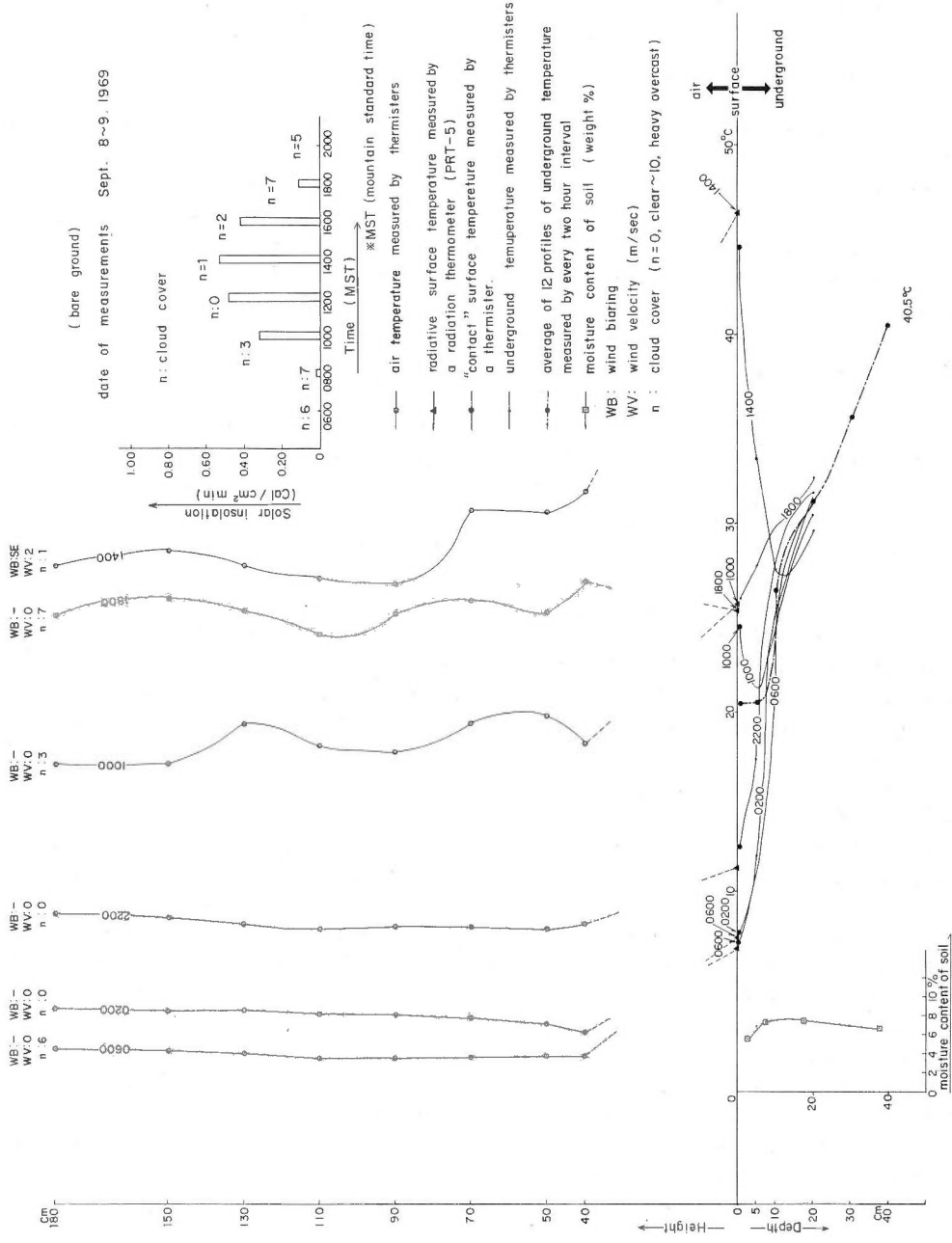


Fig. 12. Tautochrones at YS-3.

gives different radiative temperature for the same "contact" temperature. After these checks, surface temperature anomaly can be resulted in endogenic, or geothermal cause.

For the purpose of the application of thermal infrared imagery for geothermal mapping, some basic studies are very useful (DAWSON, 1964; ROBERTSON and DAWSON, 1964). Surface heat flow studies were made by the author (HASE, 1971a), and classification of the geothermal heat intensity and the experimental results on the detectable limits of geothermal heat energy at the surface in terms of heat flow value were undertaken in the study.

The mean geothermal heat energy of the earth's surface is calculated to be  $1.5 \mu\text{cal}/\text{cm}^2 \text{ sec}$ . On the other hand, the average solar energy absorbed by the earth's surface in the middle latitude ( $40^\circ\text{N}$ , for example) is about  $3,600 \mu\text{cal}/\text{cm}^2 \text{ sec}$ . Taking into the account the diurnal and the annual temperature fluctuation effect, the author classified the geothermal heat energy into three grades. Grade (I) is the geothermal heat energy more than the absorbed solar energy at the surface. Grade (II) is the geothermal heat energy less than the absorbed solar energy at the surface but more than the maximum heat flow intensity caused by the annual solar effect at the depth of "no" diurnal solar fluctuation effect (80–100 cm from the surface), and the third grade (III) is the geothermal heat energy less than the maximum heat flow intensity caused by the annual solar effect at the depth of "no" diurnal solar fluctuation effect. The boundary value of each category is basically a function of latitude.

The author considers that a geothermal heat anomaly categorized into the grade (III) will be difficult to be detected at the surface even in nighttime by the solar masking effect (S/N ratio of the geothermal surface anomaly is too small) and the Grade (II) geothermal anomaly may or may not be detected at the surface.

### III.1.2 Experimental result on the detection of geothermal anomaly

In order to ascertain these interrelationship, an experimental study was made measuring the earth-air interface temperature change at geothermal spots particularly categorized into the grade (II). Some of the results obtained at the geothermal spots of known heat discharge amount at the Sulphur Cauldron area, Yellowstone National Park, Wyoming are shown as the form of tautochrones (GEIGER, 1966) (Figs. 9, 10, 11, 12). Description of field temperature measurements and other examples of tautochrones are shown in the appendices. The heat discharge contour map was obtained by WHITE (loc. cit.) utilizing snowfalls as calorimeters. The unpublished data were provided by him soon after his temperature measurement survey (later this data was published, WHITE and others, 1971).

Through his experiments, he found that the geothermal heat intensity detected as effective outgoing radiation anomaly at the surface had a value (lowest) lying between 300 to  $900 \mu\text{cal}/\text{cm}^2 \text{ sec}$ .

The same kind of study to know the limits of detectable geothermal heat energy was made by WHITE and MILLER (1969b) and PÁLMASON and others (1970). In this study, the author could correlate the snowfall calorimetric survey data at the southern slope of Sesshō-gawara geothermal spot with automatically processed aerial thermal infrared imagery of the spot, and he obtained a result concerning the limit of detectable geothermal anomaly by aerial thermal infrared imagery to be a heat discharge amount much smaller than  $800 \mu\text{cal}/\text{cm}^2 \text{ sec}$ . The result of the analysis of automatically processed data of the imagery enabled us to identify the low S/N ratio of geothermal anomaly which was very difficult with the naked eye. This is discussed further in this chapter.

The results obtained by the above-mentioned studies are tabulated (Table 3).

### III.2 Photogeologic structural analysis

The use of aerial photographs for geologic structural analysis mapping natural features on the earth's surface has been made by many (photo) geologists. These natural linear features

Table 3. Experimental data for the lowest intensity of heat discharge amount.

Name	Year	The Lowest Intensity of geothermal anomaly detected at the surface (heat discharge; $\mu\text{cal}/\text{cm}^2 \text{ sec}$ )	Measurement Site		Reference
			Location Name	Latitude	
WHITE and MILLER	1969	150-500	Old Faithful Yellowstone U.S.A.	44°30'N	Comparison of automatic computer processed data of thermal infrared imagery (8-14 $\mu\text{m}$ , nighttime imagery) with heat discharge map by snowfall calorimetric survey.
HASE	1969	300-900	Sulphur Cauldron Yellowstone U.S.A.	44°40'N	Comparison of the earth-air interface temperature data with heat discharge map by snowfall calorimetric survey (White).
PÁLMASSON and others	1970	200-700	Reykjanes Iceland	63°50'N	Comparison of thermal infrared imagery (4.5-5.5 $\mu\text{m}$ , predawn imagery) with surface temperature data. Heat discharge is assumed applying Dawson's data (1964).
HASE	this paper	< 800	Sesshō-gawara Kusatsu-Shirane Japan	36°40'N	Comparison of thermal infrared imagery automatically processed with heat discharge map by snowfall calorimetric survey. Thermal infrared imagery (4.3-5.1 $\mu\text{m}$ , predawn imagery) was obtained on 19, Aug., 1972.

have been given a unified definition by LATTMAN (1957). His description and usage are made based upon the dimensional character of the natural features derived from his extensive experiences and technical viewpoint of optimum way of observation. According to him, the natural linear features observed in aerial photographs are distinguished into two. One is called a (photogeologic) fracture trace consisting of topographic (including straight stream segments), vegetation, or soil tonal alignment, visible primarily on aerial photographs and expressed continuously for less than 1.6 km (one mile). Only natural features not obviously related to outcrop pattern of tilted beds, lineation and foliation, and stratigraphic contacts are classified as fracture traces. Included in this term are mainly joints mapped on aerial photographs. The other one is (photogeologic) lineament consisting of topographic, vegetation, or soil tonal alignment, visible primarily on aerial photographs or photomosaics and expressed continuously or discontinuously for many kilometers (many miles).

Although aerial photographs themselves reveal only the surface distribution of natural linear features and no genetical or structural geologic informations are shown on them directly, the natural linear features are inherently related to the structural geologic elements as stated by BOYER and McQUEEN (1964). Therefore genetical meanings are better to be added as a basis of definition. It is not necessary to adhere to the definition and the author uses major linear features for longer and distinct fault resulted from natural features and the minor linear features for comparatively shorter minor faults or joints in this paper. The boundary between them is arbitrary.

### III.2.1 Reliability of structural analysis data by aerial photographs

Few geologists suspect that the major linear features are the trace of fault zones, but in case of a minor linear feature, there still arises confusion and suspicion whether it can be attributed to a geologically significant natural feature or not. A minor linear feature is rarely visible except on aerial photographs and therefore the above-mentioned suspicion may be natural.

To find the interrelationship among minor linear features, faults, joints, or fold axes, several photogeologic structural analyses were made (BLANCHET, 1957; LATTMAN, 1957; LATTMAN and MATZKE, 1961). Particularly LATTMAN and his colleague came to the next conclusions (Fracture trace used in their study may be synonymous with minor linear feature in this study).

- 1) Fracture traces, which represent zones of major joint sets in areas of flat to gently dipping rocks but are not parallel to trends of joint sets in areas of steep (greater than 5 degrees) dip.
- 2) Within a small area fracture trace orientations are not the same on rock types that are markedly different. No significant differences in orientation are found on similar lithologic types within a small area.
- 3) Steeply dipping faults may bound areas of different fracture trace orientations. The orientations are, however, relatively constant within blocks bounded by such faults.
- 4) In folded rocks the fracture trace orientations are not affected by local folds but do maintain a constant angular relationship to the regional structural trend.

In Japan, examples of the same type of study in an area, where detailed structural geologic field survey have been made, are lacking. One example of systematic study was made by SHIRAISHI and his colleagues.

As to finding parallelism between the orientation of minor linear features on aerial photographs and that measured in a field, the author recalls an example that different conclusions were obtained by two investigators for nearly the same area in the United States.

BROWN (1961) made a study on photogeologic structural analysis in north-central Texas on two field profiles extending in WNW-ESE and NW-SE direction that traversed the Precambrian to Cenozoic groups (lacking Silurian to Devonian rocks according to his simplified geologic map). Comparison was made between the linear features on aerial photographs and statistically evaluated analysis of joints made at 42 field stations in the profiles, and he came to the conclusion that consistent agreement was not obtained everywhere with aerial photographic map-

ping and field observation particularly with minor linear features. His conclusion claimed further the need for caution when applying aerial photographs for geologic structural analysis. Later, an area of about 480 km<sup>2</sup>, about 40 km southeast of Brown's profile (NW-SE direction) was studied by BOYER and MCQUEEN (1964) in same manner. They found a close parallelism of the measured systematic fractures and linear features on aerial photographs, and their conclusion differed from that of BROWN. They used aerial photographs of the scale of 1:16,200, but the author does not know what scale of aerial photographs was used in Brown's study, and thus direct correlation for the different conclusions may be difficult.

Needless to say, careful observation of aerial photographs for mapping of linear features taking into consideration of lithology, bedding, or rejection of man-made linear patterns, will increase the accuracy of the data, but there are several problems of great concern about utilization of aerial photographs for structural analysis in Japan. These are: 1) Difficulty of structural analysis due to geologic complexity of the Japanese Islands under the condition of arc tectonism in the circum-Pacific mobile belt, which is very different from continental tectonism. 2) Understanding of characteristics of structural geomorphic features formed under much precipitation which causes rapid erosion. 3) Artificial environmental disruption assists destruction of the natural surface feature.

One of the largest problems in use of aerial photographs for structural geologic analysis will be the possible human bias affected by mental effects. The weaker the morphologic character showing linear features or soil tonal and vegetation alignment becomes, the greater the psychologic effect is, and most photogeologists who made structural analysis using aerial photographs refer to this point.

Several photogeologic structural analyses have been made in Japan so far (SHIRAISHI, 1963a, b; SHIRAISHI and others, 1967; KANEKO, 1969; KANEKO, 1970; HASE and NISHIMURA, 1972). SHIRAISHI and others (1967) studied in an area of central Boso Peninsula, Chiba Prefecture. The area is composed of mainly flysch type sediments represented by alternations of sandstone and mudstone of the Miocene to Pliocene, and the regional trend of the folded sedimentary strata is ENE-WSW. Field observation and mapping of the fracture system including joints and faults were made and the result of comparison of them with mapped linear features on aerial photographs showed considerable parallelism between them. Recognition of active strike-slip faults in the Miura Peninsula, south of Tokyo was done by KANEKO (1969) and the result showed good agreement with the field geologic data. These results show aerial photographs serve for rapid regional structural analysis. Will it be possible to use aerial photographs for detailed structural analysis? The use of large scale aerial photographs, for example, 1:10,000 or more will be suitable for a help solving the solution. But aerial photographs should not be used for structural geologic analysis beyond their limits of interpretation.

In general, photographs provide too much information other than we need for our purpose, and the low contrast, subtle linear features, which are geologically significant, are often overlooked from photogeologic analysis due to the presence of the surrounding prominent features (noise), which also become a cause of subjective data by possible human mental bias. Therefore in this study, only the major linear features significantly suggesting faults or fracture zones were mapped by the stereoscopic observation of aerial photographs. The aerial photographs used are approximately of the scale of 1:40,000 taken in November, 1947 and of 1:20,000 taken in May, 1965 (Fig. 13).

### III.2.2 Film sandwich method

The film sandwich method first proposed and used for geologic purpose by WELLER (1970) is an ingenious method in terms of its enhancing effect, simple procedure, and inexpensive way. The film sandwich is formed superimposing the negative transparency over the positive one and then offsetting slightly. The negative transparency is made by the next procedure.



Fig. 13. Index map of aerial photographs used.

Using hard copying lith-type film, the negative film of the aerial photograph concerned is made first, placing the aerial photographic print on the top of the lith-film, emulsion to emulsion in order to prevent light diffusion. After it is developed, fixed, and dried, this negative film is again placed on another lith-film. By the same procedure as making a negative film, a contact positive transparency is made. A pair of negative and positive contact film is prepared for one aerial photographic print. The pair of films is put on a light table one upon the other film, observation is started by making the displacement of the film exactly in one direction. Contact between the areas of different tone remains, and weak linear features, such as soil tonal changes, vegetation alignment, or small straight stream segment are traced by enhanced film lines. An interesting result of creation of man-made shadow effect by the slight offsetting of the film tells us the textural appearance and especially emphasizes the linear features.

Aerial photographs which we use for geologic interpretation or structural geologic analysis are those basically obtained for producing topographic map. Therefore they have very high accuracy and resolution photogrammetrically but on the other hand, photographs obtained show flat tone minimizing topographic shadow for the purpose and we rarely have a chance to see the shadow enhancement of the linear features in aerial photographs taken in winter season. Shadow enhancement by low sun-angle aerial photographs is effective for analysis of geologic structure whose general trend is perpendicular to the sun light direction. Effect of shadow enhancement is remarked by many structural geologists who analyzed side-looking



radar imagery (SLAR) having a radar shadow. For particular structural geologic purpose, low sun-angle aerial photograph was taken making a very high-contrast photograph (LYON and others, 1970b).

Pseudo shadow effect created by the film sandwich method is applicable to the structural geologic analysis enhancing every direction of structural trend by changing the offsetting direction so that it may diminish the cause of the individual human bias which arises extracting subtle linear features. Furthermore, it may be useful for the mapping of minor linear features such as minor faults or joints.

One experimental study applying the film sandwich method with stereoscopic observation of aerial photographs (aerial photographs of approximate scale of 1:40,000 were used) was made (HASE and NISHIMURA, 1972). In this study, correlation analysis with photogeologically

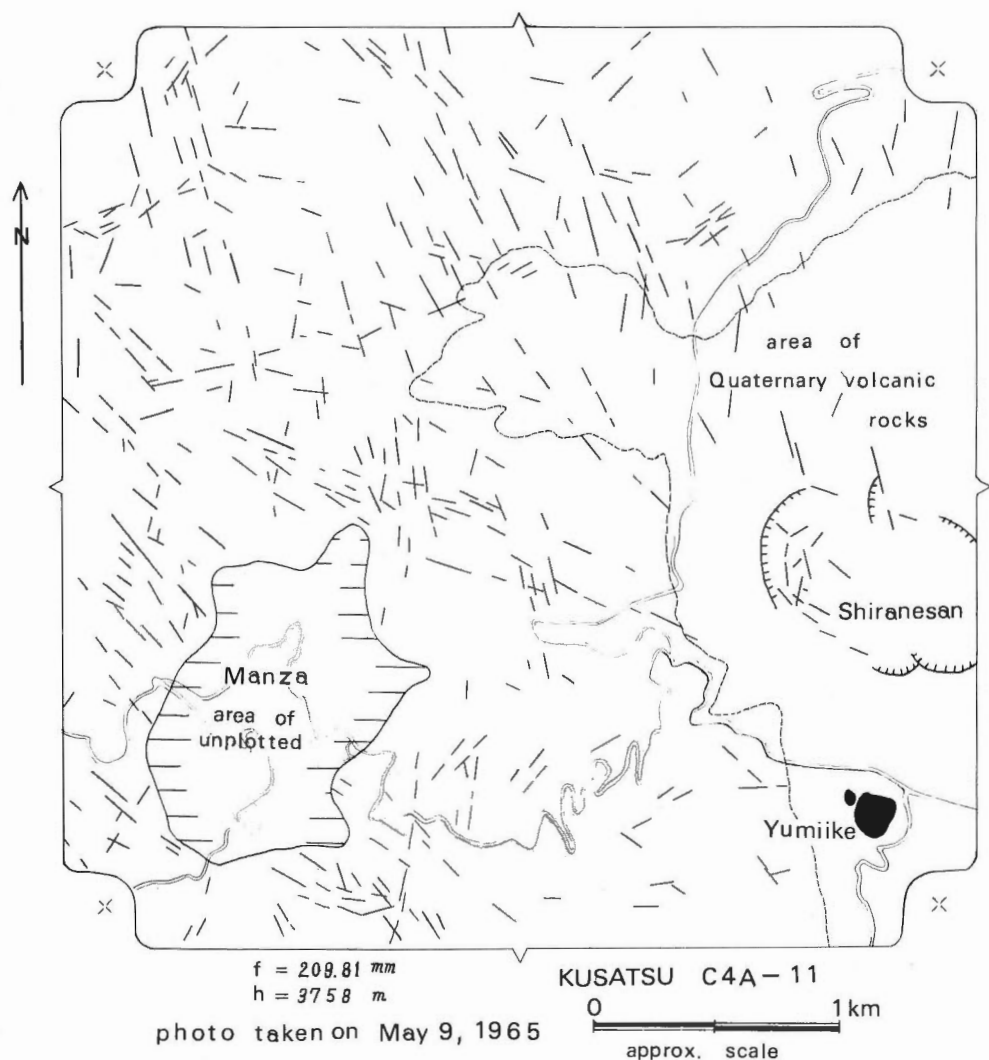


Fig. 14. An example of linear feature analysis by the film sandwich method using 1:20,000 aerial photograph (Hatched area is excluded from the analysis because the surface is artificially deformed).

plotted structural map and field observation data was made in an area in central Izu Peninsula, Shizuoka Prefecture where Miocene "basement" rocks (the Yugashima Group) are cropping out. In the area, a detailed field survey was facilitated by successive road cutting along the sightseeing road under construction (The Odoriko Line). Structural characteristics of the Yugashima Group in the area show the block movement of the basement rock bounded at the margins by steep faults or acute folds. The central area of a faulted block mass is with comparatively gentle dipping (10 to 20 degrees) pyroclastic rocks but they tend to become steep towards the margin. Only one major transverse fault trace running in NW-SE direction could be plotted with certainty by stereoscopic observation for the fault topography. The result of the film sandwich analysis, on the other hand, revealed many fracture concentration zones which were too indistinct to plot by the stereoscopic observation. And by co-utilization of the stereoscopic aerial photographic observation and film sandwich method more realistic data were

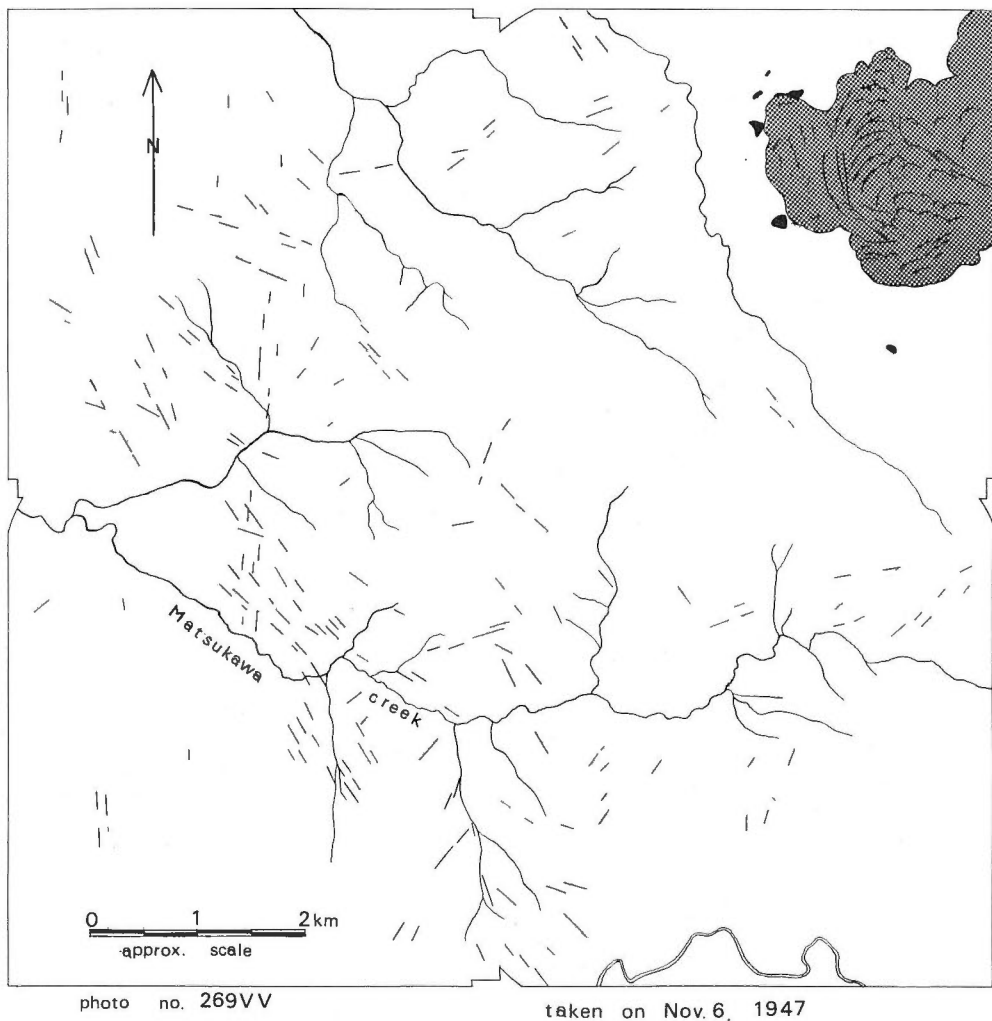


Fig. 15. An example of linear feature analysis by the film sandwich method using 1:40,000 aerial photograph (Stippled area at the northeastern corner shows a part of the distribution of the youngest lava flow of Shigasan).

provided, and thus this method was used in this study. Twenty-five pairs of negative and positive contact films developed from positive aerial photographic paper prints were prepared for the analysis. They include 20 pairs of 1: 20,000 scale aerial photographs and 5 pairs of 1: 40,000 scale aerial photographs, which are shown in the index map (refer to Fig. 13).

Film offsetting was made to horizontal, vertical, and two diagonal directions corresponding to E-W, N-S, NW-SE, and NE-SW directions respectively. Geologically significant linear features observed in each offsetting direction (offset amount 1 mm for 1: 20,000 photos and 0.5 mm for 1: 40,000 photos) were plotted on a tracing paper and finally, they were superimposed on another tracing paper. This procedure was repeated. An example of the plotted result of 1: 20,000 scale aerial photograph at the Manza Hotsprings area (Fig. 14) and also that of 1: 40,000 scale aerial photograph at an area north of the Manza Hotsprings is given (Fig. 15). Aerial photographs of the scale of 1: 40,000 have less resolution at the margin of their frame, and as they were taken in November, 1947, the snowfall season for the higher elevation of mountainous areas, and some parts were covered with snow preventing the observation. Therefore the 1: 40,000 scale aerial photographs were used for subordinate data in this film sandwich analysis.

The minor linear features plotted had the average length of 200–500 m, and the concentration zone of minor linear features was observed for several kilometers. Such zone may be structural geologically more significant and thus the zonal treatment of the linear features was made in this study. No significant differences in orientation of the minor linear features were observed among the Quaternary volcanic stratigraphic units and this may suggest that these rock units should be treated the same as lithologic types structural geologically.

There are marked differences for density or numbers of minor linear features developed between the Tertiary “basement rock” and Quaternary volcanic rocks. It is obvious that the younger the rock becomes the less the number of linear feature develops.

Structural geologic discussions of the data obtained are made in the next chapter.

Some notices obtained through structural analysis by the film sandwich method are as follows.

1) Combination of the use with stereoscopic observation is inevitable because the major linear features represented by dominant topographic features are much better plotted by the stereoscopic observation than by this method. Also artificial linear features are easily distinguished by the stereoscopic observation of aerial photographs.

2) Width of displacement should be decided taking into account the scale of the aerial photographs used (1 mm width for 1: 20,000 scale aerial photograph and 0.5 mm width for 1: 40,000 scale aerial photograph were tested proper, which correspond to 20 m on the ground). By increasing the displacement width, major linear features will be seen, but on the other hand, the minor linear features disappear and are replaced by artificial patterns.

3) In the preliminary trial, the plotting of the minor linear features by the film sandwich method over the same area was made by three persons (the author, a student in the master course of geology, and a student in the senior course of geology). The results showed variety in the numbers plotted but if the result is treated as a zone of concentration, they show considerably good agreement with each other.

4) Artificial misleading vortex pattern, pivoting one side of the film, and also twilled fabrics-type of fine parallel pattern with intersecting angle of 45 degrees in normal horizontal displacement, appear. The latter sometimes may cause confusion.

### III.3 Aerial thermal infrared imagery of the area

Thermal infrared imaging flight in the area was made first on Dec. 18th, 1971. The test flown over a part of the area by the Asia Aerial Survey Co. was a kind of preliminary flight test and hence, a proto-type imaging sensor was used in the flight. For a feasibility study of mapping of

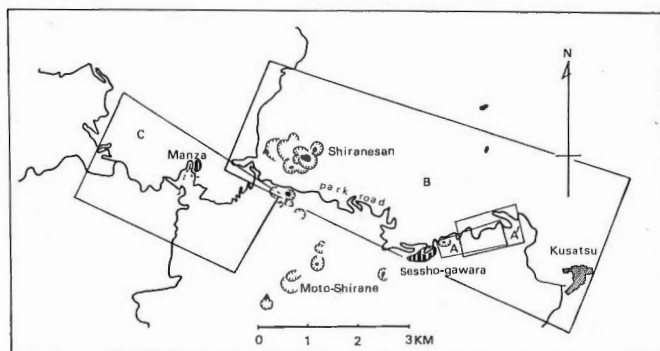


Fig. 16. Index map showing the area covered by aerial thermal infrared imaging flight.

Table 4. Specification of aerial thermal infrared flights.

	Imagery "A"	Imagery "B" and "C"
Date of Flight	Dec. 18, 1971	Aug. 19, 1972
Flight Time	09: 00 JST	04: 05–05: 30 JST
Weather Condition	Fine	Fine
Aircraft	Aerocommander (Twin Engine)	Cesna 206 (Single Engine)
Altitude (to Land)	1, 000 m	1, 600–2, 500 m
Scanner and Detector	InSb ( $\sim 5.5 \mu\text{m}$ )	Jirco, InSb ( $4.3 \sim 5.1 \mu\text{m}$ )
Temperature Resolution (NETD)	$0.4^\circ\text{C}$	$0.2^\circ\text{C}$ at $25^\circ\text{C}$
Instantaneous Field of View	6 mrad.	5 mrad.
Total Field of View	$40^\circ$	$80^\circ$
Reference Data	—	PRT-5 Radiation Temp. (along Center Line)

the geothermal distribution pattern, the Sesshō-gawara geothermal spot was selected. The flight was done in the morning of the day (09: 00 JST) soon after local sunrise of the season. But the result showed that the Sesshō-gawara geothermal spot was unsuccessfully covered by the imagery and a part of the Sesshō Lava east of the spot was barely covered because of the flight problem. Thermal infrared imagery shows a distinct flow structure of the lava which is much better distinguished than the conventional aerial photograph. The reason is due to the large scale of the imagery, and perhaps the low sun angle thermal enhancing effect contrastive higher surface temperature on the sunny side and lower one on the shaded side should be added. In this case thermal shadow may enhance the texture of the aa type of the lava flow (*Pl. 2*) (the area covered by the imagery is shown as "A" and "A'" in Fig. 16).

On Aug. 19th, 1972, another thermal infrared imaging flight was made in the Kusatsu-Manza area by the Nakanihon Kōku Aerial Surveying Co. obtaining the predawn thermal infrared imagery 04: 05 to 05: 30 JST. The imagery successfully covered many geothermally anomalous spots distributed around the summit craters area of Shiranesan, Sesshō-gawara, Kusatsu Hot-springs area, Manza Hotsprings area, and so on (Fig. 16) (Table 4).

Simultaneous ground checking survey could not be done and thus later, a field checking survey was made during Oct. 17–19th, 1972 in the major geothermal spots of the area.

### III.3.1 Interpretation of imagery

(i) Thermal infrared imagery of the Shiranesan—Kusatsu Hotsprings (*Pl. 3*). (the area

covered by the imagery is shown by "B" in Fig. 16)

The general surface temperature distribution pattern at the area is thought to be of comparatively lower temperature at the summit area of Shiranesan and vice versa at the Kusatsu Hotsprings area, reflecting the normal adiabatic humid temperature lapse rate difference of both areas (the altitude of the summit area is about 2,100 m above sea level and that of Kusatsu Hotsprings is about 1,100 m). The background temperature distribution pattern shown as a gray scale in the imagery is correspondent except for the break (abnormally warmer) at the center of the imagery. By checking the scanner and recording system, this pattern was decided to be a ground "anomaly." The rocks of this "comparatively warmer" area consist mostly of the Aoba lava, and one reason of the apparently warmer radiative surface temperature was caused by the more solar energy acceptance over the area by the topographic effect of the steep slope facing the solar insolation direction, and the difference of thermal property or emittance of the Aoba Lava with other lava units (all andesitic rocks) may be negligibly small. The cause cannot necessarily be attributed to non-geothermal surface temperature ruling factors and is thought to be the mixture of both "non"-geothermal and geothermal factors. The water surface temperature of the Mizugama was 9.5°C at the time of checking survey (Oct. 18th, 1972, air temperature 4.1°C at 15:00, fine weather). The water surface temperature of the Karagama was 10.5°C (Oct. 18th, 1972, air temperature 8.0°C at 14:15, clear sky).

On the other hand, the water surface temperature of the Yumiike was 8.5°C (Oct. 18th, 1972, air temperature 4.0°C at 16:00, clear sky), or 1.0 to 1.5°C lower than those of the above-mentioned two lakes but in the imagery the Yumiike is shown as bright as the Yugama, central crater lake containing anomalously high lakewater, though there is no positive sign of geothermal manifestation in and around the lake.

The Karagama is the shallowest (water depth was only about 30 cm at the time of measurement) but the water depth of the Mizugama and the Yumiike is about 1.5 meter. The author does not know why the surface temperature of the Yumiike was of distinctly higher temperature than that of the Mizugama in the predawn imagery taken in August. The Mizugama is encircled by fumarole effluencing geothermal spots on both western and eastern sides of the inner wall whose maximum temperature reached 87.7°C, and thus the apparent geothermal effect seemed to be greater at the Mizugama than at the Yumiike.

The surface temperature of the Yugama showed 14.6°C, being distinctly higher than other two lakewaters. This may be due to the subaqueous geothermal activity at the bottom, and the free sulphur floating is observed at about the center of the crater lake (refer to *Pl. 6*).

The high temperature geothermal anomaly at the summit craters area of Shiranesan, where explosive activities in the past ninety years were concentrated, was detected in the imagery. Particularly several steam issuing vents observed at the northern slope of the outer side of the summit craters were identified as fishhook type of surface geothermal anomaly. Fissure zones, where explosive activities took place in the explosion of 1932, are shown in dark tone of the imagery and no geothermal anomaly is observed there. The southern cusp on the eastern side of the fishhook type of geothermal anomaly is connected with the fissure zones formed in 1932 through geothermally anomalous spots observed on the eastern side of the inner wall of the Mizugama crater-bowl suggesting the existence of a ring type fracture system just outside the summit craters area. In this sense the fissure zones formed by the explosion activity in 1932 on the eastern side of the outer side of the Yugama crater can be said to be a straight segment of the ring type fracture system.

The geothermal anomaly at the summit craters area of Shiranesan is inferred to have been formed, related to the volcano geologic structure to cause ring type fissures at the surface.

In the imagery obtained, Sesshō-gawara is shown as a characteristically high temperature anomaly, and also the hollow at the southern portion of Sesshō-gawara is shown like a shining

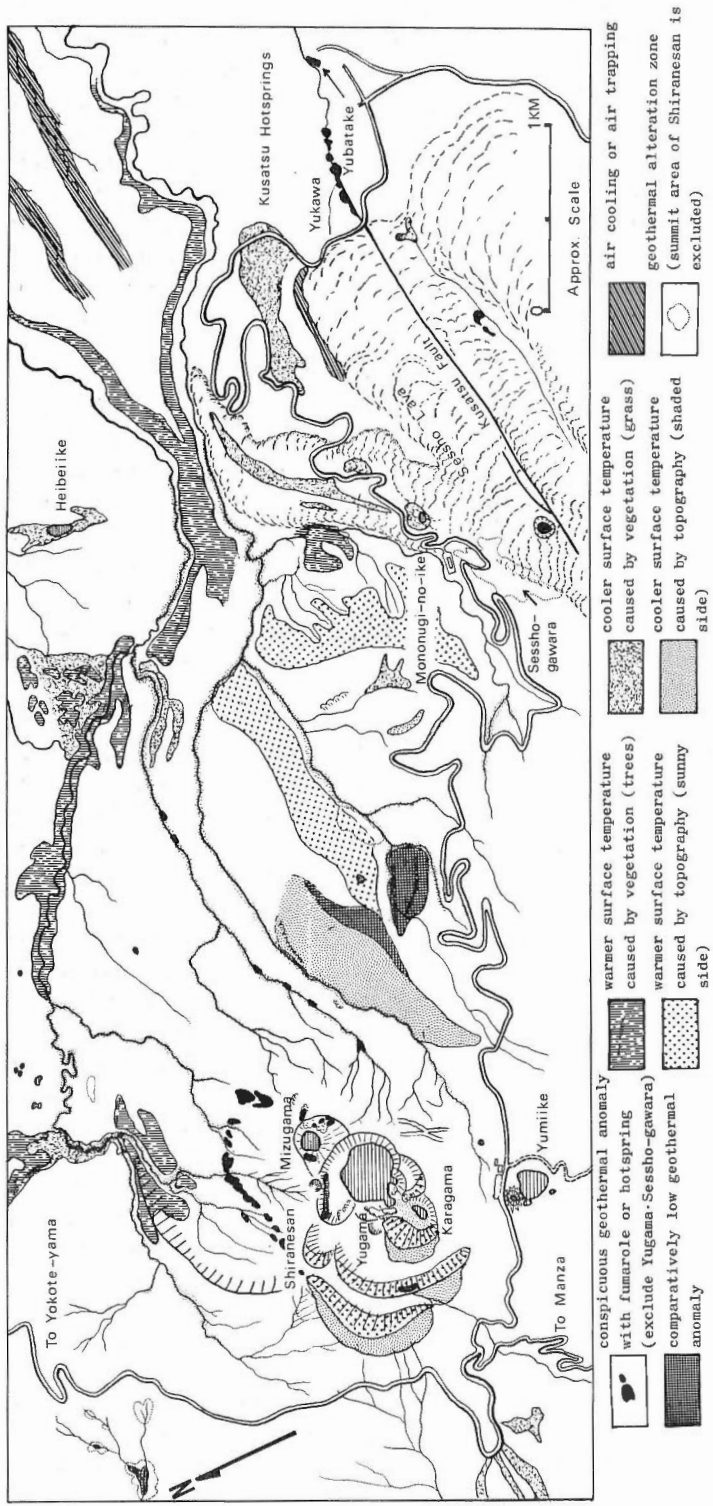


Fig. 17. Explanatory figure of aerial thermal infrared imagery at the Shiranesan-Kusatsu Hot Springs area (refer to Pl. 3 and Fig. 16).

ball by fumarole emitting geothermal activity. The detailed analysis of the geothermal pattern at Sesshō-gawara is made in the next section and omitted here.

The hot springs along the Yukawa (hotspring creek) had temperatures ranging from 62.0°C to 47.3°C (measurement, Oct. 19th, 1972; air temperature 10.8°C at 11:45, cloudy sky). A bright spot seen in the central part of Kusatsu town is a hotwater pool known as Yubatake; natural hotwater is gushing out and its temperature was 67.2°C to 57.0°C (measurement, Oct. 19th, 1972; air temperature 12.8°C at 09:00, cloudy sky).

The lower temperature pattern along the topographic low is thought to be caused by cool temperature air trapping, in turn, by the cool surface temperature. This was suggested through the stereoscopic observation of the aerial photographs, in which the topographic sag or depressions were often observed on the lava flow surface. These topographic characteristics showed good correspondence with the thermally black or thermally cold area in the imagery. Cooled air in the nighttime flowed down along the valley slope often forming a topographically concordant surface temperature distribution pattern. Concrete-topped buildings appear warmer in the nighttime and on the other hand, metal-roofed houses are cooler reflecting the difference of thermal inertia of the materials. The asphalt-surfaced road is a warm radiator in the nighttime. An interpretation of the imagery is shown in the map (Fig. 17).

(ii) Thermal infrared imagery of the Manza area (*Pl. 4*) (The area covered by the imagery is shown as "C" in Fig. 16).

Three major geothermally anomalous spots situated at, the deepest upper stream of the Manza River, the mouth of the Nigayusawa creek, and Karafuki along the Hōshōzawa creek, form foci of geothermal activity at the area (for the name of location, see Fig. 18).

The cliff at the northernmost part of the Manza River manifests a little higher temperature anomaly than that of the surrounding area. The rock consists of altered andesitic lava and its tuff breccia of the Takai Lava, and the outcrop seems to have higher temperature anomaly to some extent though distinct field measurement data are not available. The exposed rocks usually show "normal" surface temperature and are not always distinguished from the adjacent objects in the imagery. It is assumed that there exists some geothermal heat anomaly at the cliff. Geothermal anomaly characterized by the arrangement of hotgrounds at the area has N-S trend, that is to say, it is distributed along the Manza Fault.

A thermal linear pattern is observed extending its trend in NW-SE direction forming a comparatively lower temperature zone. This thermal linear corresponds with a linear feature distinguished in the stereoscopic observation of the aerial photographs. This may be formed by the topographic effect rather than by the alignment of the soil materials resulting from faulting. A hot spring is observed along the zone (see Fig. 18).

The most distinct temperature pattern other than geothermal pattern is caused by the difference of vegetation cover at the area. This vegetation effect is the most distinct surface temperature determined factor in the Manza area, and it exceeds the cool air trapping effect there. Without exception, the grass covered surface (mostly bamboo grass) is always cooler than the tree covered surface in the predawn imagery. For example, the Karafuki geothermal spot seen in the central part of the imagery forming an isolated bright spot, is surrounded by the bamboo grass, and the spot is seen in the thermally dark area.

Geometrical dark linear patterns are the grass covered surface for skiing facilities and skiing slopes. The asphalt-surfaced road is shown as a warmer object but part of the park road which was under construction and not surfaced at the time of imaging flight can not be distinguished from the surrounding objects thermally.

The Manza River is warmer at the northern part of the imagery (upper stream) and the water surface temperature gradually decreases into the surrounding temperature at the southern part (lower stream). The temperature was 54.5°C at the warmest portion and 8.0°C at the coolest

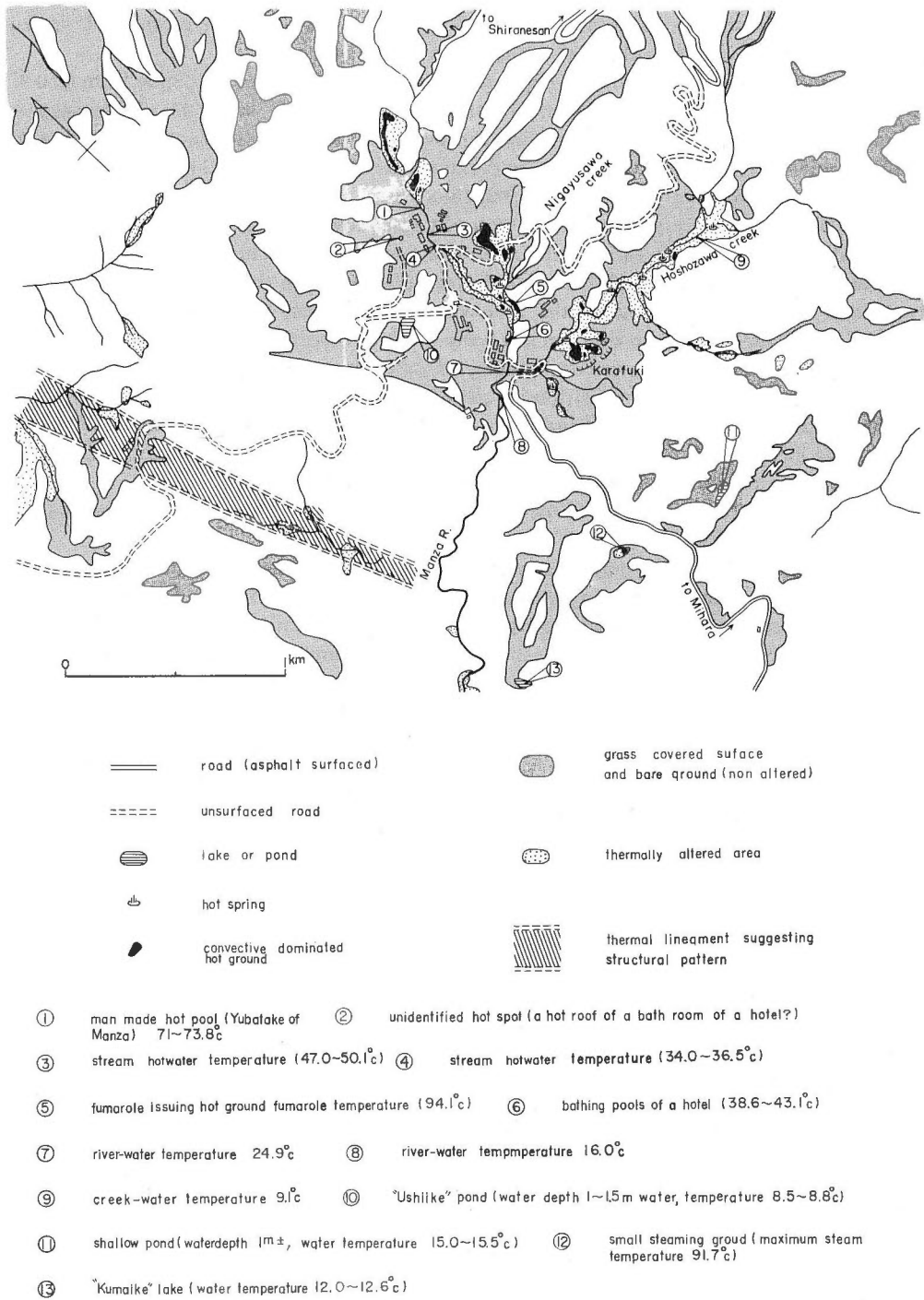


Fig. 18. Explanatory figure of aerial thermal infrared imagery at the Manza area.



measurement point (measurement Oct. 17th, 1972; air temperature 7.8°C at 14:00, cloudy).

The result of the image interpretation is shown in the map (Fig. 18).

### III.3.2 Data analysis by the automatic data reduction system

The obtained aerial thermal infrared imagery has a comparatively wide temperature range on its gray tonal scale (10°C). The objects less than one degree centigrade difference are shown as the same image tonal density at least for the naked eye.

In order to analyze a more detailed thermal distribution pattern, an automatic data reduction system was utilized for the spots of special interest. The system used is called Phosdac 1000 Digital Color System and it was constructed by the Kimoto Co.

The difference of gradual tonal change of the imagery is automatically divided into several density steps (maximally 12 steps are available) and in turn, displayed onto TV screen as a color pattern. The reduced data therefore represent a calibrated "isothermal" map of the area concerned.

Two geothermal spots, Sesshō-gawara and the Yugama crater lake were selected for the analysis.

(i) Sesshō-gawara: As formerly described, the heat discharge pattern and some quantitative heat discharge contour lines are known at the southern slope of the spot (refer to Fig. 5). Comparison of digital color data (Pl. 5) and the heat discharge map were made. The result shows that two rows of sublinear patterns (comparatively hotter pattern) in the central violet color portion may be correlated with the same pattern of the heat discharge map. The geothermal anomaly distinguished from the surrounding temperature pattern extends to the outside of the contour line shown as 800  $\mu\text{cal}/\text{cm}^2 \text{ sec}$ , and thus it can be said that the limitation of geothermal heat energy detected by the aerial thermal infrared imagery at the spot has a heat discharge amount much lower than 800  $\mu\text{cal}/\text{cm}^2 \text{ sec}$ . The result is mentioned in the former section of this chapter (refer to Chap. III-1, and Table 3).

(ii) The Yugama crater lake: Apparent thermal pattern of the water surface of the crater is mono-tonal. However, according to the result obtained from the automatic data reduction system of the spot, a comparatively darker area (black color in the color data) is distinguished at the eastern half of the lake (Pl. 6). This pattern was concluded to be formed by the driftage of the floating free sulphur according to the checking survey (Oct. 18th, 1972). At the time of visit the free sulphur was observed showing a pattern as if it was gushing from the bottom of the central part of the lake and subsequently swept eastward by the westerly wind to make a same kind of distribution pattern as observed in the color data (see Pl. 6).

It is difficult to refer the tonal change of the imagery to the surface temperature difference at this stage. The difference of emittance with water surface and floating sulphur surface may be another cause.

## IV. Interpretation of Structural Control

Structural geologic data obtained from field measurements, stereoscopic observation of aerial photographs, minor linear feature analysis by the film sandwich method, thermal infrared data, and other data are plotted in the structural geologic map (Fig. 19).

Based upon the map, an interpretation of structural control of the area studied, particularly that of the Kusatsu-Manza area is attempted and interrelationship of the geologic structure and surface geothermal anomaly is discussed in this chapter.

### IV.1 Field measurement of the fracture system

Most of the Kusatsu-Manza area is covered with Quaternary volcanic rocks and systematic fractures are less developed than elsewhere. But at the Manza area where Plio-Pleistocene

“basement” rocks named the Takai Lava are cropped out, quite a number of fractures are observed. Measurements of dip and strike of fault and joint planes were made during the field survey. The Takai Lava is of massive andesitic lava and tuff breccia at the area, the bedding

Table 5. Measurement data of fracture system.

Loc. no	Number of Measurements	Place	Formation	Rocks	Dominant Direction of Fracture System
M1	43	Manza, north	Takai Lava	massive andesite lava	NNW-SSE
M2	15	do.	do.	do.	NNW-SSE
M3	37	do.	do.	do.	NNW-SSE, NW-SE, E-W
M4	17	do.	do.	do.	NNW-SSE, E-W
M5	19	do.	do.	do.	NE-SW, E-W
M6	26	Manza, south	do.	do.	NNW-SSE, E-W, ENE-WSW
M7	27	do.	do.	do.	NNW-SSE, E-W
M8	14	do.	Older Shirane Lava	alt. of andesite lava & tuff brecc.	WNW-ESE, NE-SW, E-W
M9	20	Agatsuma Sulphur Mine	Matsuozawa L.	massive andesite	NNE-SSW, NE-SW, E-W
M10	35	Shirane Sulphur Mine	Yatoko Lava	alt. of andesite lava & tuff brecc.	N-S, NNE-SSW, E-W
M11	7	Agatsuma Sulphur Mine	Matsuozawa L.	andesite lava	(E-W, NNE-SSW)
M12	38	Karafuki	Takai Lava	massive andesite lava	NNW-SSE, NW-SE, NNE-SSW
M13	37	Manza, east	do.	do.	NNW-SSE, NW-SE
M14	32	Hoshozawa	do.	do.	N-S, NNE-SSW

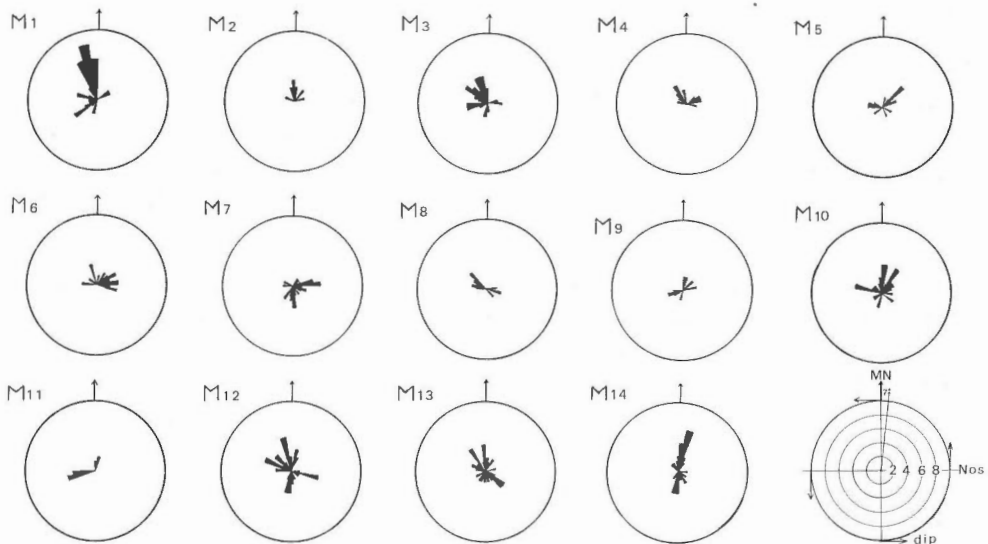


Fig. 20. Field measurement of fractures.

plane of the rock is not known, but the lava seems to have been not so steep dip (perhaps 20 degrees or less) at the area.

Systematic fractures (BADGLEY, 1965) were measured one after another at one outcrop to another by the same manner as HOSHINO and MURAI (1967). The total of 367 measurements was made over the area, mostly (305) in the Manza area and partly (35) at the vicinity of the Shirane Sulphur Mine (Table 5).

The gently dipping fracture system was excluded and only the fractures showing dip angle steeper than 40 degrees were taken into consideration (Fig. 20). It seemed that the fracture system at the Manza area could be subdivided into two areas, Manza north and Manza south, because an E-W trend fault traversed the center of the area and the density of the major linear features observed by aerial photographs were higher at the north than at the south.

With regard to the occurrence of surface geothermal anomaly, the author came to the conclusion that the geothermal anomaly at Sesshō-gawara was formed in relation to the break of the Kusatsu Fault. And one assumption could be deduced that the Kusatsu Fault which cut the Sesshō Lava might be one of a radial fracture system developed in the Kusatsu-Shirane Volcano. Topographically, the Sesshō-gawara is situated at about 1,550 m above sea level and two sulphur mines, the Shirane Sulphur Mine and the Ishizu Sulphur Mine are situated at about the same level. Since sulphur ore is formed strongly related to geothermal activity, those two areas are thought to be thermally active in the near past. The longer axis of the sulphur ore at the Shirane Sulphur Mine trends NW-SE according to the mining company's data, and it reminds us of the development of a radial fracture system as considered at Sesshō-gawara. From the development of the ring type fracture system with thermal anomaly at the summit of Shiranesan it is inferred that the geothermal anomaly at Sesshō-gawara and the development of the sulphur ores of nearly the same elevation along the middle portion of the volcanic body may have been formed at the intersection of two fracture systems. That is, the one is a radial type of fracture system developed centering the summit area, and the other is a ring type fracture system developed at the elevation of 1,550 m above sea level.

From the result of field measurement, however, he could not obtain cogent data to support this assumption. From 35 fracture systems measured at the vicinity of the Shirane Sulphur Mine, two orientations of fracture system were dominant. One trends N~NNE-S~SSW and the other is of E-W direction. The result is not contradictive with his assumption but unfortunately the data are too insufficient.

There is another sulphur mine called the Agatsuma Sulphur Mine about 3 km west of the Ishizu Sulphur Mine (for the location, refer to Fig. 21). This mine is situated at the elevation of about 1,500 m above sea level, but the regional geologic aspect of this location is hard to put on a structure geologically equal to the above-mentioned two locations and for this reason the Agatsuma Sulphur Mine was excluded from the consideration.

The fracture system measured in the field can be classified into three groups (M1, 2, 3), (M4, 5, 6, 12), and (M10), and they are shown as Schmidt net diagram (Fig. 21).

From the result of the field measurements, it can be said that the fracture system developed in the "basement" Takai Lava has two dominant structural trends of N~NNW-S~SSE and E-W in the Manza area. This structural trend shows good correspondence with the photo-geologic structural analysis data. The fracture system developed in the Quaternary volcanic rocks at the southern part of the Kusatsu-Shirane Volcano has trends of NNE-SSW and E-W.

#### IV.2 Lineagenic structural characteristics of the Kusatsu-Manza area

First, a consideration is made on the fracture system as a geothermal heat transfer path.

The main heat source at the geothermal area is thought to exist between a depth from the surface to several kilometers underground. The heat source may sometimes be a melted magma

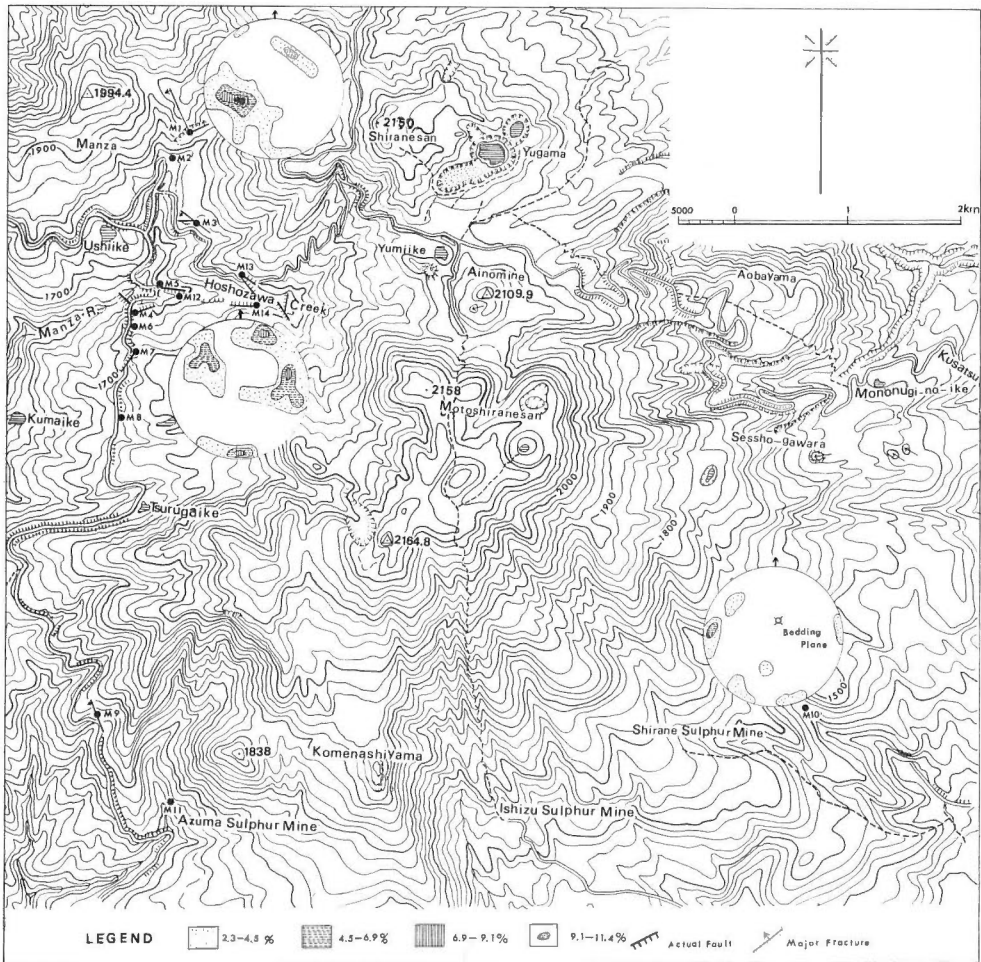


Fig. 21. Schmidt net diagram of fracture system of the Manza area and near the Shirane Sulphur mine.

body itself, an intrusive rock mass with remnant heat energy, or a secondary heat reservoir derived from them. The secondary heat reservoir is defined by the high temperature fluid mass consisting of steam, gases, or hotwater differentiated from the primary magma, and heated groundwater.

A vast amount of geothermal heat energy is transferred to the surface through the open vertical fracture system from the deeper underground. The deep-seated major fracture system as a good heat transfer path may be formed reflecting the regional stress field of the deep underground.

Fractures formed initially in the deep underground are known to be propagated to the surface perhaps by the oscillatory repeating movements of the earth's crust such as volcanic activity, earthquakes and so on. Recently RUMSEY (1971) attested the upward propagation of fractures even in unconsolidated superficial deposits by the observation of many aerial photographs in Canada.

With regard to the regional structural geologic aspect in the Kusatsu-Manza geothermal

area, several discussions on the structural control have been made thus far.

The oldest tectonic movement which might have affected the area is characterized by the supposed northwestern extension of a tectonic line of Mesozoic age called the Kanto Tectonic Line by KOBAYASHI (1941) or the Tonegawa Tectonic Line by YAMASHITA (1957).

According to YAMASHITA's tectonic map of Japan (1957, p. 3), this tectonic line trends WNW-ESE and its northwestern end seems to attain beneath the position of the Kusatsu-Shirane Volcano and extends in east southeastern direction traversing the northern margin of the Kanto Plain. However, from the result of the regional lineagenic characteristics obtained from this study, arrangements of linear features parallel to or subparallel to this tectonic line are indistinct in the area.

It is clear that the post Mesozoic regional geologic movement of the middle Tertiary Green-tuff tectonism gave great influence on the structural control in the area. As is stated before, the Central Uplift Zone proposed by IJIMA extends in NE-SW direction in the area. He proposed the existence of a tectonic line called the Suwa-Tokamachi Tectonic Line which stretches along the center of the uplift zone with the same trend in the area. He considers that the volcanic, geothermal, and hot spring phenomena in the northern Fossa Magna region is related to the uplift zone which forms a culmination zone of igneous rock intrusion.

In the Kusatsu-Manza area, the most dominant structural trend related to the Green-tuff movement is NE-SW. One of the "basement" rock units, propylites crop out at the elevation of about 1,700 m on the northwestern side of the Kusatsu-Shirane Volcano, on the other hand, the same rock facies on the eastern and southeastern sides of the volcano are observed to crop out at the elevation of about 1,100 m or 600 m lower than that of the northwestern side of the volcano. This vertical discrepancy is thought to be caused by a major fault with trend of NE-SW, running along the northwestern side of the volcano. OTA (1957) concluded that the arrangement of the summit craters of Shiranesan (the Mizugama, the Yugama, and the Karagama from north to south), and the arrangement of geothermally anomalous spots at Sesshō-gawara and its vicinity reflect the structural trend developed in the basement rocks. OTA and MATSUNO (1970) remarked that distinct difference can be observed on the arrangement of the linear features between the area of the northwestern and the southeastern half of the area. That is, they claimed that the southwestern side of the volcano was characterized by linear features with ENE-WSW and NNW-SSE trends and on the other hand, that the northwestern side of the volcano was characterized by those of E-W and N-S directions.

From the author's photogeologic structural analysis, he considers that the regional lineagenic characteristics in the region of the eastern part of the Chikuma River, northern Fossa Magna region is shown by the arrangement of linear features with NW-SE direction, and the linear features of NNW-SSE and N-S trends are a kind of diverged linear feature trend from the regional one. Structural geologic characteristics represented by the lineagenic characteristics did not show the orientation parallel to the uplift zone (NE-SW) but a direction perpendicular to it.

Interrelation of surface geothermal anomaly and structural control should be discussed in more local sense but unfortunately no cogent conclusion showing the similarity of regional structural control and surface geothermal anomaly could be obtained.

### Conclusion

A geologic remote sensing study was made in the Kusatsu-Manza geothermal area, situated in the volcanic region of central Japan. The area consists mostly of the Neogene Tertiary "basement" rocks and Quaternary volcanic rocks. Thermal activity is one of the most distinct characters of the area.

As one way of approach for understanding the geothermal system, structural geologic analysis was done to find the interrelation between geologic structure and geothermal activity. Photo-geologic analysis utilizing the film sandwich method as well as a conventional analytical method was done and thermal infrared imagery was applied for the purpose. The use of thermal infrared imagery is the practical outgrowth from photogeology, but the data interpretation is still experimental rather than an established method and these remain many thermal factors to be solved. Therefore the consideration and experiment for the quantitative analysis of thermal infrared imagery for the detection of geothermal anomaly are included in this study.

The conclusion obtained through this study is as follows:

1) The result of photogeologic structural analysis using 1 : 20,000 and 1 : 40,000 scale aerial photographs on the eastern district of the Chikuma river, northern Fossa Magna region shows the existence of regional arrangements of linear features with a general trend of NW-SE. The general trend however becomes indistinct in the area occupied by the volcanic body of the Azumaya Volcano and Kusatsu-Shirane Volcano, and is replaced by the linear features with E-W direction.

2) Minor linear features plotted by the film sandwich method and expressed as the concentration zone show good parallelism with the major linear features in terms of the arrangement of the zone whose longer axis corresponds with the general trend of the minor linear features. Zones are often formed at the extension portion of major linear features where the major linear features are not plotted.

3) The geothermal anomaly developed at the northern slope outside of the summit craters area of Shiranesan forms a part of the fissure heat discharge along a ring type fracture system.

4) At the Manza area, the geothermal anomaly characterized by the arrangement of conductive and convective hotgrounds has a N-S trend and a geothermally anomalous lineament formed along the Manza Fault. Similarly, the heat discharge pattern measured at the southern slope of Sesshō-gawara indicates that the pattern is formed by the existence of a fracture system, and is thought to be formed in relation to the break out of the Kusatsu Fault.

5) One of the experimental data to know the limits of the lowest geothermal heat intensity in terms of heat flow unit by thermal infrared imagery was obtained at Sesshō-gawara. According to the automatically analyzed thermal infrared data at the spot, the anomalously high geothermal heat energy distinguished from the adjacent thermal pattern has an amount much smaller than  $800 \mu\text{cal}/\text{cm}^2 \text{ sec}$ .

6) The geothermal heat discharge system particularly shown as hotgrounds has close inter-relationship with the fault and fracture system. Usually it is affected by the development of a local fracture system, therefore detailed understanding of the fracture system is inevitable in this sense.

The application of remote sensing methods can provide effective clue to the ultimate goal. Thermal infrared imagery gave realistic information in this study.

### References

- ANDO, T. (1957): On the Sessho-gawara geothermal spot in Gunma Prefecture. *Bull. Geol. Surv. Japan*, vol. 8, no. 3, p. 131-137 (in Japanese with English abstract).
- ARAMAKI, S. (1968): Geology of Asama Volcano. *Assoc. Geol. Collab. Japan, Monogr.*, no. 14, 45 p. 2 pls. and a 1 : 50,000 geol. map (in Japanese).
- BADGLEY, P. C. (1965): *Structural and tectonic principles*. Harper and Row Co., 521 p.
- BLANCHET, P. H. (1957): Development of fracture analysis as exploration method. *Bull. Amer. Assoc. Petr. Geol.*, vol. 41, no. 8, p. 1748-1759.
- BOYER, R. and MCQUEEN, J. E. (1964): Comparison of mapped rock fractures and airphoto

- linear features. *Photogram. Eng.*, vol. 30, no. 4, p. 630-635.
- BROWN, C. W. (1961): Comparison of joints, faults, and airphoto linears. *Amer. Assoc. Petr. Geol.*, vol. 45, no. 11, p. 1888-1892.
- CANTRELL, L. J. (1964): Infrared geology. *Photogram. Eng.*, vol. 30, no. 6, p. 916-922.
- CHUBU ELECTRIC CO. (1954): *Geothermal power generation plan at the Manza area*, 29 p. (in Japanese, mimeogr.).
- DAWSON, G. B. (1964): The nature and assessment of heat flow from hydrothermal areas. *N. Z. Jour. Geol. Geophys.*, vol. 7, p. 155-171.
- DECKER, R. W. and PECK, D. L. (1967): Infrared radiation from Alae lava lake, Hawaii. *U. S. Geol. Surv. Prof. Paper*, 575-D, p. D169-D175.
- FISCHER, W. A. (1962): The use of photographs and images for geologic procedures. *Japanese Jour. Geol. Geogr.*, vol. 71, no. 2, p. 43-59.
- , MOXHAM, R. M., POLCYN, F. and LANDIS, G. H. (1964): Infrared surveys of Hawaiian volcanoes. *Science*, vol. 146, no. 3645, p. 733-742.
- FRIEDMAN, J. D., WILLIAMS, Jr., R. S., PÁLMASSON, G. and MILLER, C. D. (1969): Infrared survey in Iceland-preliminary report. *U. S. Geol. Surv. Prof. Paper*, 650-C, p. C89-C105.
- FUJIMOTO, H. (1962): *Historical geology-Kanto District*. Asakura Shoten, 357 p. (in Japanese).
- GEIGER, R. (1966): *The climate near the ground*. Harvard Univ. Press, 611 p.
- GEOLOGICAL ASSOCIATION NAGANO PREFECTURE (1962): *Geological sheet map of Nagano Prefecture (1: 200,000)*.
- HASE, H. and MATSUNO, K. (1967): Today's infrared geology and its problems. *Prof. Yasuo Sasa Memorial Vol., Hokkaido Univ.*, p. 675-687 (in Japanese with English abstract).
- HASE, H. (1971a): Surface heat flow studies for remote sensing of geothermal resources. *Jour. Japan Soc. Photogram.*, vol. 10, no. 3, p. 9-17.
- (1971b): Surface heat discharge at southern slope of Sessho-gawara and geologic interrelation. *Bull. Geol. Surv. Japan*, vol. 22, no. 9, p. 461-471, 2 pls. (in Japanese with English abstract).
- and NISHIMURA, K. (1972): An example of study of photogeologic structural analysis using film sandwich method. *10th Annual Meeting, Japan Soc. Photogrammetry*.
- (1972): Geologic structure controlling heat flow systems at shallow geothermal underground. *Prof. Jun-ichi Iwai Memorial Vol., Tohoku Univ.*, p. 489-501 (in Japanese with English abstract).
- HILLS, E. S. (1963): *Elements of structural geology*. Science Paper Backs, London, 483 p.
- HOSHINO, K. and MURAI, I. (1967): Fracture system in Matsushiro area. *Nat. Res. Center Disaster Prevention* no. 5, p. 37-40 (in Japanese with English abstract).
- IJIMA, N. (1962): Volcanostratigraphy and petrology of the eastern part of Fossa Magna (Part I). *Bull. Fac. Education Shinshu Univ.*, no. 12, p. 86-133 (in Japanese).
- (1963): Volcanostratigraphy and petrology of the eastern part of Fossa Magna (Part II). *Bull. Fac. Education Shinshu Univ.*, no. 14, p. 91-122 (in Japanese).
- IWASAKI, J. (1897): Sulphur crystal of Kusatsu-Shirane Volcano. *Jour. Geol. Soc. Japan*, vol. 4, no. 40, p. 142-146 (in Japanese).
- KAKIMI, T. (1971): Depth of fracturing in the earth's crust. *Jour. Geol. Soc. Japan*, vol. 77, no. 5, p. 237-242 (in Japanese with English abstract).
- KANEKO, S. (1969a): Right-lateral faulting in Miura Peninsula, south of Tokyo, Japan. *Jour. Geol. Soc. Japan*, vol. 75, no. 4, p. 199-208.

- KANEKO, S. (1969b): *Structural morphology*. Kokin Shoin Co., 260 p. (in Japanese).
- (1970): Deformation of Hakone Volcano, South-west of Tokyo, Japan. *Jour. Geol. Soc. Japan*, vol. 76, no. 5, p. 247–258.
- KAWANO, Y. and UEDA, Y. (1966): K-Ar dating on the igneous rocks in Japan (IV)—granitic rocks in northeastern Japan. *Jour. Japan Assoc. Min. Petr. Econ. Geol.*, vol. 56, no. 2, p. 41–65 (in Japanese with English abstract).
- KOBAYASHI, T. (1941): The Sakawa Orogenic Cycle and its bearing on the origin of the Japanese Islands. *Jour. Fac. Sci. Imp. Univ. Tokyo, Sec. II*, vol. 5, Part 7, p. 219–578, 48 pls.
- KUTINA, J. (1969): Hydrothermal ore deposits in the western United States: a new concept of structural control of distribution. *Science*, vol. 165, p. 1113–1119.
- LATTMAN, L. H. (1957): Technique of mapping geologic fracture traces and lineaments on aerial photographs. *Photogram. Eng.*, vol. 24, no. 4, p. 568–576.
- and MATZKE, R. H. (1961): Geologic significance of fracture traces. *Photogram. Eng.*, vol. 27, no. 3, p. 435–438.
- LYON, R. J. P. (1964): *Evaluation of infrared spectrophotometry for compositional analysis of lunar and planetary soils—Part II. rough and powdered soils*. Stanford Research Inst., 172 p.
- (1970a): Terms in geologic remote sensing, a condensed glossary, A review draft for the revised edition of the American Geological Institute. *Glossary of Geological Terms*.
- , MERCADO, J. and CAMPBELL JR., R. (1970b): Pseudo Radar. *Photogram. Eng.*, vol. 37, no. 6, p. 1257–1261.
- and LEE, K. (1970c): Remote sensing in exploration for mineral deposits. *Econ. Geol.*, vol. 65, p. 785–800.
- MATSUNO, K., HASE, H. and NISHIMURA, K. (1969): On IR imagery and its application to the mapping of geothermal distributions. *Photogrammetria*, vol. 25, p. 61–74.
- MCLERRAN, J. H. and MORGAN, J. O. (1965): Thermal mapping of Yellowstone National Park. *Proc. 3rd Symp. Remote Sensing of Environment, Ann Arbor, Mich.*, p. 517–530.
- MEINESZ, F. A. V. (1947): Shear patterns of the earth's crust. *Trans. Amer. Geophys. Union*, vol. 28, no. 1, p. 1–61.
- MINAKAMI, T. (1939): Activity of Kusatsu–Shirane Volcano. *Earthquake*, vol. 11, p. 13–34 (in Japanese).
- MOXHAM, R. M. (1969): Aerial infrared survey at the Geysers geothermal steam field, California. *U.S. Geol. Surv. Prof. Paper*, 650C, p. C106–C122.
- NAKAMURA, H. and HIRUKAWA, T. (1957): Geology and hot springs in the Manza thermal area, Gunma Prefecture. *Bull. Geol. Surv. Japan*, vol. 8, no. 1, p. 1–14 (in Japanese with English abstract).
- OHASHI, R. (1914): Report of the geological survey of Kusatsu-Shirane Volcano (I). *Jour. Geol. Soc. Japan*, vol. 21, p. 233–246, 1 pl. *ibid.* (II). p. 277–294, *ibid.* (III). p. 319–324, *ibid.* (IV). p. 359–367, *ibid.* (V). p. 422–441 (in Japanese).
- (1915): Temperature change of Kusatsu Hotsprings. *Jour. Geol. Soc. Japan*, vol. 22, p. 191–202 (in Japanese).
- OTA, R. and KATADA, M. (1955): *Geological sheet map Suzaka (1: 50,000) and its explanatory text*. 54 p. (in Japanese with English abstract), Geol. Surv. Japan.
- OTA, R. (1957): *Geological sheet map of Kusatsu (1: 50,000) and its explanatory text*. 75 p. (in Japanese with English abstract), Geol. Surv. Japan.



- OTA, R. and MATSUNO, K. (1970): Reinvestigation of Kusatsu-Shirane Volcano. *Bull. Geol. Surv. Japan*, vol. 21, no. 10, p. 609-618 (in Japanese with English abstract).
- PÁLMASON, G., FRIEDMAN, J. D., WILLIAMS JR., R. S., JÓNSSON, J. and SAEMUNDSSON, K. (1970): Aerial infrared surveys of Reykjanes and Torfajökull thermal areas, Iceland, with a section of cost of exploration surveys. U.N. Symp. on the Development and Utilization of Geothermal Resources, Pisa, Italy, vol. 2, part 1. (*Geothermics, Special Issue, 2*), p. 399-412.
- ROBERTSON, E. I. and DAWSON, G. G. (1964): Geothermal heat flow through the soil at Wairakei. *N.S. Jour. Geol. Geophys.*, vol. 7, p. 134-143.
- RUMSEY, I. A. P. (1971): Relationship of fractures in unconsolidated superficial deposits to those in the underlying bedrock. *Modern Geology*, vol. 3, p. 25-41.
- SAWAMURA, K., KAKIMI, T., SOGABE, M., KOBAYASHI, I. and HASE, H. (1967): Geology and geological structure of the Matsushiro seismic area. *National Res. Center for Disaster Prevention, Issue no. 5*, p. 3-11 (in Japanese with English abstract).
- SEKIOKA, M. and YUHARA, K. (1970): Heat-flow survey with snowfall calorimeter at Owakudani geothermal area, Hakone Volcano. *Jinetsu (Geothermics)*, no. 25, p. 22-27, 4 pls. (in Japanese with English abstract).
- SELLERS, W. D. (1965): *Physical climatology*. Univ. Chicago Press, 272 p.
- SHIRAIISHI, T. (1963a): Photogeologic studies of the Tamugiyama oil field in Niigata Prefecture (I). *Japan Assoc. Min. Petr. Econ. Geol.*, vol. 49, no. 1, p. 1-21 (in Japanese with English abstract).
- (1963b): Photogeologic studies of the Tamugiyama oil field in Niigata Prefecture (II). *Japan Assoc. Min. Petr. Econ. Geol.*, vol. 49, no. 2, p. 56-66 (in Japanese with English abstract).
- , HOSHINO, K. and OITA, K. (1967): The use of photographs for structural analysis of fracture system. *Prof. Yasuo Sasa Memorial Vol., Hokkaido Univ.*, p. 707-718 (in Japanese with English abstract).
- SHIRANE SULPHUR MINE (1965): General condition of the mine—*Explanatory pamphlet of the Mi i g Co.*
- SURVEY COMMITTEE FOR KUSATSU GEOTHERMAL POWER GENERATION (1955a): *Report on the cooperative survey for geothermal power generation at Sessho-gawara*. no. 1, 52 p. (in Japanese, mimeogr.).
- (1955b): *Report on the cooperative survey for geothermal power generation at Sessho-gawara*. no. 2, 46 p. (in Japanese, mimeogr.).
- TOKYO ELECTRIC Co., CHUBU ELECTRIC Co. and COMMITTEE FOR KUSATSU GEOTHERMAL POWER GENERATION (1955): *Data for geothermal power generation at Sessho-gawara*, 14 p. (in Japanese, mimeogr.).
- TSUYA, H. (1932): Explosion of Kusatsu-Shirane Volcano. *Bull. Volc. Soc. Japan*, vol. 1, no. 2, p. 74-79 (in Japanese).
- (1933a): Explosive activity of Kusatsu-Shirane Volcano after the explosion of Oct., 1932. *Bull. Volc. Soc. Japan*, vol. 1, no. 4, p. 95-97 (in Japanese).
- (1933b): Explosive activity of Volcano Kusatsu-Shirane in Oct., 1932. *Bull. Earthquake Res. Inst., Tokyo Imperial Univ.*, vol. 11, no. 1, p. 82-112, 11 pls.
- UYEDA, S., YUKUTAKE, T. and TANAOKA, I. (1958): Studies of the thermal state of the earth—the first paper: preliminary report of terrestrial heat flow in Japan. *Bull. Earthquake Res. Inst.*, vol. 36, p. 251-273.
- VINCENT, R. K. and THOMSON, F. (1972a): Spectral compositional imaging of silicate rocks.

- Jour. Geophys. Res.*, vol. 77, no. 14, p. 2465-2472.
- VINCENT, R. K. and THOMSON F. (1972b): Recording of exposed quartz sand and sandstone by two-channel infrared imagery. *Jour. Geophys. Res.*, vol. 77, no. 14, p. 2473-2477.
- WALLACE, R. E. and MOXHAM, R. M. (1967): Use of infrared imagery in study of the San Andreas Fault system, California. *U.S. Geol. Surv. Prof. Paper*, 575-D, p. D147-D156.
- WELLER, R. N. (1970): Photo enhancement by film sandwiches. *Photogram. Eng.*, vol. 34, no. 5, p. 468-474.
- WERTZ, J. B. (1970): The Texas lineament and its economic significance in southeast Arizona. *Econ. Geol.*, vol. 65, p. 166-181.
- WHITE, D. E. (1969a): Rapid heat-flow surveying of geothermal areas utilizing individual snowfalls as calorimeters. *Jour. Geophys. Res.*, vol. 74, no. 22, p. 5191-5201.
- and MILLER, L. D. (1969b): Calibration of geothermal infrared anomalies of low intensity in terms of heat flow, Yellowstone National Park. *Abstract Trans. Amer. Geophys. Union*, vol. 50, p. 348.
- , MUFFLER, L. J. P. and TRUESDELL, A. H. (1971): Vapor-dominated hydrothermal systems compared with hot-water system. *Econ. Geol.*, vol. 66, no. 1, p. 75-97.
- YAMASHITA, N. (1957): *Chusei-dai (Cenozoic)*. Part I. Assoc. Geol. Collab. Japan, 94 p. (in Japanese).

## Appendix

Diurnal temperature-change measurements shown in Figs. 10 to 12 were made by recording 20 data points (include contact surface temperature) across the earth-air interface for a profile extending from 150 cm in height in the atmosphere to 80 cm beneath the ground.

The temperature probe used was a 38 mm diameter polyvinyl chloride (PVC) pipe with 230 cm long. The pipe is cut open around 19 pairs of windows on the pipe surface from the top to the bottom in order that 19 free-air thermistors are inserted and fitted in each window position. Space between the thermistors is stuffed with cotton balls to prevent vertical movement of the air within the pipe. All the exposed surfaces of the pipe were painted in golden color so as to minimize both direct and reflected solar radiation. The smooth surface plastic tape is used to make slit windows to evade direct and reflected solar radiation incidence on the above-surface air thermistors during daytime. Nineteen free-air thermistors are led to 20 position leads on a rotary switch box which in turn is connected to a recorder.

A hole was drilled (using "ship's bit" hand-auger of the same diameter) in the unconsolidated surface soil or sand. It takes less than 30 minutes to dig an 80 cm depth hole and the temperature probe is then inserted into the hole. The drilled hole is enlarged to some extent by shock of drilling. An opening between the probe and the hole is therefore back-filled with soil previously dug out. Twenty-four hours was allowed to elapse before beginning the temperature measurements. All thermistors are ascertained to have an error less than  $0.03^{\circ}\text{C}$  at  $0^{\circ}\text{C}$ . Five examples of temperature measurements (tautochrones) at Mono Lake geothermal area, California are shown.

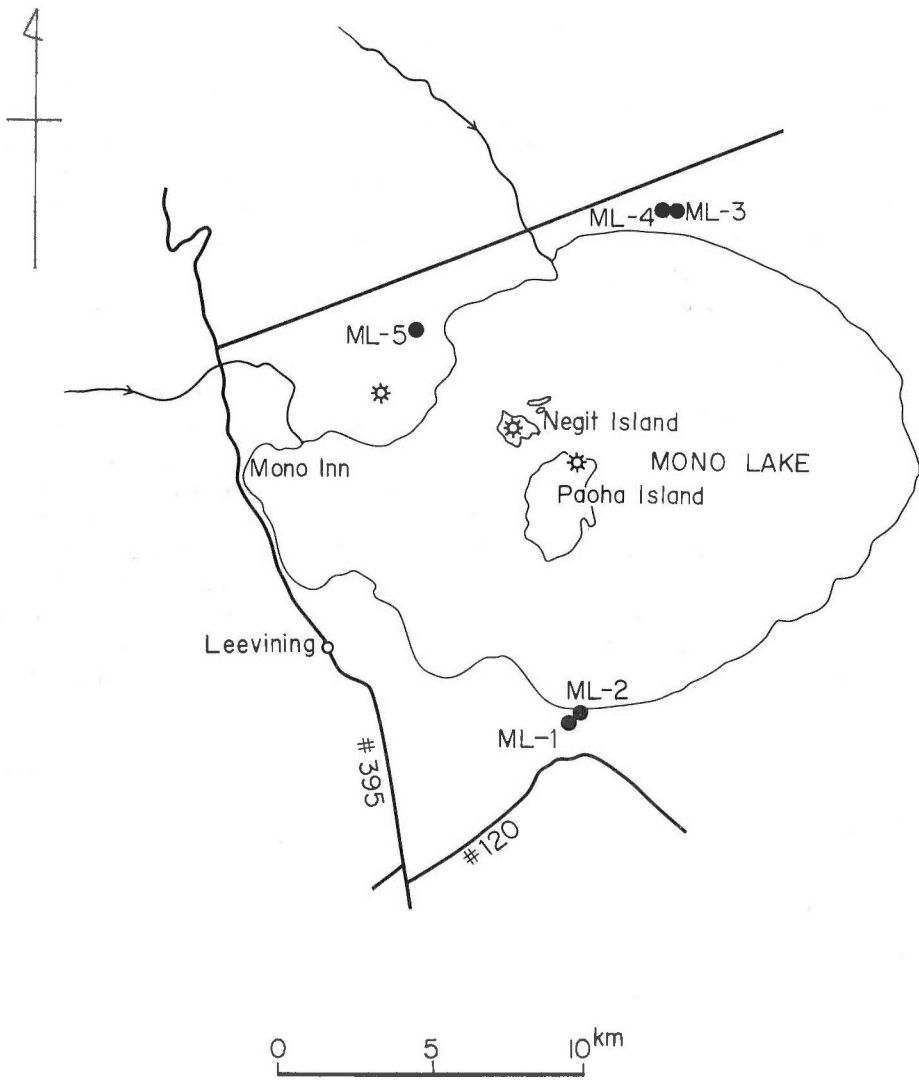


Fig. A-1. Location map showing temperature measurements sites (ML-1~5) at Mono Lake, California.

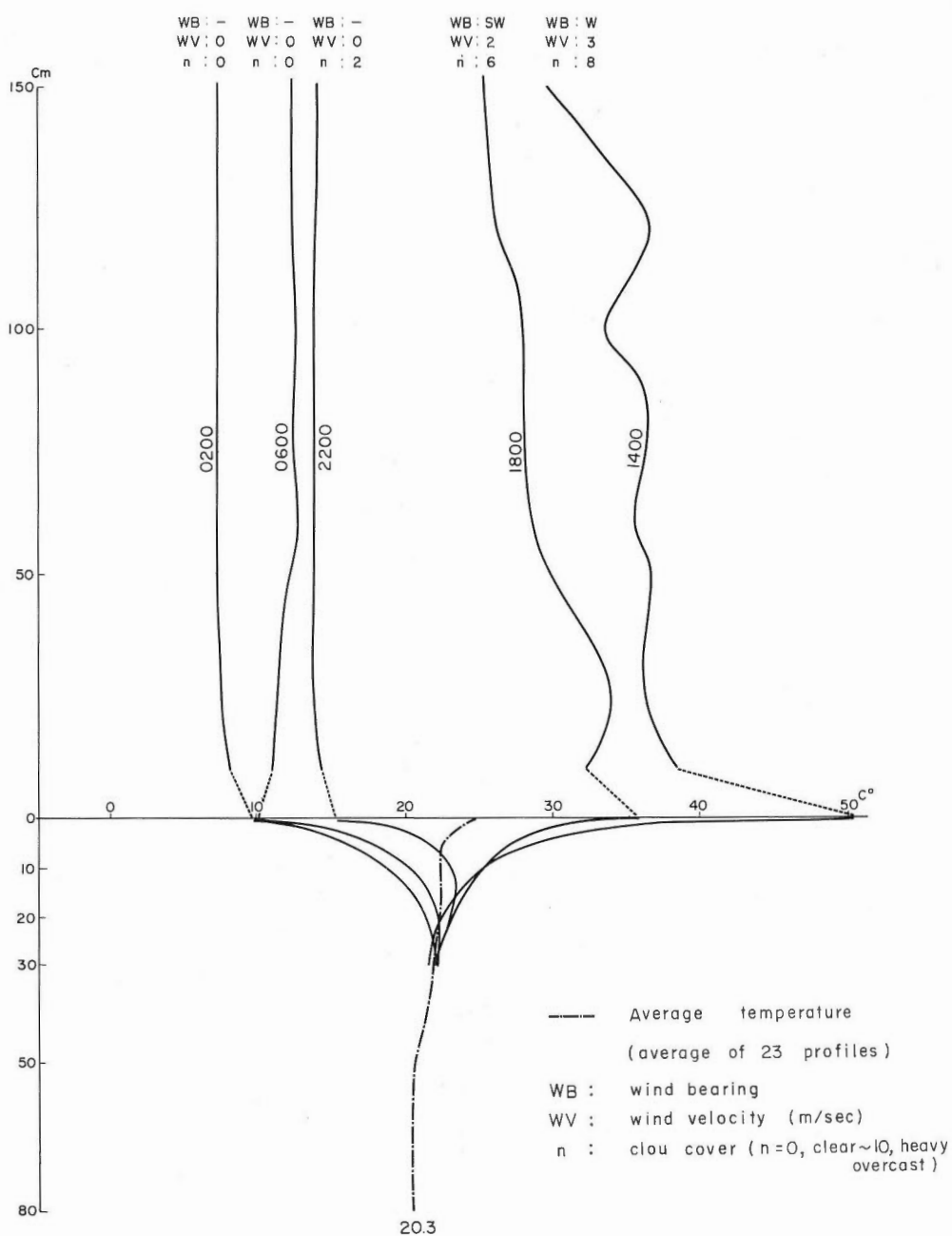


Fig. A-2. The earth-air temperature data at ML-1 "Supposed geothermal" point (rhyolite pumice-sand surface, 1~2 mm grain size) date of measurements June 4-5, 1969.

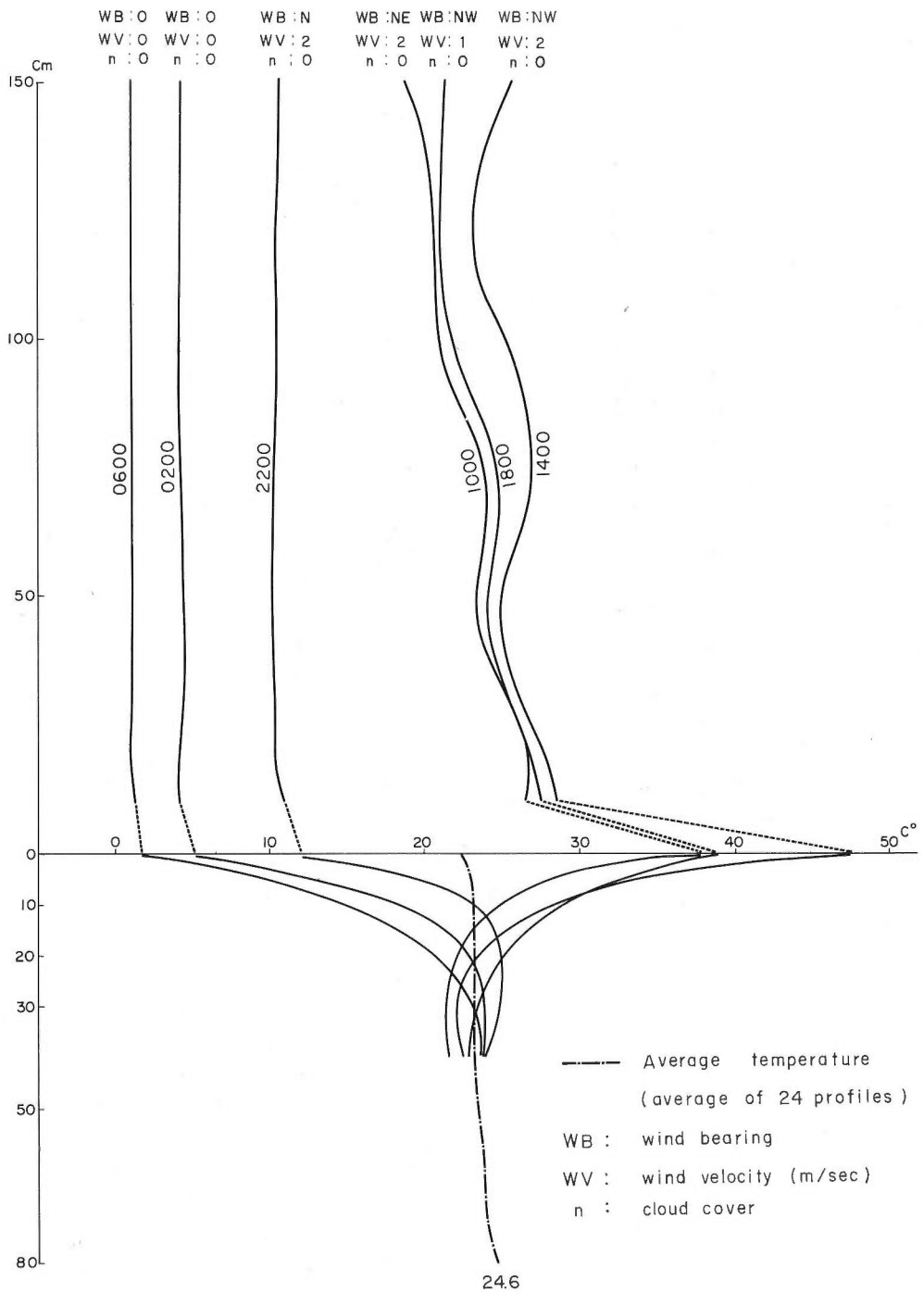


Fig. A-3. The earth-air temperature data at ML-2 geothermal point (rhyolite pumice-sand surface, 1~2 mm grain size) date of measurements May 27-28, 1969.

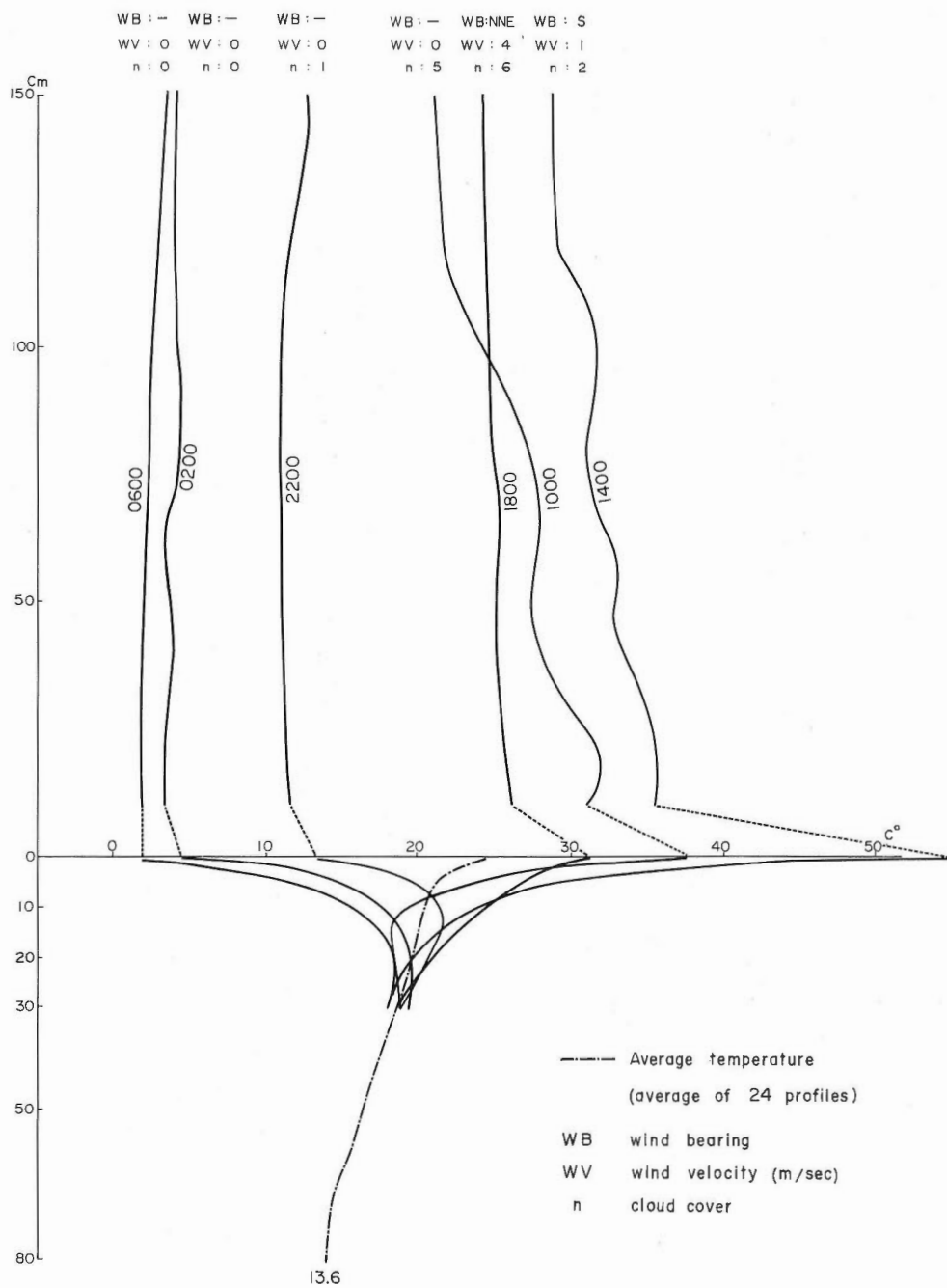


Fig. A-4. The earth-air temperature data at ML-3 "Dry surface" date of measurements May 31 ~ June 1, 1969.

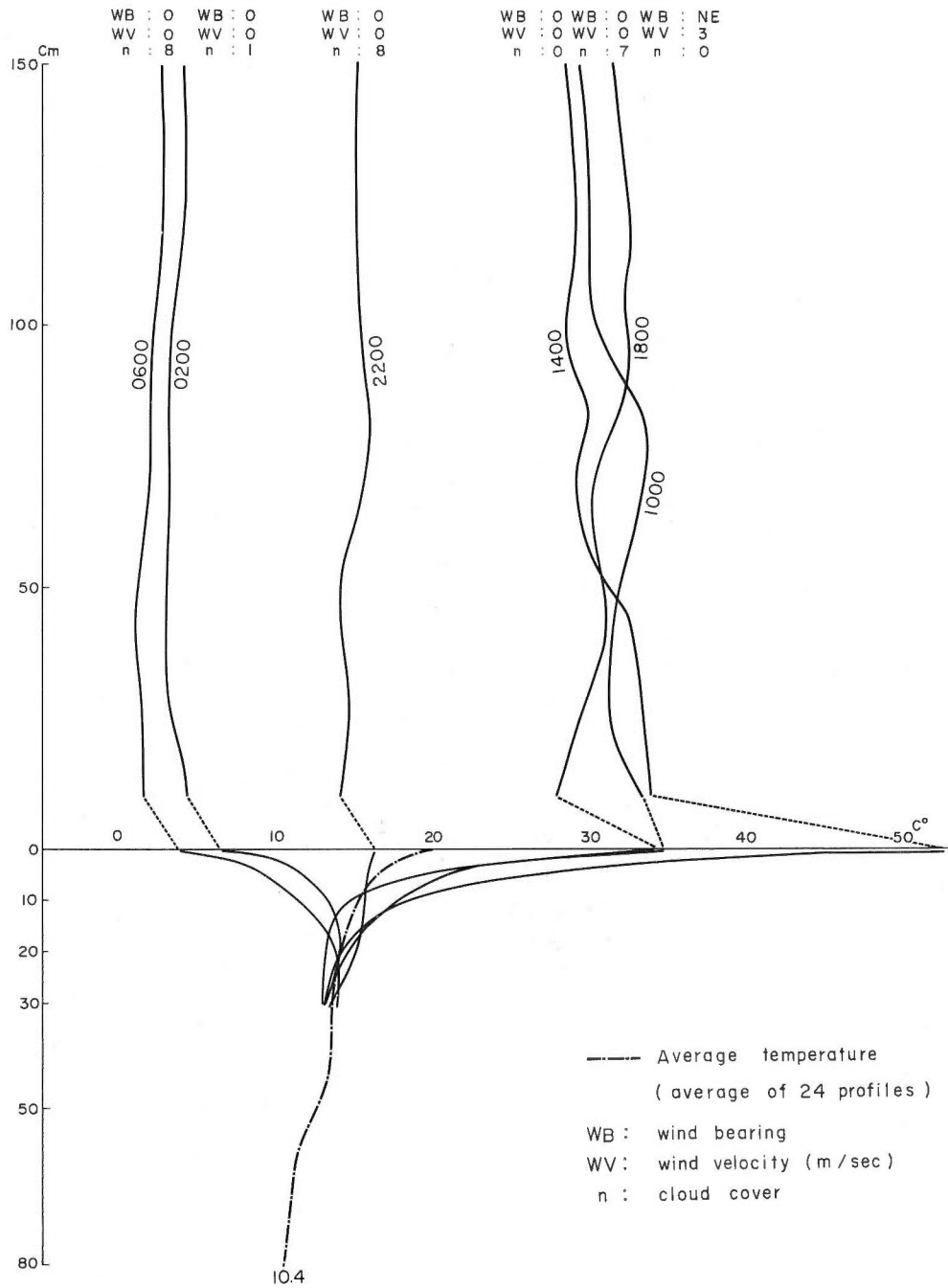


Fig. A-5. The earth-air temperature data at ML-4 "Wet surface" date of measurements May 29-30, 1969.



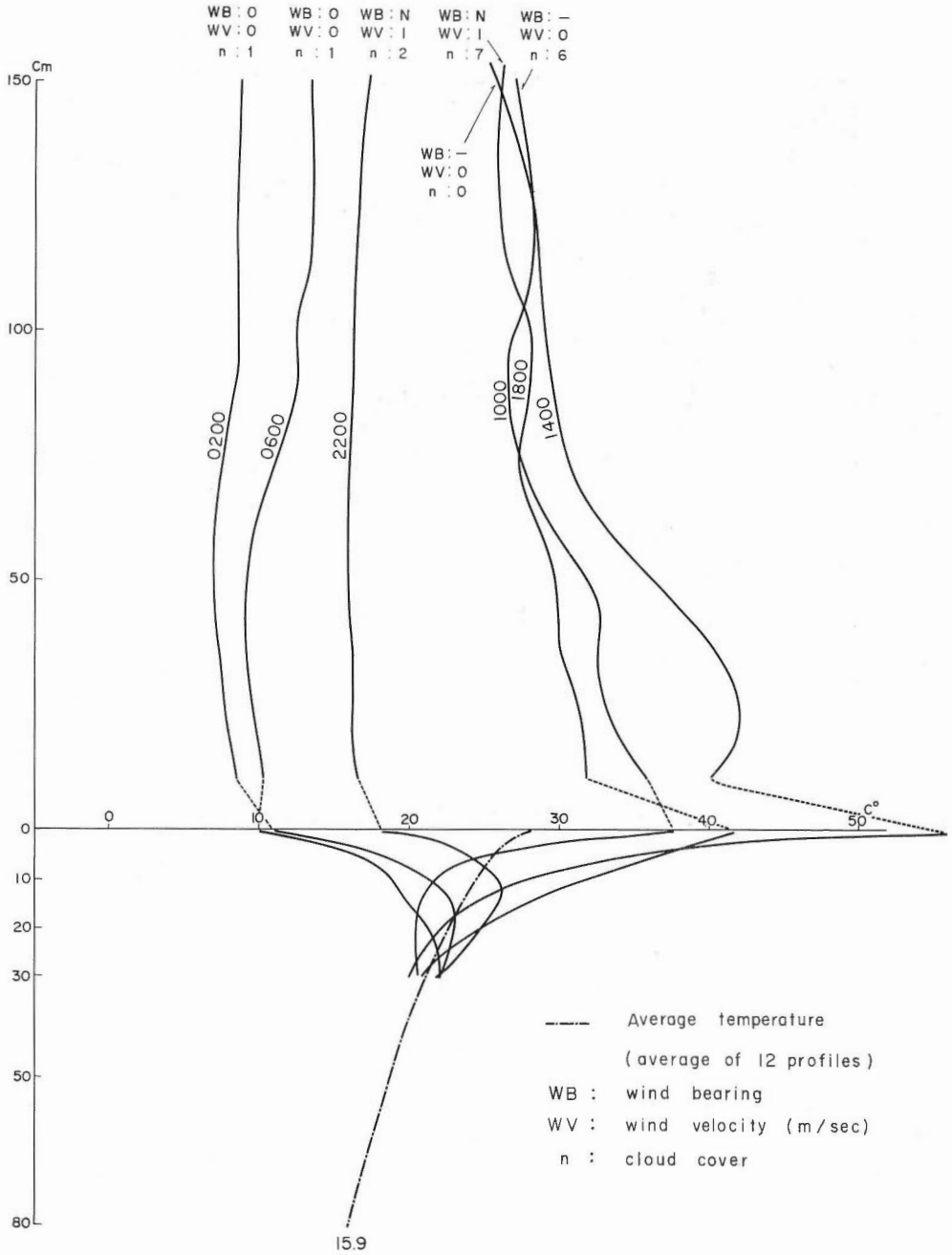


Fig. A-6. The earth-air temperature data at ML-5 (scoriaceous black colored sand surface) date of measurements June 2-3, 1969.

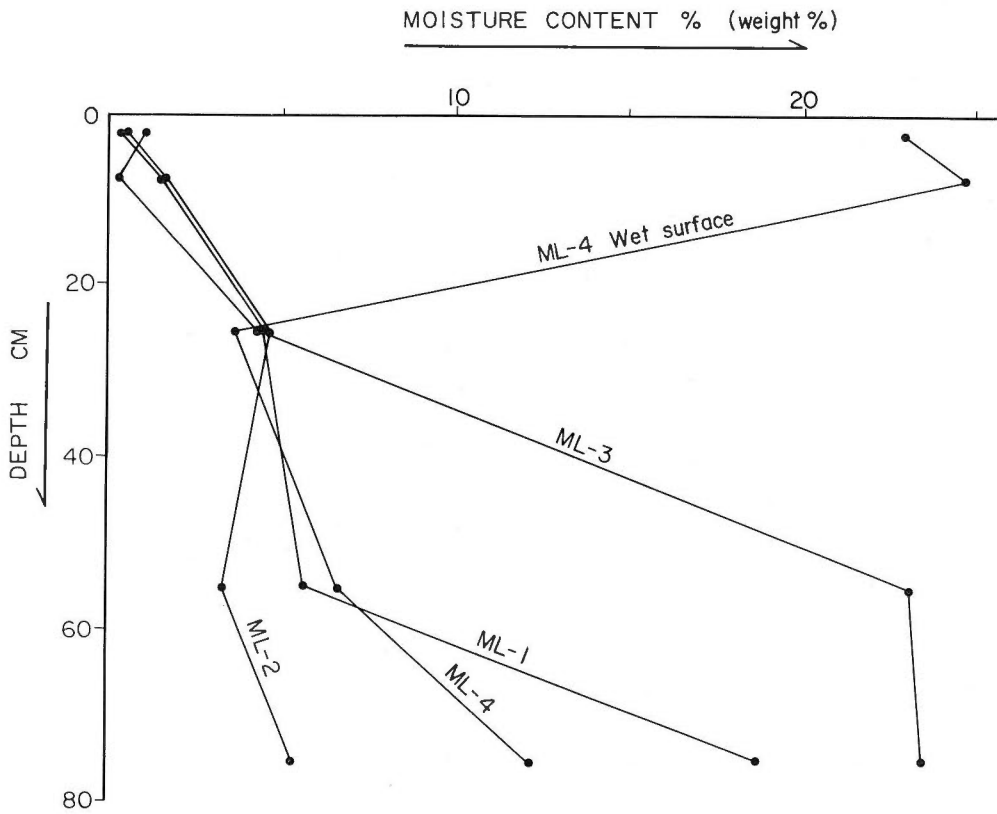


Fig. A-7. Moisture content versus depth curve of measurements sites (lacks ML-5 data).

## 草津一万座地熱地域の地質学的リモートセンシング

長谷 紘 和

### 要 旨

浅地下一地表間の地熱機構は対象地域の地質および地質構造と密接に関連することが推定され、地熱機構を理解するためには、地熱エネルギーの地表への主要運搬経路となる断層・節理など開いた割れ目の把握と地熱異常との関連をつかむことが要求される。

断層・節理などの地表トレースを地質線構造として把握する有効な手段としては空中写真による判読があげられる。また、地熱異常の面的広がり把握するためには熱赤外映像の利用が有効であると考えられる。

本論文では、群馬県北部に位置する草津一万座地熱地域を対象地として選定し、空中写真および熱赤外映像を併用して地質線構造の側面から本地域の地熱機構と地質構造との関連を解明することを試みた。

熱赤外映像の地熱目的への利用の方法論はまだ確立されておらず、本論文中には映像の解釈に関する基礎的研究が含まれている。すなわち、本地域内では、熱赤外映像を地殻熱流量との関連において定量的に解釈することを目的とし、映像によって地熱異常としてとらえられる最小限界を経験的に求めた。

草津一万座地域は東北日本列島弧の南西端と伊豆－マリアナ弧の北端とが交わる地域に位置する。第三紀中新世以降本地域はグリーンタフ変動を受け、地向斜区域となったが変動の初期に地背斜に転じ、以後今日まで陸上での火山活動が連続した地域に相当する。火山活動の形態は、初期の割れ目噴火の群生火山噴火から次第に個々の独立した火山体を形成する噴火活動へと変化し、地域内においては、本白根および白根山の南北二頂をもつ草津白根火山が第四紀以降の噴火中心となった。

本論文では初めに、主として従来の地質学的・構造地質学的研究に基づき、草津一万座地域の基盤を形成する新第三系緑色凝灰岩類およびその上位の第四系火山岩類の層序、岩質についてのべた。次に草津白根火山の有史以来の火山活動史について、爆発の中心、割れ目帯の形成、湧泉など火山地質構造に関連する形態変化を略述した。草津白根火山は有史以来たびたび爆発活動をくり返し、過去90年間に10回の活動が記録されている。有史以来の火山活動はすべて白根山（北頂）頂上付近で行なわれた。活動形式は水蒸気爆発がおもで熔岩の噴出はなく、活動の休止期に近づいているものと考えられる。

本地域は代表的な火山性地熱地域としても特徴づけられ、白根山山頂以外にも地域内には多くの地熱異常地、温泉が分布する。これらのうちでとくに顕著な地熱異常地である殺生河原、草津温泉、および万座地熱異常地の地熱現象について記載した。このうち殺生河原は透水性無水地帯に発達する地熱異常地で、高地温地表面と噴気とによって特徴づけられる。殺生河原の南側斜面において積雪を熱量計として利用し、地熱異常地表面の融雪パターンを降雪後の時間経過とともに作図し、等放熱量図を作成した。すなわち、 $1,320 \mu\text{cal}/\text{cm}^2\text{sec}$  と  $800 \mu\text{cal}/\text{cm}^2\text{sec}$  の等値線と他に2本の定性的補助線が得られた。

地熱異常に関連の深い、断層・節理の解析には空中写真を利用した。既存の、縮尺およそ4万分の1および2万分の1の空中写真を用いて、立体視観察により北部フォッサマグナ地域の主要地質線構造の把握をおこなった。また、微弱な地形的特徴や土壌の写真階調のわずかな違いによって識別される地質線構造（相対的小規模断層および節理群）の把握には擬似陰影効果による写真映像の

強調法 (WELLER によって提唱されたフィルムサンドウィッチ法) を適用した。野外調査では基盤岩が露出する万座地域を中心に、断層面・節理面の走向傾斜を主要露頭ごとに測定し、写真地質線構造解析結果と合わせて lineagenic な地質構造を考察した。

千曲川以東の北部フォッサマグナ地域において、地表面に線構造としてとらえられる断層・節理ののびには北西—南東方向の顕著な方向性がみとめられる。この lineagenic な構造特徴は北部フォッサマグナ地域におけるグリーンタフ変動の構造上の長軸方向 (culmination zone) とほぼ直交する関係にある。しかしながら独立した火山体が発達する地域では地域的な特徴をもった線構造が卓越する。草津白根火山では東西方向の地域的線構造が認められる。フィルムサンドウィッチ法によって解析された微弱な線構造ののびの方向は主要地質線構造の方向と調和的である。とくに万座地域での地表調査結果は写真地質解析結果とよい一致を示した。

本地域に発達する地熱異常の面的広がりを把握する目的で空中熱赤外線撮像が行なわれた。飛行は1971年12月18日早朝と、1972年8月19日夜明け前に行なわれた。撮像装置の検知器は InSb で波長  $5.1 \mu$  までの赤外放射エネルギーが温度映像として表示される。また万座地域の「からふき」地熱異常地を対象に地上用熱赤外線撮像装置を用いて地熱異常分布が詳細に調査された。この装置の検知器には HgCdTe が用いられ、 $8 \sim 14 \mu$  の波長領域の赤外放射エネルギーが温度映像として表示される。

1972年8月の撮像結果によれば、地域内の主要な地熱異常地が熱赤外線映像に表示された。得られた映像の解釈のために現地調査が行なわれ、また、室内においてはカラー画像解析装置を用いて温度分布の画像解析を行ない、併せて地表地熱異常現象について考察を行なった。

白根山山頂付近では、中央火口群をとりまくような半環状の地熱異常パターンが熱赤外線映像によって識別される。この地熱異常パターンは1932年の爆発の際に形成された噴気を伴う割れ目帯 (現在地熱異常はない) に連続する。この事実から中央火口群の周囲をとり巻いて地熱異常を伴う環状割れ目帯が発達することが結論された。

万座および殺生河原のように噴気と高地温異常で特徴づけられる地熱異常の分布には、地域的ではあるが規則性が認められる。万座では南北性の万座断層、殺生河原では東西性の草津断層と調和する地熱異常の配列を示し、両断層は地熱機構を考察する上で重要な断層として認識された。

熱赤外線映像濃度差をカラー画像解析装置により解析することによって判読効果を上げることが期待される。殺生河原の熱赤外線映像にこれを応用した結果、地表地熱異常として周囲の温度分布パターンから識別される地熱異常分布は積雪を熱量計として測定した  $800 \mu\text{cal}/\text{cm}^2\text{sec}$  の等放熱線よりも広がっている。この結果は熱赤外線映像による地熱異常のマッピング調査に一つの定量的利用可能限界値を与えた。本論文中にはこれまでに得られた、地表面でとらえられる地熱異常の限界を与える経験的測定結果の数例をまとめた (第3表)。

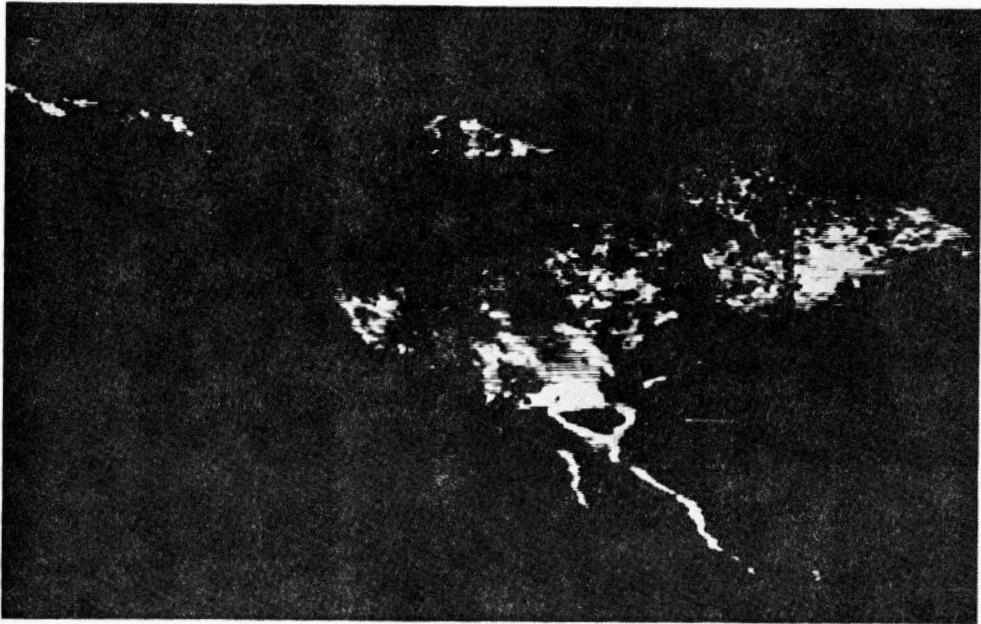
PLATES  
AND  
EXPLANATIONS

(with 6 Plates)





1. View of the Karafuki geothermal spot looking toward south (northern face)  
The spot is situated in a horseshoe-shaped place suggesting landslide topography. Many dead tree stumps around Karafuki show the occurrence of large scale landslide in the past of not older than 50 years ago. Two vapor issuing vents are seen at the central portion of the spot.

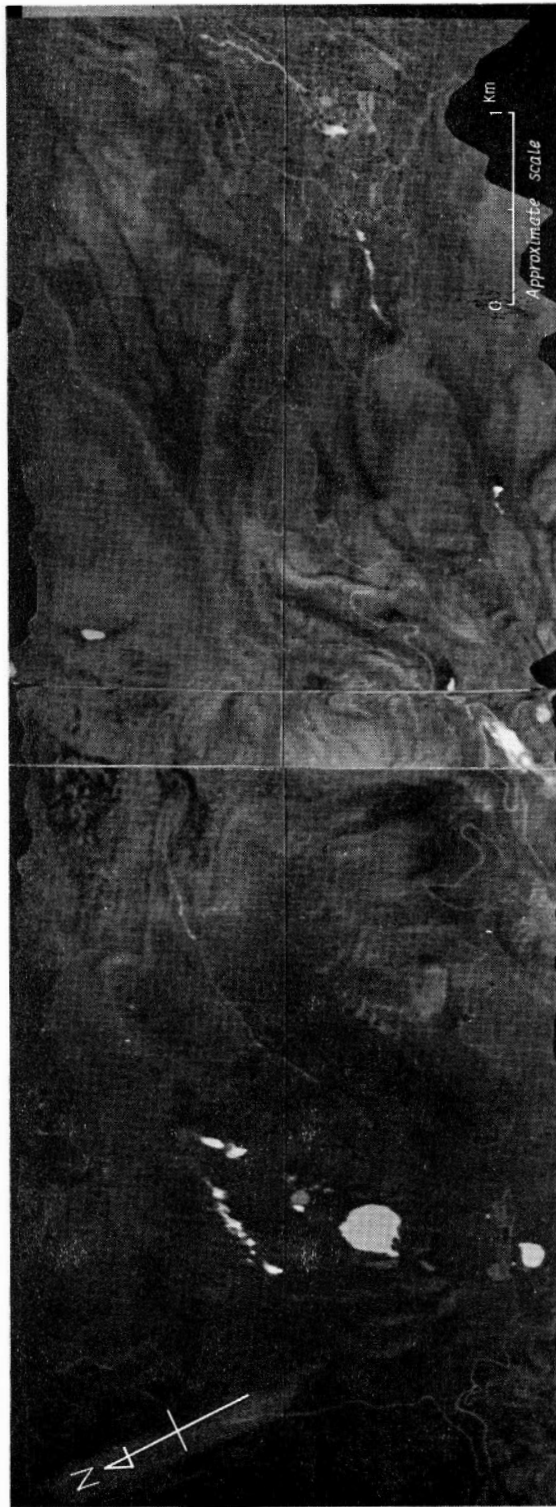


2. Nighttime thermal infrared imagery mosaic of the Karafuki geothermal spot  
The imagery was taken between 21:30m to 21:36m, Aug. 31, 1972. Air temperature during the imaging test tended 18.2°C to 17.6°C, cloud cover  $n = 10$  (overcast). Temperature range is 6°C.

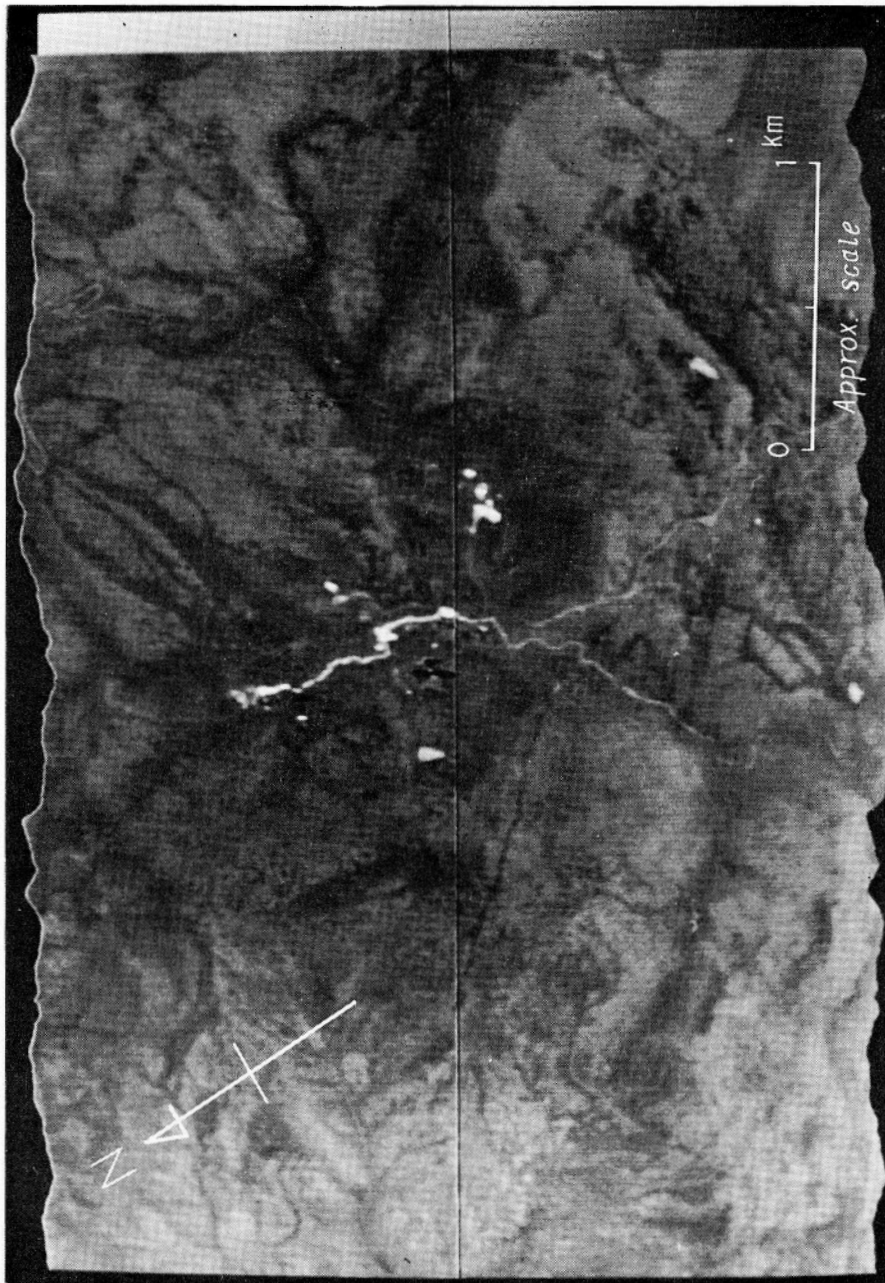


Aerial thermal infrared imagery of a part of the Sesshō Lava near at Sesshō-gawara (refer to Fig. 16)  
Imaging flight was made on 9:00 A.M. Dec. 18, 1971 (imaged by the Asia Aerial Survey Co.).

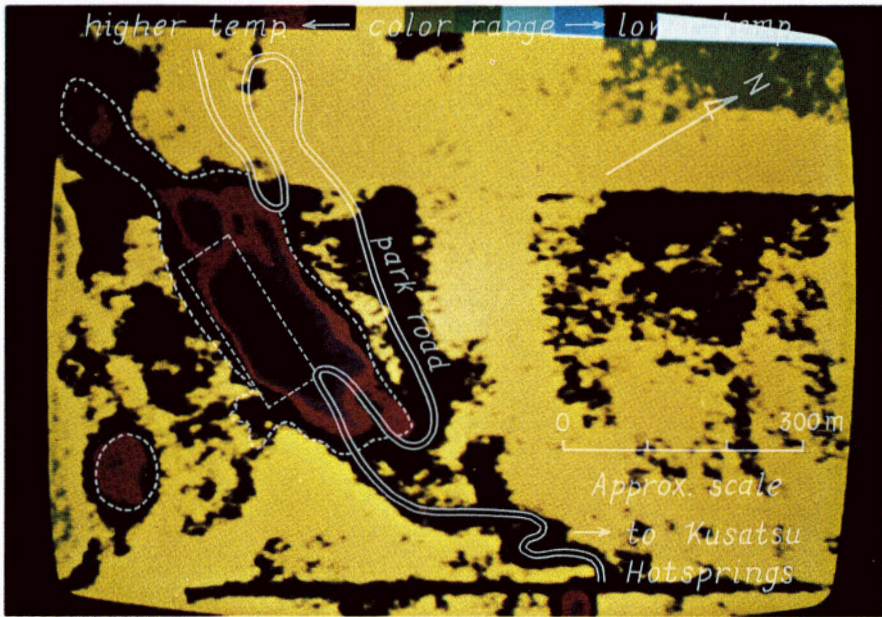






Aerial thermal infrared imagery of the Kusatsu-Shirane Volcano—Kusatsu Hotsprings area (refer to Fig. 17). The elevation of the mountain is about 2,000 m at the summit area and about 1,100 m at Kusatsu Hotsprings. Natural surface temperature pattern is broken at the middle portion of the slope (central part) by comparatively warmer thermal pattern. The reason is discussed in the paper.



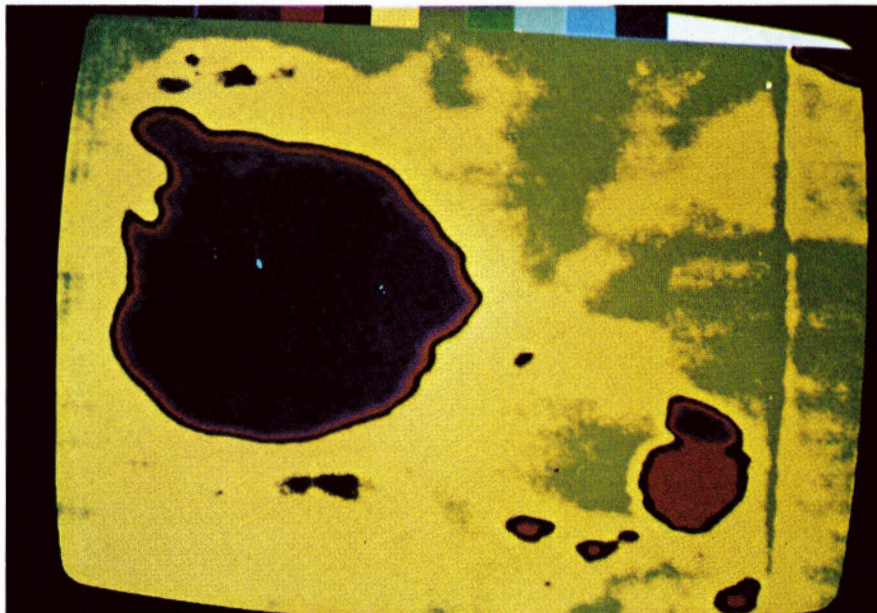
Aerial thermal infrared imagery of the Manza area (refer to Fig. 18)  
The Manza river seen in the central part of the imagery is warmer at the upperstream (northern part) and the river water temperature decreases  
nearly ambient temperature at the bottom. The Karafuki geothermal spot is seen at the center right of the imagery.



-  thermally altered area
-  area covered by snowfall calorimetric survey

Automatically processed thermal infrared imagery of Sesshō-gawara

Two rows of sublinear patterns in the central dark color portion surrounded by violet color area may be correlated with the same pattern of the heat discharge map. The geothermal anomaly distinguished from the surrounding temperature pattern extends outside of the contour line shown as  $800 \mu\text{cal}/\text{cm}^2 \text{ sec}$  (see Fig. 5). High heat discharge portion is saturated in the imagery.



1. Automatically processed aerial thermal infrared imagery of the Yugama crater lake  
Thermal pattern on the surface of the lake water is formed by the lake bottom spring and the floating free sulphur with different temperature and emissivity from the surrounding water.



2. View of the Yugama crater lake looking toward south  
Photograph was taken from the northeast crater rim.

地質調査所報告は1報文について報告1冊を原則とし、その分類の便宜のために、次のようにアルファベットによる略号をつける。

- A. 地質およびその基礎科学に関するもの
  - a. 地質
  - b. 岩石・鉱物
  - c. 古生物
  - d. 火山・温泉
  - e. 地球物理
  - f. 地球化学
- B. 応用地質に関するもの
  - a. 鉱床
  - b. 石炭
  - c. 石油・天然ガス
  - d. 地下水
  - e. 農林地質・土地質
  - f. 物理探鉱・化学探鉱および試錐
- C. その他
- D. 事業報告

As a general rule, each issue of the Report, Geological Survey of Japan will have one number, and for convenience's sake, the following classification according to the field of interest will be indicated on each Report.

- A. Geological & allied sciences
  - a. Geology
  - b. Petrology and Mineralogy
  - c. Paleontology
  - d. Volcanology and Hot spring
  - e. Geophysics
  - f. Geochemistry
- B. Applied geology
  - a. Ore deposits
  - b. Coal
  - c. Petroleum and Natural gas
  - d. Underground water
  - e. Agricultural geology and Engineering geology
  - f. Physical prospecting, Chemical prospecting & Boring
- C. Miscellaneous
- D. Annual Report of Progress

## 地質調査所報告

第 247 号

小川克郎：空中磁気図解析・解釈法の研究，1973

第 248 号

IGI, S.: The metagabbros and related rocks of the "Yakuno Complex" in the inner zone of Southwest Japan, 1973

第 249 号

尾崎次男：地下水位の観測記録，1973

第 250 号-1

第三系堆積盆地研究グループ：新潟第三系堆積盆地の形成と発展，層序編，1974

第 250 号-2

第三系堆積盆地研究グループ：新潟第三系堆積盆地の形成と発展，構造地質・地球化学編，1974

第 251 号

地質調査所：北上山地の白亜紀花崗岩類—岩石記載と帯状配列—，1974

## REPORT, GEOLOGICAL SURVEY OF JAPAN

No. 247

OGAWA, K.: A study of the method for interpretation of aeromagnetic maps, 1973 (in Japanese with English abstract)

No. 248

IGI, S.: The metagabbros and related rocks of the "Yakuno Complex" in the inner zone of Southwest Japan, 1973 (in English)

No. 249

OZAKI, T.: Observation records of ground water level, 1973 (in Japanese with English abstract)

No. 250-1

TERTIARY SEDIMENTARY BASINS RESEARCH GROUP: Stratigraphy and tectonics of Niigata Tertiary basin, vol. 1, Stratigraphy, 1974 (in Japanese with English abstract)

No. 250-2

TERTIARY SEDIMENTARY BASINS RESEARCH GROUP: Stratigraphy and tectonics of Niigata Tertiary basin, vol. 2, Structural geology and geochemistry, 1974 (in Japanese with English abstract)

No. 251

GEOLOGICAL SURVEY OF JAPAN: Cretaceous granitic rocks in the Kitakami Mountains—Petrography and zonal arrangement—, 1974 (in Japanese with English abstract)

HASE, H.

**Geologic Remote Sensing of the Kusatsu-Manza Geothermal Area,  
Central Japan**

Hirokazu HASE

Report, Geological Survey of Japan, no. 252, p. 1-56, 1974

21 illus., 6 pl., 5 tab., 7 appendix illus.

An approach for the understanding of geothermal system was made by means of photogeologic structural analysis and the use of thermal infrared imagery in the Kusatsu-Manza geothermal area. Regional lineagenic characteristic of the northern Fossa Magna including the studied area is given and surface geothermal anomaly is discussed on the basis of thermal infrared imagery, the result of lineagenic structural analysis, and field data. Some fundamental studies to know the detectable limit of surface geothermal anomaly are included.

550.36:551.21:550.836:778.35 (521.24)





昭和 49 年 8 月 12 日 印 刷

昭和 49 年 8 月 17 日 発 行

工業技術院地質調査所

川崎市高津区久本 135

印刷者 小 宮 山 一 雄

印刷所 小宮山印刷工業株式会社

東京都新宿区天神町78









地質調報  
Rept. Geol. Surv. J.  
No. 252, 1974